UNIVERSITY OF MIAMI

TROPICAL CYCLONE RAINBANDS OVER LAND IN SOUTH FLORIDA: MULTI-WAVELENGTH RADAR OBSERVATIONS AND THEIR EDUCATIONAL APPLICATIONS

By

Shaunna Donaher

A DISSERTATION

Submitted to the Faculty
of the University of Miami
in partial fulfillment of the requirements for
the degree of Doctor of Philosophy

Coral Gables, Florida

August 2012

UNIVERSITY OF MIAMI

A dissertation submitted in partial fulfillment of
the requirements for the degree of
Doctor of Philosophy

TROPICAL CYCLONE RAINBANDS OVER LAND IN SOUTH FLORIDA: MULTI-WAVELENGTH RADAR OBSERVATIONS AND THEIR EDUCATIONAL APPLICATIONS

Shaunna Donaher

Approved:

_____ Bruce Albrecht, Ph.D. Professor of Meteorology and Physical Oceanography	_____ M. Brian Blake, Ph.D. Dean of the Graduate School
_____ Frank Marks Jr., Ph.D. Research Meteorologist and Director NOAA/AOML Hurricane Research Division Miami, Florida	_____ Paquita Zuidema, Ph.D. Associate Professor of Meteorology and Physical Oceanography
_____ Kevin Kloesel, Ph.D. Associate Professor and Associate Dean for Public Service and Outreach University of Oklahoma	_____ Okhee Lee, Ph.D. Professor of Childhood Education New York University

DONAHER, SHAUNNA (Ph.D., Meteorology and Physical Oceanography)
Tropical Cyclone Rainbands Over Land in South Florida: Multi-wavelength Radar Observations and their Educational Applications (August 2012)

Abstract of a dissertation at the University of Miami.

Dissertation supervised by Professor Bruce Albrecht.
No. of pages in text. (202)

This dissertation investigates the wind structure observed in outer rainbands of three tropical cyclones in August and September 2008 in South Florida. Average wind profiles during fourteen stratiform periods are evaluated using a velocity-azimuth display (VAD) technique applied to Level-2 Miami (KAMX) WSR-88D data to study wind structure in high vertical resolution from a height of 65 meters to 6550 meters above ground level. The maximum horizontal wind speed in the rainbands is typically observed between 1000-1500 meters in height, with occasional evidence of a secondary horizontal wind maximum near 3500-5000 meters. This secondary maximum is found to be stronger than the low-level maximum in four cases of stronger storms observed at further distances (425-450 km) from storm center. Storm-relative wind components are calculated, and radial wind profiles show a mean switch from radial inflow at low levels to radial outflow around 2500-3000 meters AGL. The radial inflow maximum is around 500 meters, while maximum outflow is much more variable. Temporal variability within one four hour period is examined, and an ascending and strengthening low-level wind maximum is seen, along with a decrease in the low-level radial inflow over time.

Low-level winds are studied in great detail using the high resolution VAD data. All rainbands show a logarithmic wind speed decrease below 500 meters; friction velocity and aerodynamic roughness length are calculated in this log-wind regime for each band. Although the roughness length is found to be higher and much more variable than previous observations, using the calculated components for a fit between 65-120 meters AGL allows for an estimate of wind speeds up to 500 meters above ground level with good accuracy.

Variability within the four longest stratiform periods is examined in high temporal and vertical resolution using X-band radar and wind profiler data. Vertical features extending from the near-surface up to the height of the melting level are present in the majority of the cases and are found to have wavelengths of 3.6-5.3 kilometers in the horizontal. Possible forcings behind these features are hurricane boundary layer rolls triggered near the surface and thermodynamic forcing triggered at and above the melting level. Results do not suggest that one forcing is consistently dominant, but rather that the forcings are acting in conjunction, causing a new scale of wavelength that does not connect directly with previous observations of hurricane boundary layer rolls.

Finally, an educational study is conducted using wind profiles from three stratiform cases to evaluate the use of field data in undergraduate meteorology classroom. An inquiry-based lab approach and a traditional “cookbook” lab approach were tested, with student attitude toward science and content knowledge and retention evaluated. Results indicate that both approaches allowed for comparable content knowledge growth, although neither had a direct impact on student views towards science labs.

This dissertation is dedicated to my husband Ryan for his unwavering support.

ACKNOWLEDGEMENTS

Several people were instrumental in the completion of this work, and I would like to acknowledge their efforts and support.

First and foremost, I would like to thank my advisor, Dr. Bruce Albrecht. He has been an amazing mentor and role model and I appreciate his patience and guidance throughout this project. My experience at RSMAS has been incredible and I feel fortunate to have been able to participate in so many amazing field projects and research opportunities. I would also like to thank Dr. Albrecht for his support in adding education research to this RSMAS PhD. This dissertation marks a new interdisciplinary connection for RSMAS research, and I am thankful for his encouragement to pursue all of my research interests.

Dr. Paquita Zuidema was also instrumental in the encouragement of this work. Her efforts to include the education research mean more to me than I can put into words, and for that I will be eternally grateful.

I would like to thank Dr. Frank Marks for sharing his seemingly endless hurricane and remote sensing expertise. Dr. Marks helped to make my transition into hurricane research seamless, and I am thankful for the opportunity to collaborate with him, and for all of his kind comments during our interactions.

Dr. Kevin Kloesel was also a valuable committee member whose enthusiasm and support was always appreciated. He generously volunteered his class as a study group for the educational component of this work, and provided many constructive comments on

this document. His passion for meteorology was very motivational towards the accomplishment of my task.

Dr. Okhee Lee-Salwen is another individual who was instrumental to the educational component of this work. I cannot thank her enough for agreeing to serve on my committee and for her helpful and encouraging comments on my work and research path.

Special thanks are also due to Drs. Pavlos Kollias and David Nolan for their valuable comments on the proposal and first stages of this work.

This dissertation would not have been possible without the efforts of NCAR EOL during the CPS experiment. In particular, Dr. William Brown was instrumental in data collection and providing guidance during data analysis. I am thankful for the opportunity to spend time in Boulder working on this data set, and I am grateful to him for hosting me.

I would also like to thank Dr. Sandra Yuter of NC State for providing a part of the data used in this analysis and for her support.

Many thanks are due to the UM radar group, including Virendra Ghate, Xue Zheng, Ming Fang, Eunsil Jung, and Tom Snowdon. Vinny, Xue and Tom each played a large role in CPS data collection and instrument maintenance. Ming generously provided the VAD data used in this study. Dan Voss also provided computer support throughout the project. Special thanks go to our former undergraduate assistant Bri Winkler for her assistance in preparing for the field project and for all the work she helped with at the field site.

I am thankful for the opportunity to be exposed to interesting work being done by my classmates and colleagues at RSMAS and in TAL, and feel fortunate to have been a member of this community.

Moreover, the support from my friends in Miami and afar has helped to make the past 8 years even more enjoyable. I couldn't have done this without the friendship of Corinne, Laura, Emily, Andrew, Rachael, Chris, Kristen, Amy, Bryan, Evan, Kelly J., Kelly G., Josi, Katie, Stephanie D., Aaron, Shelly, Stephanie S. and Liz. Love you guys!

Finally, I would like to thank my family for their constant love and support throughout my entire academic career. Knowing that my parents Susan and Tony, brother Kevin, in-laws Helen and Kevin, sister-in-law Erin, and grandparents Alexia, Norman and Maryann believed in me helped tremendously in this pursuit. I cannot thank my husband Ryan enough for his love and his support of this dream. His constant encouragement makes me feel like I can conquer the world.

This work was supported by NSF grant 663684.

TABLE OF CONTENTS

LIST OF FIGURES

LIST OF TABLES

LIST OF EQUATIONS

Chapter 1: Introduction

1.1 Motivation

Observational studies on the structure of tropical storm and hurricane rainbands have become more prevalent since the end of World War II, when radar began to be used for meteorological purposes (Powell 1990a). In the past few decades, the majority of these observations have occurred over the oceans using data from C- and X-band radar collected during research flights (e.g Barnes et al. 1983; Marks 1985; Jorgensen 1984; Barnes and Stossmeister 1986). There have also been a few studies of rainbands making landfall, some with scanning weather radar (e.g Skwira et al. 2005; Spratt et al. 1997; Blackwell 2000; Stewart and Lyons 1996) and some with wind profilers (e.g May et al. 1994; May 1996; Sato 1991). However, these landfalling studies are less prevalent due to the challenge of planning for data collection with highly variable landfall potential, as well as the inability to perform research flights at low levels over land. Landfalling systems are thought to be different from oceanic systems as they have enhanced cooling in the middle and upper levels of the atmosphere due to the loss of oceanic heat and moisture, advection of drier air from over land, enhancement of rainband convection over land leading to mesoscale saturated downdrafts, and enhanced turbulent entrainment of dry air from above the top of the hurricane boundary layer (Powell 1987). Landfalling tropical cyclones can also be influenced by continental aerosols acting as CCN that invigorate convection at the cyclone periphery and weaken the storm (Khain et al. 2010).

Capturing data from landfalling tropical systems is challenging due to safety concerns, instrument limitations, and logistical difficulties. Although recent studies have collected such observations (e.g. Knupp et al. 2006), they often only use one or two

instruments for data collection, or have limited vertical resolution (e.g. 105 meters during Knupp et al. 2000) or heights (e.g. below 10 meters during Masters et al. 2010) that they can analyze. There are several reasons that it is important to understand the vertical structure of winds in rainbands over land. First, knowledge of the vertical variation of wind speed is critical in urban areas where high-rise structures may experience winds much stronger than those at the surface (Franklin et al. 2003). Second, the vertical wind profile may be responsible for the generation of low-level roll structures such as those seen in Morrison et al. (2005) and Lorsolo et al. (2008), and modeled by Foster (2005). Wind gusts near the surface are also important, as they can cause significant damage near the shoreline, but can decrease rapidly inland due to surface friction (Powell, Dodge and Black 1991). Additionally, wind shear may play a role in promoting tornado genesis over land (e.g. Novlan and Gray 1974; Gentry 1983; Baker et al. 2009) making understanding the amount of low-level shear in landfalling storms important.

In this study, data collected during the Cloud Precipitation Study (CPS) field experiment are used to study a total of 24 rainbands collected from one tropical storm and two hurricanes as they pass over a field site in South Florida. The availability of multi-wavelength radar observations allows for the characterization of the detailed vertical structure of these rainbands, creating a high-resolution representation of rainbands over land, including the variability within them. Since the largest impact of tropical cyclones on human activity and vegetation is felt within the lowest 100 meters of the hurricane boundary layer, it is important to fully understand the processes that are occurring near the surface-- an area that is mostly missed during research flights.

These data are used to compare the vertical structure of wind profiles from rainbands of storms of different intensities and distances. The two-to-four meter vertical resolution of the Velocity-Azimuth Display (VAD) data set below 500 meters allows for high-resolution examination of the log-wind regime in the hurricane boundary layer (HBL). In this work, the HBL is defined dynamically, following Kepert (2001), as the shallow area closest to the surface that is influenced by the frictional disruption of the gradient wind balance (Ekman layer). The HBL has a logarithmic increase in wind speeds from the surface up to a wind maximum (usually located between 500-1000 meters above ground level, Montgomery and Smith 2010) that tops the HBL. The HBL is an area that is often unsampled during research flights but is crucial to understanding the impact of tropical cyclones on human activity and vegetation. In addition to the VAD data, data sets from other instruments can also be utilized to study the upper-level winds that are frequently missed by dropsondes, and to compare non-precipitating periods before and after rainband passage with stratiform periods within the rainbands.

Commonly, rainband studies show radial and tangential wind components (e.g. Barnes et al. 1983; Ishihara et al. 1986), but relatively few show the mean horizontal wind (e.g. Knupp et al. 2006; Marks et al. 1999) and many of these analyses are limited to the lowest 2000-3000 meters of the atmosphere due to dropsondes being released from 700hPa. This study examines both the mean wind and wind component profiles from 65 meters above ground level up to 6550 meters over land, and allows for comparison of wind profiles among three different storms using the same instrumentation.

The motivation of this work is to examine the dynamics of tropical cyclone rainbands over land using a variety of remote sensing instruments. This includes a focus

on the vertical structure of the wind components including locations of wind maxima and inflection points, conditions in the surface layer (defined as the lowest 200 meters of the atmosphere), and changes during rainband passage. This work will improve the understanding of the conditions that occur in an urban coastal environment with rainband passage, especially in the surface layer where winds can have a large impact on structures. This is especially important when evaluating the influence that variations in wind speed with height can have on high-rise buildings. Additionally, high-resolution studies (30 seconds temporally) of mesoscale wind variability and turbulence in four stratiform rainband cases are presented with a goal of relating observed variability to hurricane boundary layer (HBL) rolls or other turbulence features (e.g. those observed by Lorsolo et al. 2008 and Gall et al. 1998). The observations from rainbands over land can be compared with previous flight observations over water to highlight similarities and differences in conditions. With an increased knowledge of landfalling hurricane rainband conditions, simulations and forecasts of hurricane impacts could be improved before a storm comes close enough to impact land.

The remainder of Chapter 1 provides an overview of previous studies related to hurricane rainbands, as well as the scientific objectives behind this work. Chapter 2 describes the experiment and instrumentation used for the remainder of the analyses shown in this dissertation. In Chapter 3, observations from 14 stratiform rain periods within 8 outer rainbands over land in South Florida in August and September 2008 are presented. This chapter describes individual profiles of mean wind speed and direction, as well as storm composites and individual profiles of radial and tangential wind broken down by storm occurrence. This chapter also examines the temporal variability during

rainband passage, first within one rainband and then by presenting case examples of radial and tangential profile changes before, during and after rainband passage. Section 3.5 focuses on the HBL winds, first examining the log-wind regime and calculating friction velocity and aerodynamic roughness length by rainband, and finally by comparing the ratios of surface winds to those at the top of the BL. The ratios calculated from the 14 stratiform cases over land are compared with previous observations of surface to HBL wind ratios over land and water to showcase the differences between land and ocean wind conditions. In Chapter 4, case studies from four of the stratiform rainbands are used to examine the small-scale (< 1 km) vertical variability and draw comparisons between the features seen and previously observed HBL rolls (e.g. Lorsolo et al. 2008, Morrison et al. 2005).

Chapter 5 transitions from the analysis of rainband observations to investigating their potential for use in an undergraduate meteorology classroom. In this chapter, an educational research study is described that uses three stratiform rainband cases to test two approaches to a meteorology lab exercise. Chapter 6 concludes with a summary of the conclusions reached during this work.

1.2 Background

Detailed research into hurricane processes began in the 1940's, when radar was transported from its military World War II purpose and used for weather observations. Major features such as the hurricane eye and rainbands were identified as early as the 1940s (Marks 2003). The development of airborne Doppler radar in the 1980s led to the ability to study the detailed structure of these systems over water during research flights

(e.g Marks 1985, Willoughby et al. 1984, Marks and House 1987, Powell 1990b, Barnes et al. 1991), albeit with temporally limited data (May 1996). In the past, observations of tropical cyclone rainbands over land were limited due to limited coastal radars and the low probability of a storm hitting a specific region in a given year. For the past two decades however, almost every mile of United States coastline has had coverage by a 1998 Next-Generation Doppler Weather Surveillance Radar (NEXRAD WSR-88D), so storms passing near or over land can be studied (e.g Skwira et al. 2005, Lorsolo et al. 2008). However, despite the improvements in spatial coverage, the large (S-band) wavelength of the WSR-88D radar makes it challenging to study features with spatial scales less than 500 meters that occur in tropical cyclone rainbands passing nearby without additional data manipulation.

1.2.1 Aircraft Observations

Early work describing the structure of hurricane rainbands is based on data collected from research flights into storms in the late 1970s and early 1980s. A schematic of typical rainband structure was published by Barnes et al. in 1983. This schematic is still widely used today and can be seen in Figure A1 in Appendix A. Barnes et al. used a minimum radar reflectivity of 25 dBZ to threshold where rainbands existed, and then composited 26 aircraft passes of a rainband of Hurricane Floyd (1981) to develop a schematic of the rainband in crossband-height coordinates (Figure A1a) and x,y coordinates (Figure A1b). Using the 25 dBZ contour, the rainbands are seen to lean radially outward with height. Stratiform conditions with a bright band exist on either side of convective cells, which are defined as local maxima of radar reflectivity extending

along the aircraft track at least 2000 meters with horizontal gradients that exceed 2 dBZ/km. The mesoscale average flow and convective scale updrafts and downdrafts are more three-dimensional than just a simple two-dimensional radial overturning. The air from the subcloud layer rises, but the air at 2000-3000 meters AGL descends. The rainband is found to become more stratiform closer toward the storm center.

Barnes et al. (1983) hypothesized that small-scale transports, especially convective scale vertical motions, are responsible for the observed equivalent potential temperature fields. The subcloud layer is modified by the convective scale downdrafts causing a reduction in θ_e (Barnes et al. 1983). However, they noted that this schematic may be biased based on flight location in the rainbands, and if the flights had sampled elsewhere in the rainbands, a very different thermodynamic, kinematic and reflectivity structure could be present.

As seen in the conceptual schematics shown in Figure A1, there is low level flow toward the eye and a reversal of flow away from the eye around 6 km. Barnes et al. (1983) state that strong radial inflow is mainly confined to the lowest 1000 meters of the HBL. This radial inflow transports angular momentum into the inner core, compensating for frictional loss (Marks 2003). Later work by Barnes and Stossmeister (1986) shows radial flow toward the eye below 2000 meters altitude in early stage rainbands and away from the eye below 2000 meters altitude in late stage rainbands. Barnes and Stossmeister (1986) found that the tangential winds were always positive (cyclonic) below 2 km, with peak values of ~40 ms^{-1} occurring around 500-1000 meters above ground level. In contrast to these results, Jorgensen (1984) showed that rainbands do not have a pronounced tangential wind max and have a more cellular nature of reflectivity and vertical motion.

This discrepancy may be explained by May et al. (1994), who state that "The variations of the radial and vertical velocity across the rainbands is more complex and appears to be characteristic of the mesoscale circulations associated with stratiform precipitation in trailing squall-line anvils." With this statement, they are suggesting that rainband characteristics can vary widely depending on where in the rainband sampling occurred.

When discussing tropical cyclone rainbands, it is important to note the differences between principal and secondary rainbands. The principal rainband is the prominent spiral feature that extends outward toward one side of the vortex. It commonly has cellular convection along its axis and stratiform precipitation falling from an anvil on its outer side. Observations of the principal rainband generally show a cross-band circulation consisting of a mesoscale updraft sloping outward with height, with inflow at low levels and outflow at high levels (Marks 2003), similar to the Barnes et al. (1983) schematic shown in Figure A1. The secondary rainbands are less prominent spiral-shaped features that vary greatly in terms of intensity and amount of convection. Most contain weak shallow convection but some have convection and outer wind maxima that rival the eyewall in intensity (Willoughby, Marks and Feinberg 1984). Secondary rainbands occur at a larger distance from the storm center, and have been shown to have decreased strength and increased depth of the low level radial inflow layer (Zhang et al. 2011). For example, Ishihara et al. (1986) examined an outer rainband at 300 km from the center of Typhoon 8305 and found the height of reversal to outflow to be at 1500 meters above ground level (AGL) on the inside edge of the rainband and 3600 meters AGL on the outside edge of the band.

Marks (1985) analyzed airborne radar data in Hurricane Allen (1980) to show that

tropical cyclone rainbands were characterized by areas of enhanced reflectivity embedded in a region of stratiform rainfall that contained a distinct bright band just below the height of 0^{o}C isotherm (between 4-5 km) due to the lower reflectivity of ice crystals above the melting level. These rainbands, like those observed by Barnes et al. (1983), were shallow with tops of radar echoes between 7-9 km. In the rainbands, peak reflectivity values were between 42-48 dBZ, and mean rainrates were about 1.8 $mmhr^{-1}$. Stratiform precipitation is more extensive in the rainbands, and was found to cover areas 10 times larger than the convective precipitation (Marks 2003), making understanding the stratiform region a high priority.

In non-stratiform regions, Jorgensen and Willis (1982) found peak vertical velocity (w) values of about 12 ms^{-1}. Convective cells with positive vertical velocities exceeding 1 ms^{-1} for several kilometers were common. Convective-scale downdrafts of 3-5 ms^{-1} associated with high reflectivity regions are also common. Previous rainband studies (e.g. Barnes et al. 1983) have shown that the reflectivity maxima are correlated with stronger vertical velocities and are the initial location for the thermodynamic modification of the subcloud layer (Barnes et al. 1991). In both convective and stratiform regions in rainbands, updrafts outnumber downdrafts by at least a factor of two and updrafts are wider and stronger than downdrafts (Black, Burpee and Marks 1996). The mean vertical velocity ($\overline{w}$) has been found to be positive at all heights, except in the stratiform region below 3 km, where $\overline{w}$ was weakly downward. Minima in $\overline{w}$ values were found between 5000-6000 meters AGL in all regions. Above 5 kilometers the mean reflectivity decreases with height which indicates that microphysical processes are efficient in converting liquid water to ice and that updrafts are not strong enough to

transport much liquid water or graupel above the melting level (Black, Burpee and Marks 1996). The maximum flux in the rainbands was located near 1 km, which indicates that HBL convergence is efficient in producing upward motion.

With the collection of data from additional tropical cyclone rainbands, Powell (1990a) was able to expand upon the rainband schematic produced by Barnes et al. (1983). Powell's model is shown in Figure A2 in Appendix A. In this model, the inner side of the rainband is the preferred region for downdrafts, with the peak updraft typically at the rainband axis (center of 25 dBZ contour). Stratiform rainfall is generated from the anvil and is present on the outer side of the axis with a bright band existing a little bit higher than Barnes et al. (about 4500 meters AGL), extending out up to 20 km from the rainband axis. There is also a smaller stratiform region on the inside of the higher reflectivity cell. Inflow is restricted to the lowest 2000-3000 meters AGL, with outflow above 3000 meters AGL. The high reflectivity cores in the cellular regions extend up as high as 9000 meters AGL with some stratiform rain present above the cells, which is advected downwind while falling. Some rainbands had cellular features upband (upwind slope), caused by the movement downwind of the lower part of the cell with the mean wind at a faster rate than the upper part of the cell. These observations agree with the mechanism of rainband development described by Atlas et al. (1963) where rainbands consist of large stratiform areas that are transported from upwind convection at the speed of the radial velocity. Powell claimed that the higher reflectivity cells developed, matured and decayed over periods of 15-30 minutes and that 60-70% of drafts in these cells are updrafts. The convergence maximum occurs at the bottom of the higher reflectivity cellular regions. Divergence maxima may be found on either side of the rainband 5-10

km away from the convective activity, which suggests mesoscale compensating subsidence. These convective vertical motions are similar to those observed in mesoscale convective lines sampled during the tropical GATE experiment in 1974 (Barnes et al. 1993).

A more recent study of two Category 5 storms (Katrina and Rita, 2005) by Hence and Houze (2008) took place during the Hurricane Rainband and Intensity Change Experiment (RAINEX). They used dual-Doppler X-Band radar observations to validate and expand upon the Barnes et al. (1983) updraft model to create their own schematic of hurricane circulations, shown in Figure A3. Their theory of the circulation includes a layer of strong convergence, which is shallowest and most intense at the base of the sloping reflectivity core. The top of this convergent layer slopes upward and outward with increasing radial distance from the storm center. A layer of divergence, which also slopes upward and radially outward, caps the low-level convergence in the region of the convective cell. The outward sloping updraft lies just above the region of maximum convergence. The radially inward flow at lower levels (below 4000 meters AGL) passes under the reflectivity cell and turns upward, rises, and flows back outward at 8000-10,000 meters AGL. On a local scale this circulation mimics the in, up and out circulation behavior of an eyewall.

In terms of the wind field described by Hence and Houze (2008), a secondary wind maximum extends from about 1000 meters up to 6000 meters AGL where the speed of the wind abruptly decreased. The peak of this wind maximum (also known as the tangential jet) is located at about 4000 meters AGL. There is a positive vorticity anomaly

on the radially inward side of the jet and negative vorticity anomaly on the outside of the jet.

In the plane-view, Hence and Houze (2008) state that the higher reflectivity cores closer to the eyewall are newer, and that they weaken and eventually dissipate as they move downband. However, despite advances in technology in the decade since the Barnes et al. (1983) paper was published, Hence and Houze (2008) claim that multiple Doppler radars still have not been fully utilized to infer the convective scale circulations.

The three main schematic models of hurricane motions discussed so far describe the secondary circulation of the storm, and are mainly focused on mesoscale motions within rainbands. While some convective-scale (< 5 km) details have been added since the original Barnes et al. model in 1983, the understanding of small-scale (< 1 km) motions in tropical cyclone rainbands has not developed as thoroughly due to the challenges of observing these detailed and highly variable rainband features. Black, Burpee and Marks (1996) found that there is a larger frequency of small (< 1 ms^{-1}) vertical velocity values in flight level data than in Doppler data, indicating that small scale-motions may not be completely captured by aircraft Doppler radar.

1.2.2 Landfalling Observations

In order to study features with sub- kilometer spatial scales, it is often necessary to focus on landfalling systems that can be observed with higher resolution instrumentation, such as WSR-88Ds (e.g. Morrison et al. 2005) and scanning X-band (e.g. Knupp et al. 2006). Research on these small-scale features has mostly been carried out over the last decade, and has been focused on finescale bands (e.g. Gall et al. 1998) and

hurricane boundary layer (HBL) rolls (e.g. Lorsolo et al. 2008).

Finescale bands are smaller in size than typical rainbands, with horizontal scales of about 10 km across and wavelengths of 10 km. They move with the tangential wind and spiral outward in a clockwise fashion (Gall et al. 1998). These small-scale features are similar to HBL rolls, although they extend up to 5000-6000 meters AGL, a factor of ten higher than the 600 meter mean depth observed in HBL rolls by Lorsolo et al. (2008). One theory is that these finescale bands are triggered by a combination of Kelvin-Helmholtz instability and HBL shear (Romine and Wilhelmson 2006). The HBL shear could be due to the reversal of radial winds at the top of the HBL (Nolan 2005) as seen in the various hurricane motion schematics of crossband-height flow. Model results suggest that finescale bands are more likely to form in strong storms, with the banding increasing as the storm approached land due to increased vertical wind shear (Romine and Wilhelmson 2006).

On an even smaller scale than finescale bands, recent studies have observed sub-kilometer scale horizontal roll vortices, suggesting that the HBL is predisposed to form rolls. These rolls, which have also been found in non-hurricane boundary layers (e.g. Weckworth et al. 1997; Weckworth et al. 1999), can influence the transfer of momentum across the boundary layer and at the surface as well as enhance the fluxes of heat and water vapor. Lorsolo et al. (2008) found HBL rolls to be present in both Hurricane Isabel (2003) which was a stratiform case, and Hurricane Frances (2004) which was a convective case. Although every case examined by Lorsolo et al. (2008) showed HBL rolls, in Isabel the rolls were near-linear structures, while in Frances they were more

cellular. In over 90% of the cases, the rolls features were oriented within 20^{o} of the mean near-surface wind direction.

Morrison et al. (2005) used WSR-88D data during four hurricane landfalls to show alternating bands of enhanced and reduced residual radial velocities aligned with the mean wind direction, which they also suggest are HBL rolls. These rolls have a mean depth of 660 meters AGL and mean wavelength of 1450 meters, though wavelengths were found to extend up to 3000 meters and depths up to 1500 meters in some cases.

HBL rolls have been found both in the rainbands and in stratiform regions of storms. Wurman and Winslow (1998) found peak wind gust variability on time scales of 2.5 seconds below 500 m, alternating on and off with calmer winds near the point of landfall of Hurricane Fran (1996). They propose that these are HBL rolls with wavelengths between 100-600 meters superimposed on larger-scale flow patterns. The rolls form parallel to the wind shear in environments that are convectively unstable. A major question in the scientific community is what is the contribution of these rolls to the turbulent fluxes and how to parameterize them in numerical models (Foster 2005).

One final area of interest related to landfalling hurricane rainband observations relates to their potential to generate tornados. The strong amount of vertical wind shear in the HBL has been shown to “spin up” lower atmospheric winds, which can couple with updrafts to form tornadoes (Spratt et al. 1997). Novlan and Gray (1974) found this to be especially true when the vertical shear was large from the surface up to 1500 meters AGL. Gentry (1983) found that the majority of hurricanes and about 60% of tropical storms spawn tornados. As storms move over land, the likelihood of tornados increases due to the increased surface friction (Baker et al. 2009). As tornados can cause extensive

damage to structures, it is important to understand the typical wind profiles in the lowest 2000 meters to more accurately predict the conditions that are likely to spawn tornados.

1.2.3 Wind Profiles

The highest resolution observations of wind speed profiles in hurricane rainbands come from dropsondes (e.g Franklin et al. 2003; Schwendike and Kepert 2008; Zhang et al. 2011) which have become very prevalent in oceanic flights in the past decade. These sondes are released from aircraft typically flying at 700 hPa, and fall to the surface collecting measurements with a vertical resolution of 5-7 meters. Dropsondes allow for the study of the HBL with in-situ measurements, something that is challenging to do with aircraft, as they cannot fly low enough. In particular, aircraft cannot measure HBL winds over land, which is an important area to understand the wind variations with height that can impact tall buildings. Unfortunately, dropsondes use is less frequent over land than over water, so detailed wind profile measurements over land must be collected using another data source, such as the VAD technique.

To evaluate mean sonde profiles, Franklin et al. (2003) composited 630 sondes over 2 years, shown in Figure A4. Their composite of outer rainband sondes shows a low-level wind max at 1 km, with a logarithmic profile in the mean wind below 300 meters AGL (Figure A5). They also found a ratio of near-surface (10 meter) winds to 700 hPa winds of 0.78 in nonconvective storm profiles.

Similarly, Zhang et al. (2011) composited 790 sondes in 13 hurricanes and found a clear separation between thermodynamical and dynamical HBL heights. The dynamical HBL height decreased with decreasing radius to the storm center. The thermodynamic

HBL height also decreased with decreasing radius to the storm center, but was about 400 meters shallower than the dynamical HBL height within the radius of maximum winds (RMW).

Schwendike and Kepert (2008) compared sondes by storm quadrant for Hurricanes Danielle (1998) and Isabel (2003). They found substantial variability in the structure of the HBL, with a horizontal wind maximum at 500 meters AGL near the storm eyewall that rises to 1500 meters AGL at 100 km radius. They also found a surface (40 meters AGL)-to-aloft (2000 meters AGL) ratio ranging from 0.6-0.7 in the outer core. While the development and frequent use of dropsondes has significantly increased the understanding of wind structure in hurricanes, they can drift while falling as they are blown around by the strong wind speeds, so the information they provide is not a true representation of a vertical profile in a rainband but rather a trajectory profile.

Other ways to retrieve wind profile measurements in hurricane rainbands include wind profilers (e.g. May et al. 1994) and the VAD technique, which is described in more detail in Section 2.2.1. Wind profilers typically have 200-500 meter vertical resolution (e.g. May 1996). The VAD technique provides horizontal wind measurements with a mean vertical resolution of 7 meters, making it comparable to the vertical resolution of dropsondes and radiosondes.

1.2.4 Modeling Studies

In addition to remote and in-situ observations, hurricanes can also be studied using numerical models. An early simulation by Jones (1986) showed model rainbands for 288 hours at the end of a 13-day experiment. These rainbands were seen to be forced

by quasi-stationary spiral bands of upward motion occurring in the low troposphere (~800 hPa level) around the moving vortex. The rainbands contained convective events lasting between 0.5-1 hour with strong subsidence capping the convection. In the model, this subsidence always occurred over rainbands in front of the vortex, but not always behind it. The rainband region showed a trend towards stabilizing as time progressed, and as static stability increased, rainband activity also increased. Jones (1986) hypothesized that mesoscale events may control rainband activity. Jones also showed an asymmetry in radial winds with height in the rainbands. More recent modeling studies on rainband motions have shown results similar to the schematics of rainband motion based on observations (e.g Barnes et al. 1983; Powell 1990a; Hence and Houze 2008). Schwendike and Kepert (2008) modeled the HBL winds in Hurricanes Danielle (1998) and Isabel (2003) to show that the strongest azimuthal winds occur near the top of, but still within, the HBL. Schwendike and Kepert (2008) analyzed various regions of the storm and found the strongest radial inflow in the right front quadrant of Hurricane Danielle and in the left front quadrant of Hurricane Isabel. Franklin et al. (2005) used a Tropical Cyclone Model (TCM3) with explicit cloud microphysics to study tropical cyclone rainbands, and found that their model was able to capture many of the features observed in tropical cyclone rainbands, including the updraft cores in the rainbands sloping radially outward with height. They also found that all convective vertical velocity profiles had a maximum in upward motion located at 250 hPa and a sharp gradient from the surface to about 850 hPa. Chen and Yau (2001) used the high-resolution PSU-NCAR non-hydrostatic mesoscale model (MM5) to examine the role of potential vorticity in sustaining rainbands and overall storm strength. They found potential vorticity (PV)

anomalies at the top of the HBL due to the interaction with friction. These PV anomalies act to produce upward motion that gives rise to inner bands. The PV interaction with the top of the HBL is similar to that described by Nolan (2005) and can influence the development of finescale bands and HBL rolls.

Modeling studies can also be used to examine the responses of hurricane rainbands to various types of forcing. A theoretical modeling study of hurricane wind field response to rainband heating was recently presented by Moon and Nolan (2010). Their results show characteristic flow structures of purely convective rainbands, purely stratiform rainbands, and mixed rainbands. When viewed along-band, all rainband types were seen to have an overturning secondary circulation with a secondary wind maximum on the radially outward side of the rainband. All rainband types except purely convective rainbands had mid-level radial inflow along the rainband that descends to the surface. The convective rainbands frequently had stronger secondary overturning circulations associated with upward motion, while the stratiform rainbands were the main driving force behind the descending mid-level radial inflow. Upward vertical motions were found to be strongly coupled with heat sources within the rainband. As modeling techniques continue to evolve, higher-resolution understanding of hurricane rainband processes can continue to advance, especially of smaller-scale features such as finescale bands (e.g Romine and Wilhelmson 2006) and HBL rolls.

1.2.5 Summary

Previously, observations of tropical cyclone rainbands over land were limited due to widely spaced coastal radars, the inability to fly at low levels over land, and the small

possibility of a storm hitting a specific region in a given year. For the past two decades however, almost every mile of the United States coastline has had coverage by a WSR-88D, so storms passing near or over land can be studied (e.g Skwira et al. 2005; Lorsolo et al. 2008). Unfortunately, the likelihood of a storm passing close enough for rainband analysis is still limited. Though several previous studies have examined rainbands using WSR-88Ds (e.g. Spratt et al. 1997; Blackwell 2000; Stewart and Lyons 1996), and through VAD techniques (e.g. Kim et al. 2009), this work evaluates the wind profiles during stratiform rainbands at a high resolution by combining WSR-88D Level II Data with the VAD technique, similar to Marks et al. (1999) and Morrison et al. (2005). With this technique, the mean vertical resolution of the VAD observations is about 7 meters, which is comparable to that of 5 meters by Franklin et al. (2003), and 6 meters by Schwendike and Kepert (2008) and Zhang et al. (2011) using dropsondes. While the VAD technique retrieves winds from a volume scan, the resulting horizontal winds are representative of a much larger area rather than a point measurement. In stratiform conditions, this technique is preferable to observations from dropsondes, which can drift significantly with the azimuthal wind in high wind regimes (Aberson 2008). The increased resolution from dropsondes and the VAD analysis is significantly higher than the 500 meter vertical resolution previously seen in aircraft radar data (Hence and Houze 2008) and 200 meter vertical resolution seen in landfalling wind profiler studies (May et al. 1994), allowing for an improved understanding of wind structure.

1.3 Scientific Objectives

The main goal of this dissertation is to improve the understanding of the processes that occur within the vertical structure of tropical storm and hurricane rainbands over land, with a strong focus on creating a high-resolution (< 10 meters vertically) representation of the wind motions and comparing observations over land to those over water. An additional goal is to use case studies from this work to conduct educational research with a group of undergraduate meteorology majors.

The specific scientific goals and questions to be addressed in this study are:

I. Characterize the vertical structure of the rainband
    a. Where are the wind maxima and inflection points located?
    b. What are the differences in dynamics between rainbands?
    c. How does the wind speed vary in the surface layer?
    d. How do wind profiles change before, during, and after a rainband passage?

II. Study the small-scale vertical motions and turbulence
    a. How do the vertical motions vary in a rainband?
    b. What is the relationship among surface drop size distribution (DSD), rainrate, and draft structures?
    c. How do convective rolls force circulations above the hurricane boundary layer?

III. Investigate the best way to use field data in the classroom
    a. Does an inquiry-based learning approach using real-world data enhance students' understanding about the nature of science or improve their attitude

towards science?

b. Is this approach effective at conveying content knowledge in an undergraduate meteorology classroom?
c. Is this approach more or less effective at improving content knowledge growth and retention and/or attitude towards science than a traditional approach?
d. What are the challenges associated with an inquiry approach and a traditional approach and how can they be overcome?

This study represents one of the first times that a wide variety of instrumentation were able to capture data from multiple landfalling systems. While many rainband observations have been made in the past, the variety of radars operating at different wavelengths in this analysis allows for the examination of the small scale turbulence and fluxes in the rainbands in the HBL, and the examination of wind profiles at a very high vertical resolution from 65 meters to 6550 meters AGL. It is important to characterize the low-level wind patterns in rainbands because they are thought to have the largest impact on human activity as a storm makes landfall. It is also important to understand the vertical variability seen in these seemingly benign stratiform rainbands, as they could still contain turbulent features. Finally, educational literature has paid very little attention to the use of actual data in higher education classrooms, and the data collected in this study provides a unique opportunity to examine two potential teaching approaches to see if one increases student learning and attitude toward science more than the other.

Chapter 2: Experiment Description and Data Sets

This chapter describes the experiment location, duration and instrumentation used for data collection. Section 2.1 provides details about the experiment location and timing, and Section 2.2 describes the instrumentation. The data sets used for rainband analysis are presented in Sections 2.3 and 2.4.

2.1 Experiment Description

The original objective of CPS (Cloud Precipitation Study) was to characterize and understand the properties of the small scale vertical velocity and drop size distribution structure of thunderstorm anvils and fair weather cumuli. The field experiment took place in South Florida over 8 weeks in August and September 2008, a time chosen because summertime sea breeze fronts often converge over the center of the peninsula, causing strong afternoon storms. However, this time of year is also in the middle of the Atlantic hurricane season, and four tropical cyclones passed near the vicinity of the field site. This study focuses on the observations of the rainbands during three of the storm passages. This field experiment was a collaborative field effort between the University of Miami Rosenstiel School of Marine and Atmospheric Science (RSMAS), the National Corporation for Atmospheric Research Earth Observing Laboratory (NCAR EOL), and North Carolina State University (NC State).

The experiment was based at the University of Miami South Campus (CSTARS) in Southwest Miami, Florida, located about 15 miles west (inland) of Biscayne Bay at 25.61^{o}N, -80.39^{o}W (see Figure 2.1). A back-up generator system allowed for continuous operations during any disruption of the commercial power grid during stormy conditions.

The terrain in South Florida is flat, with no locations higher than 10 meters elevation. The CSTARS campus is in a residential neighborhood and is surrounded by tall trees, thus the near surface (~10 feet) observations of wind speed are most likely underestimates and are supplemented with wind measurements at 14.5 meters and 18 meters altitude from a nearby tower located on top of one of the CSTARS buildings.

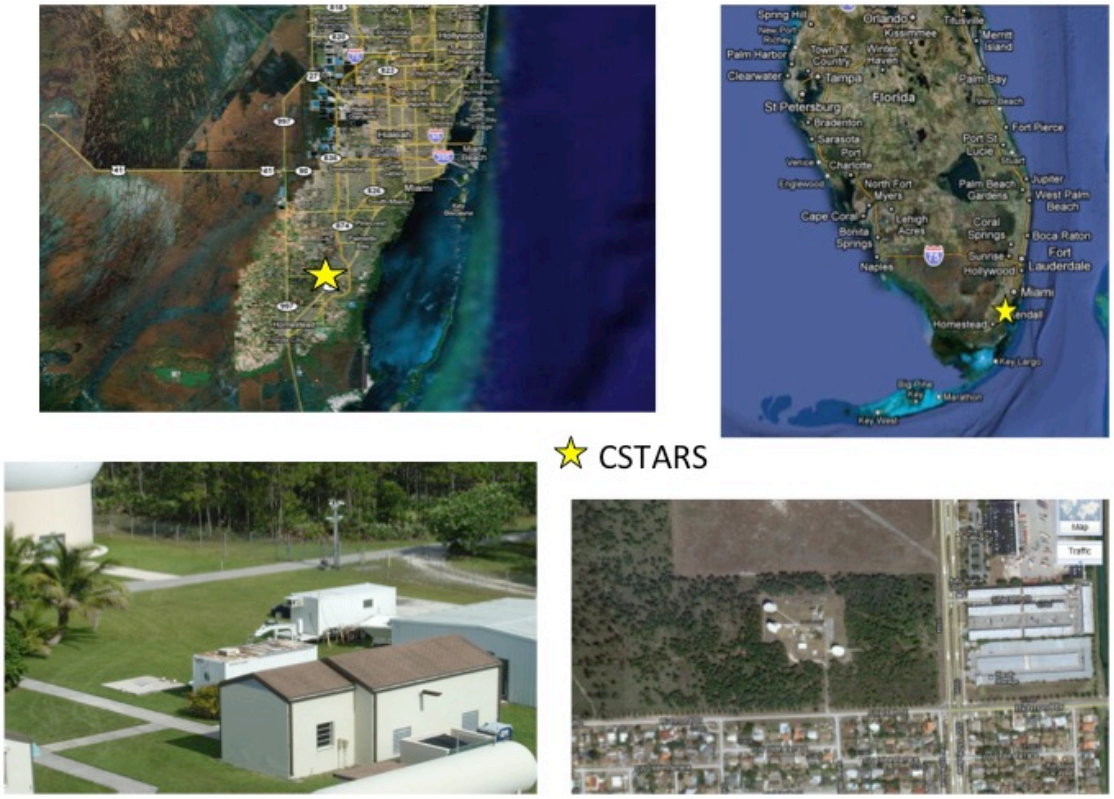

Figure 2.1: Location of data collection at CSTARS. Counterclockwise from upper right: Florida peninsula with CSTARS shown as the yellow star; a closer zoom of Southeast FL with CSTARS location; an overhead view of CSTARS, with the instrument containers from NCAR and UM visible; a birds-eye view of CSTARS. Images from maps.google.com.

2.2 Instrumentation

During this study, multiple wavelength radars were operating, including a vertically pointing X-band radar from RSMAS and a 915 MHz (33 cm) wind profiler (Multiple Antenna Profiling Radar, MAPR) from NCAR EOL that provided high-resolution (1-30 second) vertical mappings of reflectivity, Doppler velocities, and winds in the column above CSTARS. Data from the nearby scanning Miami WSR-88D (KAMX) provided the vertical and horizontal structure of winds and reflectivity. To complement the remote sensing data sets, rawindsonde launches were made up to 3 times daily from the site to provide the thermodynamic and wind profiles. A list detailing the most relevant launch times to rainband passages is given in Table 2.3, and photos of the instrumentation at the field site are shown in Figure 2.2. Surface precipitation drop size distributions were collected with a high temporal resolution (10 second) Parsivel disdrometer provided by North Carolina State University and a lower resolution (1 minute) Vaisala WXT experimental capacity plate rain sensor from NCAR. Other standard meteorological observations are combined with remote sensing data to help create a more complete understanding of tropical cyclone rainbands and their influence on surface conditions.

2.2.1 WSR-88D

The main observing instrument used for wind analysis in this work is the scanning S-Band WSR-88D. Vertical profiles of the horizontal wind are retrieved from the Level 2 WSR-88D KAMX data using a Velocity-Azimuth Display Technique (VAD, Browning and Wexler 1968). This technique involves scanning a complete circle around the radar at

a fixed elevation angle. As the beam rotates, the radar provides an output of the radial velocity, which is plotted as a sine function against the azimuthal angle. The amplitude and phase of the sine curve give the wind speed and direction (respectively) at each range gate. Due to the close proximity of the field site to the KAMX radar (2.8 km to the east), reliable wind information is obtained from the VAD from 65 meters AGL to 6550 meters AGL. The mean vertical resolution is ~ 7 meters, and varies with altitude from a minimum of 2 meters at 65 meters AGL to a maximum of 85 meters at 6000 meters AGL. The VAD scans took about 5-6 minutes depending on the operating mode of the radar, and covered a total volume of ~4,800 km^3. At the highest elevation angle of 19.5^o, an area of 51 km^2 was scanned at 45 meters above radar level (20 meters), while an area of 1058 km^2 was scanned at 6500 meters above radar level.

Figure 2.2: Photos of instrumentation from the field site at CSTARS. The picture on the left shows the wind profiler (MAPR) in the center of the image, the NCAR container to the right, and the UM container with the X-band and W-band antennas in the background. The right image shows scientists preparing to launch a rawindsonde in front of the NCAR container.

Successful application of the VAD technique insures that only wind structures comparable to and longer than the diameter of the range circle of the WSR-88D are included in the data set. This technique removes high-resolution structures, making it

ideal for studying stratiform and homogenous precipitation fields around the radar site. Thus, Chapter 3 of this study focuses only on stratiform periods during the rainbands in order to describe the vertical profiles of wind speed in the stratiform rainbands.

As described above, the VAD technique involves using Level II WSR-88D data to convert radar-relative winds into horizontal winds with height. By making the assumption that conditions are close to homogenous in the radius of the radar beam, the VAD output essentially converts a volume scan into an average vertical profile. This technique provides high-resolution wind speed and direction profiles with each complete scan, about once every 5-6 minutes. These VAD wind profiles over stratiform time periods are averaged for each rainband case, and then smoothed in the vertical with a 5-point running mean prior to analysis.

Although the VAD technique is useful for providing high (~7 meter) vertical resolution winds, data issues can arise due to the nature of the data collection process. For instance, the time lapse in a complete scan may miss important short-lived features lasting less than 5 minutes. Due to the spreading nature of the beam as it moves away from the radar, shorter wavelength features near the radar may also be missed. Also, gaps in the scanning circle can exist. The tilt angles of the scanning beam may go through just a portion of an atmospheric feature rather than the entire feature, which could skew the averaging. Additionally, the radar beam undergoes refraction at the melting level, which could cause a bias in the data that should be taken into consideration when evaluating wind speed maxima at this height. Finally, though the average fall speed of droplets is removed through the VAD technique, it is likely that changes in drop sizes would lead to changes in fall speed that still remain in the data set.

An example of smoothed wind profiles for a stratiform period in a rainband during Tropical Storm Fay is shown in Figure 2.3, and includes calculation of mean radial and tangential wind profiles using the central storm location from the closest time period in the National Hurricane Center's North Atlantic Hurricane Database, or HURDAT (Stewart and Beven 2009) which are discussed in Section 3.3. Figure 2.3 shows mean profiles of horizontal wind speed, direction, radial wind, and tangential wind from VAD analysis during the 18-minute Stratiform Band 9b. The mean horizontal wind profile shows a log-wind regime below 500 meters AGL, and a low-level wind maximum between 1000-2000 meters AGL, with a secondary wind maximum around 4500 meters AGL, which is the height of the melting level. The wind direction profile shows a general SSE direction (direction of rainband approach), with veering winds with height. The radial profile shows low-level radial inflow below 500 meters, a reversal to radial outflow at 3000 meters, and a secondary radial inflow just above the melting layer. The tangential wind profile is similar in structure and strength to the mean wind profile, indicating that the tangential component dominates the mean wind. Although the VAD technique has a mean vertical resolution of 7 meters and can measure the small-scale variations in wind and reflectivity during homogenous precipitating conditions, the MAPR is useful because of its ability to measure clear-air velocities through Bragg scattering. By combining these data sets, rainband wind events can be compared to time periods before and after the rainbands pass over the experiment site, of which a case example is shown in Section 3.4.2.

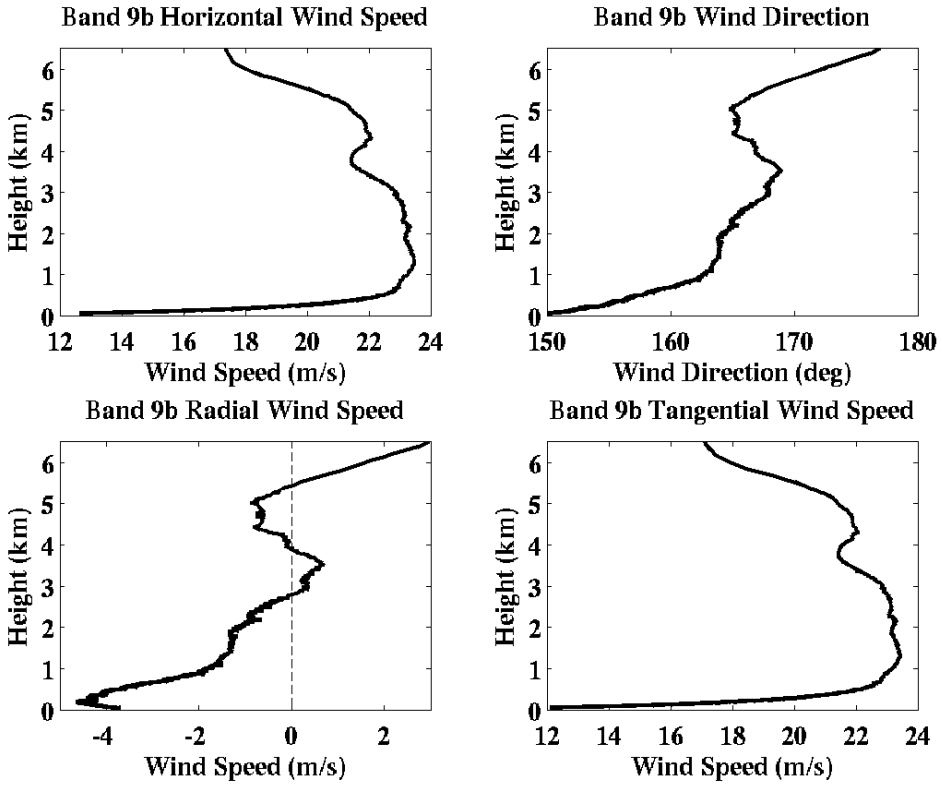

Figure 2.3: Mean profiles of Stratiform Case 9b horizontal wind speed (upper left), wind direction (degrees east of north, upper right), radial wind speed (lower left) and tangential wind speed (lower right), produced using VAD Technique of KAMX Level II data.

2.2.2 MAPR

One of the other main observing instruments used in the wind analysis is the MAPR (for details see Cohn et al. 2001). The MAPR operates by using three (or four) vertically pointing beams arranged in a triangular (or square) pattern. A single vertical beam transmits, while the diffraction pattern formed by energy backscattered from the atmosphere is received using three or more spatially separated receiving antennas. As air flows over the beams, atmospheric features are tracked across the receivers and the time lapse between spaced antennas gives wind measurements at each height. The MAPR has a time resolution of 30 seconds, which is considerably faster than the 10-15 minutes

required by traditional Doppler beam swinging wind profilers (Cohn et al. 2001). During CPS, the MAPR was operated with a variable range resolution between 100-200 meters. The lowest level that the MAPR can accurately observe is about 400 meters AGL, and depending on the operating mode it collected data up to 4.5 or 10.2 kilometers AGL. Operating at a wavelength of 33 cm, the MAPR attenuation by rain is limited and allows for reflectivity, Doppler velocity, and turbulence intensity (spectrum width) observations with height.

The MAPR data were made available in several formats, including unprocessed moments (30-second averaged), and post-processed 5- and 30- minute averaged moments. The longer time scale average files are not useful during the rainbands because the air motions typically exceeded the post-processing thresholds and the data were removed. This means that the majority of the wind profiler analysis is done using the 30-second moment data. The exceptions to this are the periods before and after the rainband passage. Although the MAPR can collect data in clear air conditions, it is limited in how high it can provide information without any targets to backscatter from. This means that the higher resolution MAPR data set needs to be supplemented with the averaged moment MAPR data sets in order to fill in upper air wind motions for the time periods before and after rainband passage in order to accomplish scientific goal Id. This is done in Section 3.4.2.

Although the MAPR is useful for providing profiles of wind speed and direction with height, it has had limited previous usage in conditions as rainy and windy as the rainbands of this study. As such, an unexpected issue was discovered where it appears that the vertical rainfall rate may be contaminating the horizontal wind speeds. This is

described further in Section 2.3.3, and comparison profiles of MAPR wind speeds, VAD-retrieved wind speeds, and rawindsonde wind speeds are presented in Figure 2.6. This contamination appears to bias the tangential and horizontal wind components by over 5 ms^{-1}, which is an issue that should be kept in mind when comparing the MAPR winds to other instruments. Examples of MAPR reflectivity and velocity are shown in Figures 2.7c and 2.7d, and an example of MAPR wind components is shown in Figure 4.2.

2.2.3 X-Band

Observations from the vertically pointing X-band radar data were intended to be used with the WSR-88D VAD and MAPR observations. Unfortunately, the radar receiver saturated under the rainband conditions, making the reflectivity data less useful. The Doppler velocities from the X-band appear to be unaffected by the saturation and represent the sum of the precipitation and the air velocity. In this study the X-band data are used to determine starting and ending times of the stratiform periods during rainbands, for establishing the level of the melting layer, and for vertical velocity information. The X-band data has a vertical resolution of 60 meters and a temporal resolution of 1 second. An example of X-Band signal-to-noise ratio and vertical velocity is shown in Figure 2.7a.

2.2.4 Rawindsondes

Wind, temperature and moisture profiles are retrieved up to three times a day with Vaisala RS 80-15 GH Rawindsondes. Table 2.3 details sounding occurrences closest to rainband periods, although on several occasions rawindsondes were not launched due to logistical challenges related to the tropical storm conditions in the region. An example of

a wind speed profile from a sounding on August 17, 2008 at 1700 UTC is shown in Figure 2.6 (red line). Although the sounding profile is treated as a point measurement, it is important to remember that the sounding drifts as it rises, and may have been blown out of the rainband completely. For this reason, the sounding profile should be more comparable to the VAD wind profile (volume scan) than the MAPR profile (point measurement). The one-second temporal resolution of the sonde allowed for high resolution (average of 3.3 meters) vertical data collection, but the transient nature of the balloon implies that it may only capture pieces of atmospheric features, or may miss them entirely.

2.2.5 Surface Instruments

Surface wind observations were obtained at three heights above the ground level. The lowest wind speed information comes from the NCAR Vaisala WXT-520 at 10 feet (3 meters), with a one-minute temporal resolution. Although this is the standard height for surface observations, CSTARS was surrounded by trees about 6 meters high, which reduced the wind speeds measured near the ground to levels much lower than typical open exposure over land. For this reason, wind observations from RM Young sensors located at heights of 14.5 and 18 meters on a tower at the CSTARS site are used to provide wind speeds, gusts, and wind direction data at a two-minute temporal resolution.

Ground-based measurements of particle size and fall speed were obtained using a Particle Size and Velocity (Parsivel) disdrometer (see Yuter et al. 2006 for details). This 10-second data set was post-processed and averaged into a one-minute temporal resolution by NC State. The post-processing algorithm often filtered out all data under the

atypical rainband conditions, with 34% of stratiform rainband data removed. The remaining data set provides information about rainrate, reflectivity, particle count, liquid water content, and volume-weighted mean drop diameter (D_m).

Additional surface drop size information was provided by the Vaisala WXT experimental capacity plate rain sensor from NCAR. This one-minute resolution data set provided 8 drop size bins (1 mm, 1.25 mm, 1.6 mm, 2 mm, 2.3 mm, 3.2 mm, 4 mm, and 5 mm), though the instrument may not be as sensitive to the smaller bin sizes (William Brown, personal communication).

2.3 Data Set

The four storms influencing the CPS site were Tropical Storm Fay (8/17-8/22), Hurricane Gustav (8/30-8/31), Tropical Storm Hanna (9/5), and Hurricane Ike (9/9-9/10). Although none of these storms' eyewalls passed over CSTARS, rainbands from the majority of the storms did pass over the field site. Careful analysis of NWS WSR-88D loops coupled with vertically pointing X-band data shows 20 rainbands during Fay, 2 during Gustav, none during Hanna, and 2 during Ike, for a total of 24 distinct rainbands. Because of this large data set, rainband data was collected during storms of varying strength (tropical storm to Category 4 hurricane), rainbands at distances from 100-800 km from the storm center, rainbands approaching the site from a wide range of directions, and rainbands lasting over the field site for anywhere from 15 minutes to 3.5 hours depending on whether they were observed cross-band or along-band, as shown in Figure 2.4.

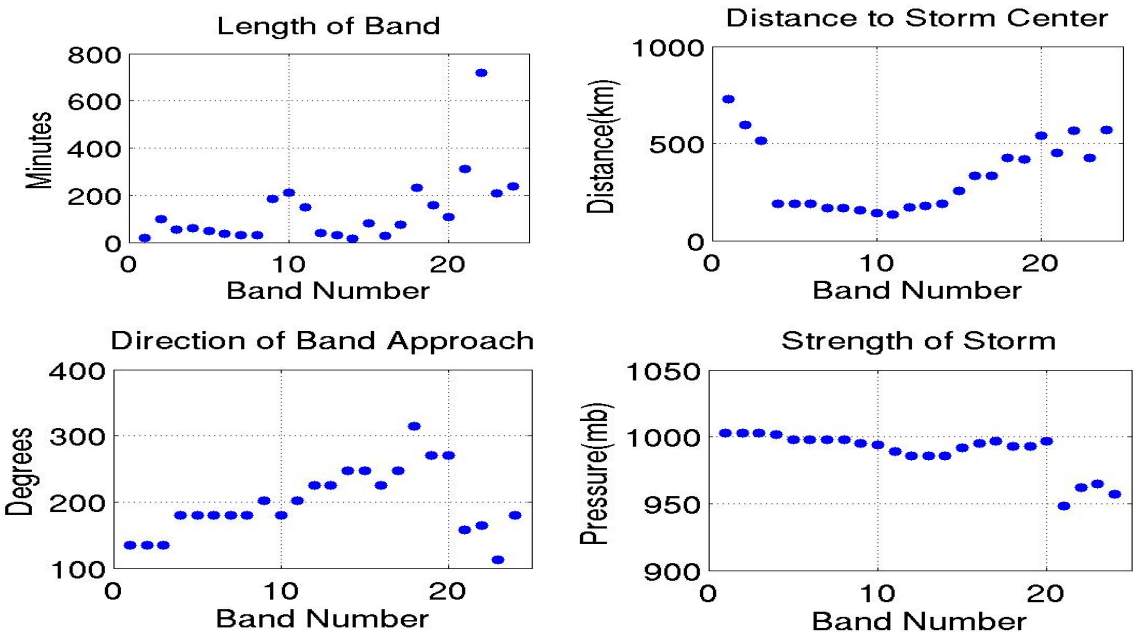

Figure 2.4: Clockwise from upper left: Statistics of rainband duration, distance to eye of storm, direction of rainband approach, and strength of storm. Rainbands are numbered 1-24 in order of occurrence. Storm statistics are taken from NHC best track data.

Table 2.1 shows a detailed summary of basic rainband and storm statistics during each of the 24 distinct rainbands. Rainband start and stop times are included, and it can be seen that while the majority of the rainbands were observed in the afternoon and early evening local time, rainband data were captured over a variety of times, durations and conditions.

2.3.1 Storm Descriptions

This section uses the Tropical Cyclone Reports from the National Hurricane Center (Berg 2009; Beven and Kimberlain 2009; Stewart and Beven 2009) to describe the basic storm characteristics of the three storms in which rainbands were sampled, including the best track and meteorological statistics. Gustav was the strongest storm

sampled, with maximum wind speeds around 120 mph during the two rainband passages. Ike was a weak hurricane at the time of rainband observations, while Fay remained a strong tropical storm throughout its duration. Due to Fay's path across Florida, several rainbands were sampled under a wide variety of conditions, both near and far from the center of the system. Tracks from the 3 storms are shown in Figure 2.5, with each box representing the center of the storm at 0000 UTC each day. Complete storm tracks for each storm are shown in Appendix A Figures A6-A8.

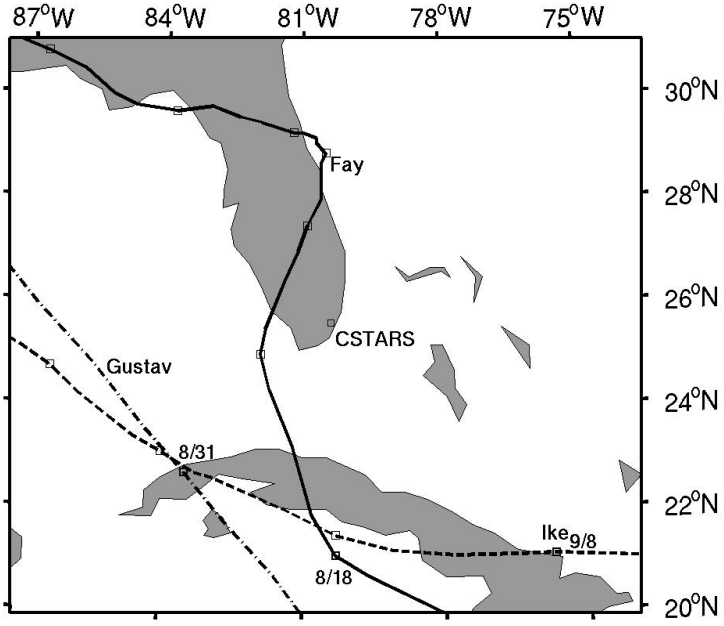

Figure 2.5: Map of Florida and Cuba. The marker represents the location of vertically pointing instruments from the CPS experiment at the University of Miami South Campus (CSTARS). The tracks of the three storms with rainbands sampled at CSTARS are also shown. Storm tracks are center positions from HURDAT. The symbols on the tracks are at 24-hr intervals beginning at 00 UTC each day.

Table 2.1: A summary of characteristics observed during each of the 24 rainbands. Storm information is from NHC best track data set. Total rainfall information is from the WXT, which had operating issues during Bands 20 and 21.

Storm	Band #	Date	Start time (UTC)	End time (UTC)	Total Rain-band Length (min)	Direction (from)	Total Rain (mm)	Storm Press-ure (hPa)	Max Sust. Wind Speed (kt)	Dist. To storm center (km)
Fay	1	8/17/08	9:15	9:35	20	SE	1.49	1003	45	729.5
Fay	2	8/17/08	16:20	18:00	100	E	0.84	1003	45	597
Fay	3	8/17/08	20:00	21:54	54	SE	2.11	1003	45	513.2
Fay	4	8/18/08	16:45	17:45	60	S	5.34	1002	50	190.6
Fay	5	8/18/08	19:30	20:20	50	S	5.98	998	50	189.6
Fay	6	8/18/08	20:40	21:18	38	S	9.06	998	50	189.6
Fay	7	8/18/08	22:18	22:48	30	S	0.32	998	50	166.9
Fay	8	8/19/08	0:13	0:44	31	S	0.30	998	50	166.9
Fay	9	8/19/08	1:21	4:36	185	S/SSW	4.02	995	50	156.1
Fay	10	8/19/08	5:00	8:30	210	S	15.67	994	50	142.6
Fay	11	8/19/08	9:00	11:30	150	S/SSW	5.86	989	50	135.6
Fay	12	8/19/08	17:00	17:40	40	SW	2.38	986	55	170
Fay	13	8/19/08	18:30	19:00	30	SW	5.73	986	55	180.2
Fay	14	8/19/08	19:32	19:47	15	W/SW	5.23	986	55	190.4
Fay	15	8/20/08	6:25	7:46	81	NW/SW	9.61	992	45	254.7
Fay	16	8/20/08	14:27	14:54	27	SW	0.98	995	45	332.9
Fay	17	8/20/08	17:24	18:39	75	W/SW	11.68	997	45	332.9
Fay	18	8/21/08	17:12	21:05	233	NW	0.01	993	50	425.6
Fay	19	8/21/08	22:30	01:09 (8/22/08)	159	W	22.23	993	50	417.9
Fay	20	8/22/08	19:12	21:00	108	W	n/a	997	40	541.9
Gustav	21	8/31/08	1:24	6:36	312	S/SE	n/a	948	120 *Cat4	452.6
Gustav	22	8/31/08	9:00	19:00	720	S/SSE	15.16	962	105 *Cat3	564.9
Ike	23	9/9/08	15:26	18:54	208	E/SE	12.13	965	70 *Cat1	427.4
Ike	24	9/10/08	15:06	19:03	237	S	0	957	80 *Cat1	568.3

Fay

Fay was a long-lived tropical storm that made eight landfalls – including a record four landfalls in Florida – and produced torrential rainfall that caused extensive floods across the Dominican Republic, Haiti, Cuba, and Florida. Fay became a tropical depression on August 15, 2008 just west of the northwestern tip of Puerto Rico. The depression moved westward and made landfall in the Dominican Republic. Despite being over land, the system strengthened to a tropical storm based on flight-level wind information obtained from Air Force Reserve Unit and NOAA reconnaissance aircraft. After leaving Haiti, the tropical storm continued its westward trek and moved over the Windward Passage, then turned west-northwestward and strengthened slightly under a favorable upper-level wind flow pattern, before it made landfall along the south-central coast of Cuba. After crossing over Cuba, Fay emerged over the Straits of Florida and encountered moderate southwesterly vertical wind shear and dry mid-level air, which inhibited significant strengthening. Fay continued traveling north-northwest at 12 mph until making landfall near Key West, Florida at 2030 UTC on August 18th. After passing north of Key West over the warm waters of Florida Bay, data from land-based WSR-88D Doppler radars and reconnaissance aircraft indicated Fay was becoming better organized as the vertical wind shear began to decrease. The storm made landfall along the southwestern Florida coast between Cape Romano and Everglades City at 0845 UTC 19 August with 55 knot winds. Shortly after landfall, a well-defined eye feature developed in both satellite and radar imagery. As the eye of Fay moved northeastward across the wetlands of the Florida Everglades toward Lake Okeechobee, Fay had maximum winds of 65 mph, and a wind field of tropical storm strength winds extending 175 miles.

Fay steadily weakened as it continued to move northeastward until the center reached the Atlantic waters off the east-central Florida coast late on the 19th. Fay slowed substantially to a northward forward speed of 3-4 knots as the cyclone skirted the coastal region near Cape Canaveral. Convective rainbands continued to develop and persist inland over the majority of the Florida Peninsula. The slow forward speed of Fay allowed heavy rain elements to 'train' across the same areas for several hours, which allowed for the sampling of the same rainbands for several hours. The majority of the 20 rainbands sampled during Fay occurred between August 18th and 21st as the storm first passed south of the field site, then turned north and made landfall to the west (between Cape Romano, FL and Everglades City, FL) before slowly traversing to the northeast over the next few days.

On August 21st Fay turned westward and made its third Florida landfall near Flagler Beach. A general westward motion was maintained across the northern Florida peninsula and cyclone emerged over the extreme northeastern Gulf of Mexico late on August 22nd. Fay made its fourth and final Florida landfall – and eighth overall landfall - just southwest of Carrabelle in the Florida panhandle around 0615 UTC August 23rd. The storm turned toward the west-northwest and weakened to a depression northeast of Pensacola, FL.

Gustav

Gustav formed from a tropical wave that moved westward from the coast of Africa on August 13, 2008, and became a tropical depression on August 25th northeast of the Netherland Antilles. From there it rapidly intensified to become a hurricane early on August 26th. Gustav made landfall on the southwestern peninsula of Haiti, then traveled

over westward Jamaica and moved northwestward to make landfall in the Cayman Islands. Gustav again rapidly intensified to a Category 4 as it hit western Cuba on August 30th.

Gustav weakened over Cuba, and it continued to weaken over the Gulf of Mexico on August 31st as it moved northwest at 15 mph. An upper-level trough west of Gustav caused some southerly vertical wind shear, and satellite imagery suggested that mid- to upper-level dry air became entrained into the cyclone. This combination appears to have prevented strengthening over the warm Gulf waters as the storm passed far to the west of the field site and two rainbands pass over the field site. However, the hurricane grew in size as it crossed the Gulf. On August 31st, tropical-storm-force winds extended roughly 175 miles from the center in and hurricane-force winds extended roughly 70 miles from the center. Gustav made its final landfall near Cocodrie, Louisiana, around 1500 UTC on September 1st with maximum winds near 90 knots (Category 2).

Ike

Ike was a long-lived Cape Verde hurricane that caused extensive damage and many deaths across portions of the Caribbean and along the coasts of Texas and Louisiana. Ike originated from a well-defined tropical wave that moved off the west coast of Africa on August 28th and became a depression on September 1st, then quickly strengthened to a tropical storm that same day and then gradually intensified over the next two days as it moved west-northwestward over the tropical Atlantic. Ike became a hurricane on September 3rd when it was centered about 600 nautical miles east-northeast of the northern Leeward Islands. Building mid-level high pressure over the western

Atlantic caused the hurricane to turn to the west late on September 4th. The high was strong enough to induce a west-southwesterly storm motion.

Due to low shear, Ike reached a Category 4 status on September 6th as it passed over the Turks and Caicos. Ike made landfall on September 8th in eastern Cuba and then moved northwestward along the southern edge island while losing strength. On September 10th, Ike turned west-northwest and the outer wind maximum started to contract and become the more dominant feature as it moved into the Gulf of Mexico. From there, Ike turned to the northwest, and made landfall on the north end of Galveston Island, Texas, on September 13th. During the time of rainband sampling of Ike, it was moving west-northwest at about 13 mph. Tropical storm force winds extended almost 200 miles from the center and hurricane force winds extended 35 miles from the center on September 9th and 80 miles from the center on September 10th.

2.3.2 Availability of Instrumentation for Rainband Observations

Due to the challenges of operating sensitive instruments in a remote field location, as well as having science personnel on site during tropical storm conditions, there were a few occasions where specific instruments were not able to collect data for certain time periods. Table 2.2 summarizes the operation of the main instruments during the 24 rainbands. Soundings were the most difficult to coordinate with restrictions on personnel hours and maximum wind speed limitations; thus, the availability of upper air profiles during the rainband time periods varies widely. Table 2.3 displays the 12 best sonde launches for use in rainband analysis and their timing in respect to the rainbands. The u and v wind components from the soundings can also be converted to storm-relative

radial and tangential winds using the central storm location and are useful to compare with radial and tangential winds calculated from the wind profiler.

Table 2.2: A list of major instrumentation and their operating capabilities during the 24 rainband passages during CPS.

Instrument	**Technical Specifications**	**Operating Times During Rainbands**	**Measurement**
Ceilometer	Laser Diode	All	Cloud-base height with time
Disdrometer- Parsivel (NC State)	50 cm^2 sampling area	All	Drop size distribution at surface
W-Band Doppler radar (UM)	94 GHz (3.2 mm)- vertically pointing	Bands 23 and 24 only	High-resolution Doppler spectra, cloud and precipitation microphysics and dynamics
Microwave Rain Radar- MRR (NC State)	35 GHz Vertically pointing	All	Cloud microphysical properties
X-Band Doppler Radar (UM)	9.4 GHz (3.2 cm)- vertically pointing	All rainbands except Band 1	Cloud dynamics and precipitation physics
Wind Profiler- MAPR (NCAR)	915 MHz (32.8 cm)	All	PBL 3-D winds, inversion height, clouds
Rawindsonde	Vasiala RS-80 15 GH	See Table 2.3	Atmospheric moisture and wind structure
WSR-88D	S-band 2.8-3.0 GHz (10.0-11.1 cm)	All	Scanning Doppler spectra
Met. Obs and Surface Rain (NCAR)	Capacity plate (WXT)	22.5 out of 24 rainbands (missing half of Band 21 and all of Band 22 during Gustav). Band 20 is missing 40 minutes as well.	Surface rainfall, temperature, humidity, and winds

Table 2.3: A list of rawindsonde launches that occurred close to rainband passages and are most useful for this study.

Date	Launch Time (UTC)	Relationship to Rainbands
8/17	1702	During Band 2
8/18	1359	Stratiform rain before Band 4
8/19	1611	Small rain events in between Bands11 and 12
8/20	1459	At end of Band 16
8/20	2151	After 3 large rainbands (Bands 15,16,17) have ended
8/22	2105	Just after end of Band 20
8/31	1500	Band 22 slowing moving north over site
8/31	1800	Band 22 still moving north over site
8/31	1938	After Band 22 ended
9/09	1501	Just before Band 23
9/09	2008	After Band 23, rain shield just skirting the site
9/10	1509	Before Band 24 (non-precipitating band)

2.3.3 Data Processing

The first challenge of this study was the acquisition, collection and quality control of the various data sets used in this study. The University of Miami Radar Meteorology Group (UMRMG) was the primary investigator for the CPS experiment and was primarily responsible for the preparation, deployment, data collection and real-time processing of the X-band and W-band radars. UMRMG was also actively involved in the operation and data collection of some of the other instruments at the field site, including the MRR and Parsivel from NC State, as well as keeping a log of weather conditions and instrument status. This participation in the experiment provided immediate access to real-time plots from all of the instruments, and to actual data from the X-band and W-band radars, but not from the MRR, Parsivel, rawindsondes, ceilometer, MAPR, and surface instruments. The raw and post-processed data from the MAPR, ceilometer, rawindsondes

and surface instruments were generously provided by Dr. William Brown and other scientists from the National Center for Atmospheric Research (NCAR) Earth Observing Laboratory (EOL). Post-processed data sets from the Parsivel were provided by Dr. Sandra Yuter at North Carolina State University (NCSU), although the post-processing algorithm often filtered out all data under the atypical rainband conditions, with 34% of stratiform rainband data removed.

Despite plans to collect vertically pointing radar data from multiple radars simultaneously, challenges involving faulty instrumentation and unavailability of computers for data processing meant that the W-band radar only operated during Hurricane Ike and only provides backscatter intensity information for the last two of the 24 rainbands. This means that the original goal of using the Mie scattering technique (Kollias et al. 2002) to study drop size distribution throughout the rainbands had to be reevaluated.

One challenge of radar data is that vertical velocity air measurements will be contaminated by the fall rate of any precipitation present. Without an accurate representation of the rainfall rate throughout the HBL it is very difficult to present an accurate mapping of true vertical air motions. Any downward (towards radar) motion seen from vertically pointing radar data is due to a combination of rainfall rate and actual air motions. Rainfall rate can vary based on drop size (see examples in Section 4.3.2 and Figure A9), so it is not possible to completely deconvolve the various components.

Additionally, the fall rate of precipitation may contaminate the MAPR data set. Even though the radar antennas are designed to track the features seen in the backscatter intensity, those features may be influenced by the downward motion of the rain, which

could be causing the overestimation of MAPR wind speeds shown in Figure 2.6. This figure shows mean horizontal winds during a non-rainband lightly precipitating case, and shows that the VAD and sounding winds match well with differences that can be explained due to timing and movement of sonde, while the MAPR overestimates the wind speeds, usually by 5-10 ms^{-1}. In Figure 2.6, bars are shown representing one standard deviation of variance within the 15-minute time period averaged for the MAPR and VAD profiles. Although the sounding profile values do typically fall into the low range of possible MAPR values if variance is included, the large (10 ms^{-1}) variance seen in the MAPR data casts further doubt upon the quality of the MAPR wind speed values.

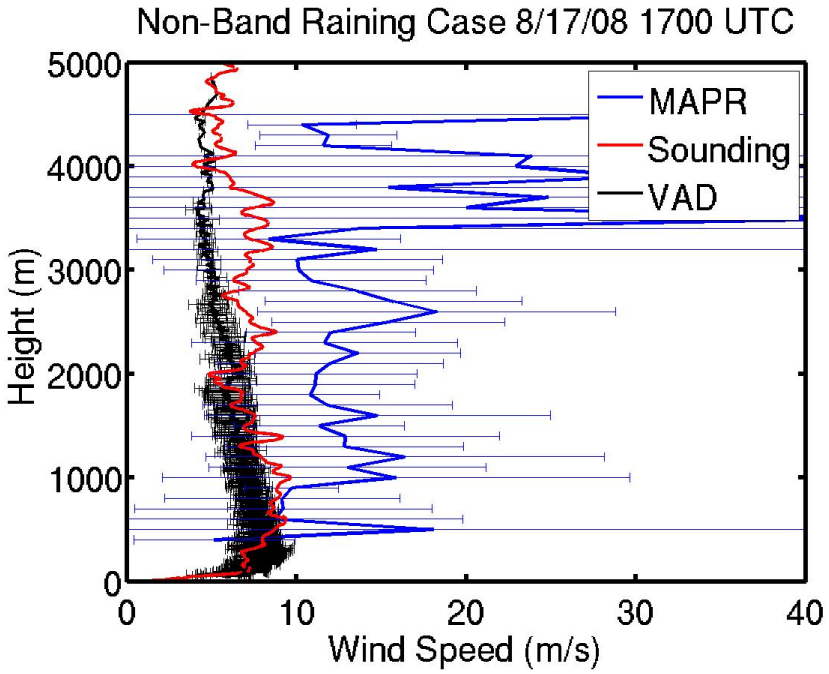

Figure 2.6: Comparison of VAD (black), MAPR (blue), and sounding (red) horizontal wind speeds during a lightly precipitating, non-rainband time period. Bars representing one standard deviation of variance over the 15-minute time period used to calculate the mean VAD and MAPR winds are also shown.

2.4 Stratiform Data Set

Since stratiform conditions are ideal to examine using the VAD technique, Chapter 3 of this study focuses only on stratiform-type periods within the previously described rainbands. The radar returns for all 24 rainbands were subjectively examined to identify the stratiform portions of the rainbands, where an obvious bright band existed around 4500 meters AGL, X-Band signal to noise ratio (SNR) remained relatively constant, and rainfall was light and fairly steady. In total, 14 stratiform-type cases were found, all in outer rainbands (see Table 2.4), and encompass cases lasting from 6 -165 minutes at distances of 135-452 km from storm center. Stratiform cases could either consist of an entire rainband (e.g. Band 4/Case 4a), one stratiform period within a rainband (e.g. Band 11/Case 11a), or several stratiform cases within a rainband (e.g. Band 9/ Cases 9a, 9b, and 9c). Stratiform cases are numbered after the rainband in which they are observed, and lettered to distinguish what order they occurred within the band.

An example illustrating the features of Band 21 and Case 21b is shown in Figure 2.7. Figure 2.7a shows SNR and vertical velocity from the X-Band for the entire five hours of Band 21, which includes the stratiform periods 21a (1:51-4:36 UTC) and 21b (5:30-6:00 UTC). Figure 2.7d shows the same variables, but from the MAPR data set. These two data sets are in excellent agreement with vertical velocity values, and show similar structure in SNR intensity and melting layer height. Figure 2.7c shows a close-up of Case 21b using MAPR data, and is an excellent example of the consistent bright band associated with the melting layer, as well as a fairly uniform rainrate seen in the vertical velocities. Figure 2.7b shows a PPI from the Miami WSR-88D at the start of Band 21b, along with a black arrow showing the mean rainband motion. Figure 2.8 shows the

rainfall rates during 21b, from the Parsivel sensor, which shows variability ranging from 0.5-3.5 $mmhr^{-1}$ on scales of 2-3 minutes. Although this may seem to be significant variability given the homogenous vertical velocity signal shown in Figure 2.7c, the differences between rainrates during this rainband are less than a tenth of an inch per hour, showing that the rainfall observed during this case is very light.

Table 2.4: Stratiform cases during rainbands.

Case #	Date	Start Time (UTC)	End Time (UTC)
4a	8/18/2008	16:40	17:40
5a	8/18/2008	19:54	20:00
9a	8/19/2008	2:06	3:36
9b	8/19/2008	3:53	4:11
9c	8/19/2008	4:18	4:30
10a	8/19/2008	5:09	5:21
10b	8/19/2008	5:27	5:48
11a	8/19/2008	9:54	10:06
18a	8/21/2008	17:42	18:30
18b	8/21/2008	20:00	20:42
21a	8/31/2008	1:51	4:24
21b	8/31/2008	5:30	6:00
23a	9/9/2010	17:27	17:38
23b	9/9/2010	17:51	18:12

For the remainder of this work, the stratiform cases are referred to as Bands (e.g. Band 9b), even if they are not oriented in distinct or entire rainbands. In Chapter 3, the 14 stratiform cases are analyzed by the storm they occurred in, as that groups them by storm

maximum strength of 50 kts for the cases during Fay, 120 kts for the two Gustav cases, and 70 kts for the two Ike cases.

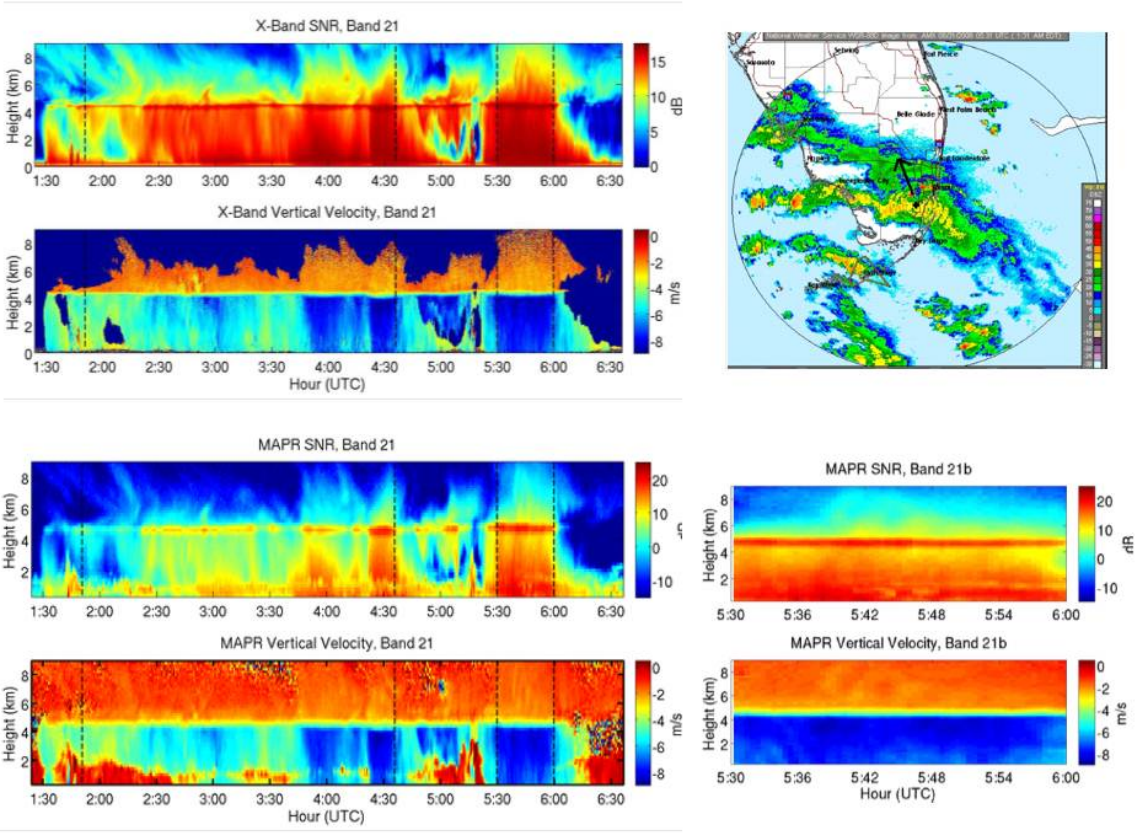

Figure 2.7: Clockwise from top left (2.7a): X-band Signal to Noise Ratio (SNR) and vertical velocity for all of Band 21, from Hurricane Gustav. Stratiform periods 21a and 21b are outlined. 2.7b: WSR-88D image from KAMX at 5:31 UTC, corresponding to the start of Band 21b. Black marker shows CSTARS location and arrow shows rainband motion. 2.7c: MAPR SNR (in dB, top) and vertical velocity (in meters per second, bottom) during Band 21b. 2.7d: MAPR SNR and vertical velocity for all of Band 21. Stratiform periods 21a and 21b are outlined. It should be noted that SNR from the MAPR and X-Band are uncalibrated and are shown to show overall rainband structure, not specific reflectivity values. Negative vertical velocities represent motion towards the radar and are due to a combination of rainfall rate and actual vertical motion.

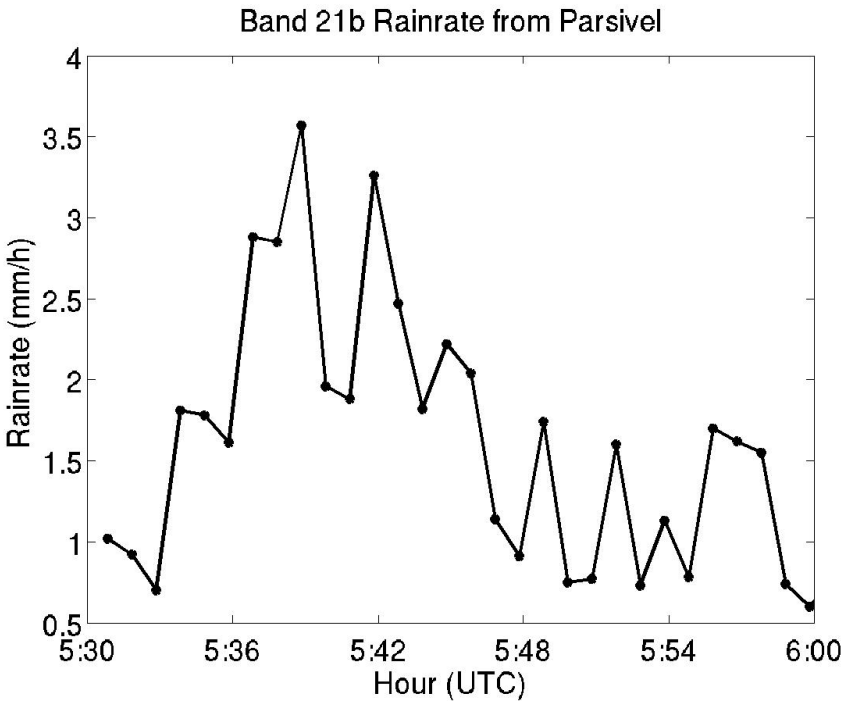

Figure 2.8: Parsivel rainrate ($mmhr^{-1}$) during Band 21b.

Chapter 3: Wind Structure in Stratiform Rainbands over Land

3.1 Motivation

There are several reasons that it is important to understand the vertical structure of winds in rainbands over land. First, knowledge of the vertical variation of wind speed is critical in urban areas where high-rise structures may experience winds much stronger than those at the surface (Franklin et al. 2003). Second, damage is often caused by wind gusts near the surface (Powell, Dodge and Black 1991), making understanding low-level wind variability important. Third, the vertical wind profile may be responsible for the generation of low-level roll structures such as those seen in Morrison et al. (2005) and Lorsolo et al. (2008), and those modeled by Foster (2005). Additionally, wind shear may play a role in promoting tornado genesis over land (e.g. Novlan and Gray 1974; Gentry 1983; Baker et al. 2009) making understanding the amount of low-level shear in landfalling storms important.

With the VAD data set, vertical structures of wind profiles from stratiform rainbands of storms of different intensities and distances can be compared. The high resolution (~7 meters vertically) of this data set allows for examination of the log-wind regime in the HBL that is often unsampled during research flights but is crucial to understanding the impact of tropical cyclones on human activity, tall buildings and vegetation. Data sets from other instruments used at the field site can also be combined in order to study the upper-level winds that are frequently missed by dropsondes, and to compare non-precipitating periods before and after rainband passage with stratiform periods within the rainbands.

In this chapter, observations from 14 stratiform rain periods within 8 outer rainbands over land in South Florida in August and September 2008 are presented. Section 3.2 shows individual profiles of mean wind speed and direction, as well as storm composites. Section 3.3 documents individual profiles of radial and tangential wind broken down by storm occurrence, and Section 3.4 examines the temporal variability, first within one rainband, and then by presenting case examples of radial and tangential profile changes before, during and after rainband passage. Section 3.5 focuses on the hurricane boundary layer (HBL) winds, first examining the log-wind regime and calculating friction velocity and aerodynamic roughness length by rainband, and finally by comparing the ratios of surface winds to those at the top of the HBL. The ratio results from the 14 stratiform cases over land are compared with previous observations of surface to HBL wind ratios over land and water. Section 3.6 summarizes the work presented and conclusions reached in this chapter.

The 14 stratiform cases described in Sections 3.2 and 3.3 are analyzed by the storm they occurred in, as that groups them by storm maximum strength of 50 knots for the cases during Fay, 120 knots for the two Gustav cases, and 70 knots for the two Ike cases.

3.2 Mean Horizontal Wind

Powell and Black (1990) indicate that the vertical profile of the horizontal component of the wind speed in the HBL has a logarithmic profile up to the base of the maximum wind speed level, usually between 500 and 1800 meters AGL. This wind maximum outside of the eyewall is normally found near the top of the frictional boundary

layer (or HBL, Franklin et al. 2003). Above the level of horizontal wind maximum, there typically is a decrease in wind speed with height due to a weakening of the radial pressure gradient in the warm core system, as well as a region of weak or no shear up to 2 kilometers. The Powell and Black (1990) flight-observed profile is also similar to that observed using GPS dropsondes by Franklin et al. (2003), where the low-level wind max occurs around 500 meters near the eyewall and rises to about 1000 meters AGL in outer vortex regions, and the peak wind values are only about 10% stronger than the 700-hPa flight-level winds, with a logarithmic profile below 300 meters. Though Powell and Black (1990) construct wind speed profiles from flight-level winds at 0.5 km, 1.5km, and 3 km, Franklin et al. (2003) use about 200 outer vortex dropsondes with 5 meter resolution to measure the wind speed profiles. These sondes can drift horizontally while falling, but since they are averaged they provide a useful high-resolution (5-7 meter) vertical profile data set to compare with the 14 individual VAD wind speed profiles below 3000 meters.

The 14 VAD profiles of wind speed with height in the stratiform rainbands all show similar features to the profiles described by Powell and Black (1990) and Franklin et al. (2003). Figure 2.3 shows an example from Band 9b, where the maximum horizontal wind speed (V_h) of 23 ms^{-1} is located at a height of 1300 meters AGL, although the wind speeds vary little from 1000-3000 meters AGL. The wind speed decreases from 3000 meters to 4000 meters AGL, and then a secondary wind maximum is observed around 4500 meters AGL, which is the height of the melting level as indicated by the X-band observations. Below 800 meters AGL, the horizontal wind speed decreases exponentially. Figure 2.3 shows just one case example, but plots of the

remaining 13 cases show that maximum winds range from 14-24 ms^{-1} with wind maxima between 1300-3900 meters AGL. Figure 3.1 shows all 14 stratiform cases, broken down by storm. The wind profiles in the 9 cases during Fay (Bands 4a, 9a, 9b, 9c, 10a, 10b, 11a, 18a, 18b) show a maximum in the horizontal wind speed between 1000-1500 meters AGL. Bands 4a, 5a, 9a , 9c, 10b, and 18b show a double wind maximum structure similar to Case 9b (Figure 2.3), although the secondary maximum is not always as prominent. These secondary wind maxima could be due to thermodynamically driven circulation at the melting level (Moon and Nolan 2010). Rainbands during Gustav (21a,b) and Ike (23a,b) also show the double wind maximum structure, but in these cases the maximum horizontal winds speeds are stronger in the upper maximum than the lower maximum, which is located around 4000 meters AGL in Band 21a, and 3500 meters AGL in the remaining three cases. These four rainbands with the stronger upper wind maximum feature were observed from stronger tropical systems, and they indicate that even at far distances from the storm center this secondary maximum can be stronger than the low-level wind maximum. A similar upper-level secondary wind maximum was seen during a rawindsonde launched at Charleston, SC when Hurricane Hugo (1989) was 170 km from making landfall (Powell et al. 1991), further supporting that stronger storms may have a secondary wind maximum above the melting layer.

All 14 of the VAD profiles show a logarithmic decay of wind speed in the HBL. In every case, this log-wind regime extends to a height of about 200 meters. The log-wind profile still exists from 200 meters to the height of the wind maximum (top of HBL), but it has a slope that differs from that in the near-surface (below 200 meters) portion of the HBL. This is similar to the composite profile of outer vortex dropsondes by Franklin

et al. (2003), where the depth of the entire log-wind region exists up to 700-800 meters, but the exponential slope changes in the lowest 200 meters. The log-wind regime is discussed in greater detail in Section 3.5.1.

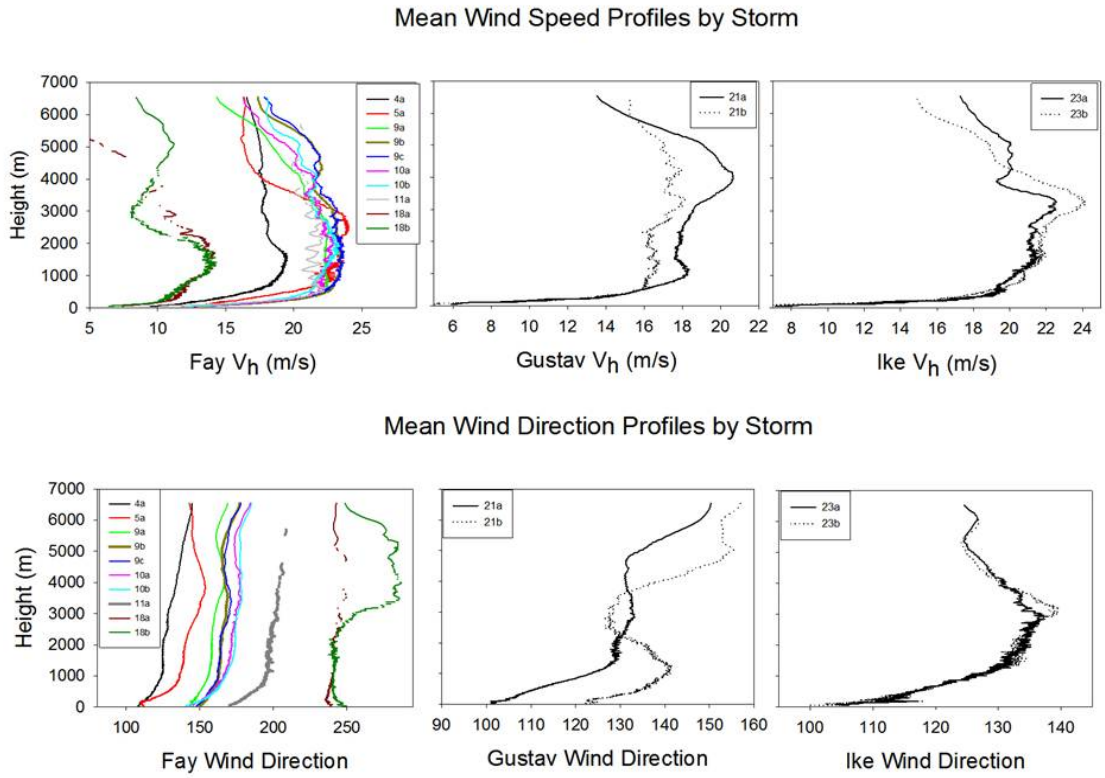

Figure 3.1: Upper Panels: Mean VAD profiles of horizontal wind speed with height during 14 stratiform rainband cases. The 10 cases from Fay are shown in the left panel, the two cases from Gustav are in the center panel, and the two cases from Ike are shown in the right panel. Lower Panels: Same storm breakdown as above, but with mean VAD profiles of horizontal wind direction with height, in degrees east of north.

Figure 3.1 also shows the VAD profiles of high-resolution structure in wind direction in each of the individual stratiform rainbands. The majority of these rainbands are coming from the southeast, so all of the profiles have an easterly or southerly profile, except for Bands 18a and 18b which have a westerly/southerly profile. As seen in Figure 3.1, the majority of the profiles show an easterly wind component near the surface.

Twelve of the 14 profiles show a nearly constant veering of wind direction up to the height of the wind maximum. In these cases, the wind veers 20-30^{o} over the lowest 1000-1500 meters. In contrast, Marks et al. (1999) analyzed hourly profiles of 6-minute VAD-derived wind direction during the landfall of Hurricane Fran (1996). They found little change in wind direction over the lowest 400 meters, followed by a sharp veering in wind direction of 50^{o} up to the height of the wind speed maximum. Although their low-level constant wind direction is constant over 5 hours of Fran's outside eyewall making landfall, the results shown in Figure 3.1 are more consistent with that of a friction layer and show similar variations as those seen by Knupp et al. (2006) using wind profiler measurements during the landfall of Tropical Storm Gabrielle (2001) in Florida. One additional feature of note is the time progression of wind direction profiles during TS Fay, seen in the lower left panel of Figure 3.1. The legend lists the stratiform rainbands in order of occurrence over four days, and Fay's path around the field site is evident. The observations on August 18th (4a and 5a) have the largest easterly component, which gains a southerly component on August 19th (Bands 9a-11a) as Fay turns northward to the west of the field site. On the 21st (18a and 18b), the storm is now well north of the field site and moving east/northeast, as is evident by the west-southwest wind direction profile. There is very little evidence of temporal changes in wind direction changes with height during Fay, other than the sharp veering at 3000 meters AGL seen in Band 18b which appears to be associated with a minimum in the wind speed profile.

Figure 3.2 shows the composite horizontal wind speed profile for each storm, and though it can be seen that there is no trend in maximum storm wind speed vs. observed wind speed profiles at the field site, the rainbands from Fay show a general decrease in

wind speed with height above 2500 meters AGL, while the Ike rainbands show a distinct narrow wind maximum just above 3000 meters AGL. Marks and Houze (1984) mention finding mesoscale features observed at a 3000 meter flight level near the core of Hurricane Debby (1982), but overall there is very little discussion of jet features observed at this height in the rainband literature. Although this it is a consistent feature in both of the Ike rainband profiles, the sample set is too small to speculate on the dynamics in Ike that may be causing this feature. In Figure 3.2, the eight Fay cases do show evidence of a small increase in wind speeds located at the height of the melting level (4500 meters), though it is mostly smoothed out by compositing. The lack of variability seen around the melting level height in the Ike and Gustav composites is likely due to the fact that each one contained only 2 stratiform rainband cases, thus while some of the individual cases had a strong wind maximum at this height, averaging causes no wind maximum to appear in these profiles. The rainbands observed during the strongest storm (Gustav, 120 knots) show a strong upper level wind maximum, though it is much broader and exists from 3000-5000 meters AGL. From Figure 3.1, a change in wind direction is observed at this height in Band 21b, but not in Band 21a. Rainbands during Gustav and Ike were observed father from the storm center (430 km for Ike and 450 km for Gustav versus an average distance of 162 km for Fay), which may help to explain some of the variability in wind patterns. Although Gustav was the strongest storm at the time of rainband observations, it had a small wind field (tropical storm and hurricane force winds extending 200 and 70 nautical miles from the center respectively, Beven and Kimberlain 2009) which explains why the wind speeds in the VAD profile are lower than the other two storms. Although the center of Ike passed 430 km from the field site, its large wind field (tropical storm and

hurricane force winds extending 240 and 100 nautical miles respectively, Berg 2009) gave measured wind speeds comparable to those during Fay. Figure 3.3 shows the mean horizontal wind from 12 of the 14 VAD cases, along with variance bars representing one standard deviation off of the mean. This averaging does not include Bands 18a and 18b, since they differ substantially from the other horizontal wind speed profile structures. Although these two rainbands occurred during Tropical Storm Fay, they were observed at far distances from the storm center and may be more squall-line (e.g. Gamache and Houze 1982) in nature, and thus are removed from the averaging. Many of the wind maxima features in this composite are smoothed out by combining all of the profiles, although the constant presence of the logarithmic decay in wind speed strength near the surface is evident, as is a decrease in wind speed above 3 kilometers.

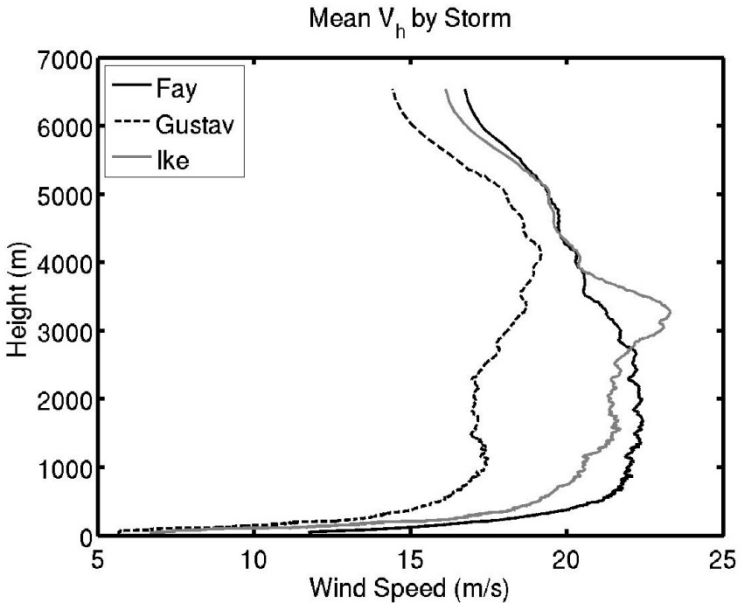

Figure 3.2: Composite of VAD profiles by storm maximum wind speed at time of rainband observation. The solid black line represents the mean of rainbands observed when Fay had a maximum sustained wind speed of 50 knots. The solid gray line represents rainbands observed when Ike had a maximum sustained wind speed of 70 knots. The dashed black line is the mean of rainbands observed when Gustav had a maximum sustained wind speed of 120 knots. Bands 18a and 18b have been excluded from the composites due to their large differences in wind speeds from the other cases.

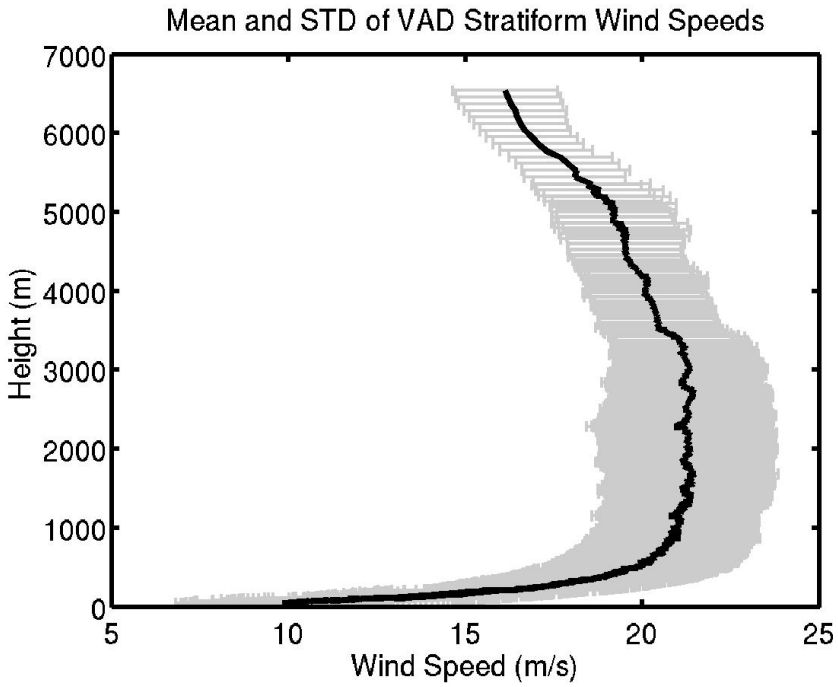

Figure 3.3: Mean VAD horizontal wind speed during all stratiform cases (thick black line) except for 18a and 18b, with one standard deviation (gray bars).

3.3 Radial and Tangential Winds

To discuss the wind profiles within the context of the storms it is useful to represent them into the radial and tangential wind components relative to the center location of the tropical cyclone. These wind profiles are calculated using the central storm location from the closest time period HURDAT data (Stewart and Beven 2009; Beven and Kimberlain 2009; Berg 2009). In this coordinate system, negative radial wind speeds represent wind blowing towards the center of the storm, positive radial winds are moving away from the eye of the storm, and positive tangential winds represent cyclonic flow around the storm center.

3.3.1 Radial Wind Profiles

Figure 3.4 shows mean profiles of radial winds during 11 of the stratiform cases from both the VAD (solid dark blue line) and MAPR (solid black line). These profiles agree nicely, with a switch from radial inflow near the ground to outflow located around 3000 meters AGL. Peak radial inflow at low levels (300-400 meters) is well defined by the high resolution of the VAD, a feature that is missed with the lowest range gates of the MAPR being at 400 meters. Although the MAPR data shows a second radial inflow above the melting level (4500 meters), the VAD winds indicate outflow at all heights above the HBL.

Individual profiles of radial wind by storm are shown in the upper panels of Figure 3.5. These profiles show that the lowest radial wind shifts occur during Ike at just above 1000 meters, but the highest occur during Gustav at heights above 4000 meters AGL. The majority of radial shifts from inflow to outflow during Fay are located between 2500-3000 meters. This is in agreement with observations from Barnes et al. (1983) where the radial shift occurs between 2500-4000 meters AGL at radial distances of 70-110 km from the storm center. The individual profiles of radial wind shown in Figure 3.5 indicate a maximum radial inflow below 500 meters in every case except 18a and 18b, which varies in strength between 3-8 ms^{-1}. This is in agreement with the peak radial inflow around 500 meters observed by Marks et al. (1999) during the landfall of Hurricane Fran (1996). Schwendike and Kepert (2008) report finding a shallower inflow layer towards the storm center over the ocean in Hurricane Danielle (1998), but evidence of that is not seen in this data set. Maximum radial outflow is less consistent and exists at a wide variety of heights between 3000-6000 meters AGL and values between 0-4 ms^{-1}.

Several of the Fay cases and both Ike cases show a secondary radial inflow, located at heights between 4500-5500 meters AGL. This weaker inflow likely arises from a balanced response to heating (Zhang et al. 2011). One profile during Gustav has a secondary radial inflow (Band 21b), but it occurs at a lower height of 3 km, and unlike the Fay and Ike cases, this secondary inflow is stronger than the low-level inflow. Maximum values of radial outflow are less than maximum values of radial inflow, and Bands 9a and 18a show no evidence of having any radial outflow. Nine out of the 14 stratiform rainbands show evidence of peak radial outflows of about 2 ms^{-1} located around 3500 meters AGL, which corresponds to a clockwise shift in wind direction at the same height (Fig. 3.1). Only two of those nine cases (23a and 23b) also have a peak in tangential/horizontal winds at these heights, which mean that those cases probably have a layer of stronger winds at this height due to the strength of Hurricane Ike. The wind shifts in the remaining seven cases could be due to a secondary circulation causing increased storm outflow at heights above the HBL but below the melting layer.

3.3.2 Tangential Wind Profiles

Individual profiles of mean tangential winds from each stratiform case are shown by storm in the lower panels of Figure 3.5. All profiles are positive, which is expected due to tropical cyclone circulation in the Northern Hemisphere. These profiles show that a maximum in the tangential wind is typically observed between 1000-3000 meters AGL, and is fairly constant in value by rainband over this height range. Although most profiles decrease in speed with height above 3000 meters, a few of the cases do show evidence of a second maximum in the tangential wind at about 4000 meters, especially the Gustav

and Ike cases where the upper maximum is stronger than the lower maximum. These results are also in agreement with the rainband schematic from Barnes et al. (1983) that shows tangential wind peaks between 1000-2500 meters AGL at radial distance of 50-110 km, with an occasional secondary peak around 4000 meters AGL depending on the flight location relative to the cells moving along the rainband. Individual profiles of tangential wind are similar in magnitude and structure to the individual rainband profiles of horizontal wind (Fig. 5), indicating that as expected the tangential wind component is the most significant to the overall wind speed. As in Figure 3.1, Bands 18a and 18b differ greatly in strength and structure from the other Fay cases. Like the other profiles, they have a low-level tangential wind maximum just above the top of the HBL, but the tangential wind speed drops off at a faster rate in these cases than in the other Fay, Gustav and Ike cases, signifying that Bands 18a,b could be more squall-line in nature, which could result in a weaker coupling between the surface winds and winds aloft. This could also be related to the direction of rainband approach, as these two cases are in westerly flow, indicating a longer fetch over land before reaching South Florida.

An average profile of tangential winds is shown in Figure 3.6 using smoothed data from both the MAPR and VAD. These profiles differ significantly in magnitude and also in terms of features. The VAD, which is higher resolution, has features of wind maximums blended out by compositing the rainbands together. However, while the MAPR data may have atypically high mean values, it does show more structure, including a tangential wind peak around 1500 meters AGL, as well as smaller tangential peaks at 3000 meters AGL and 5200 meters AGL. Both data sets show decreasing tangential winds above 5500 meters, in accordance with ocean observations by Barnes et

al. (1983), but lower than the 4000-8000 meter AGL maxima found during landfall of Tropical Storm Flo (1990) by May et al. (1994).

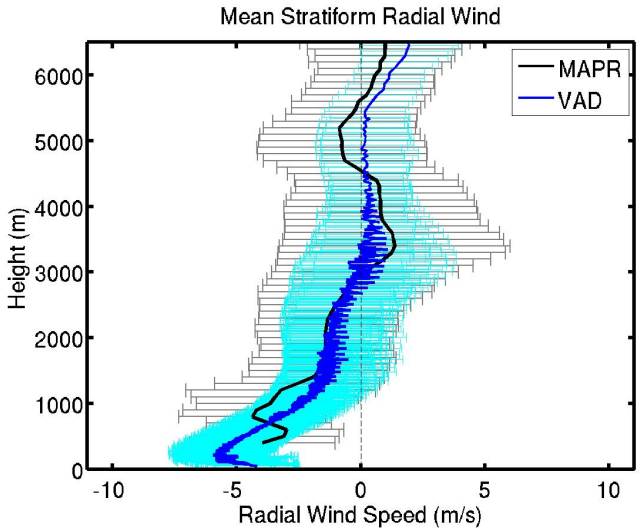

Figure 3.4: Mean radial wind profiles with height from VAD (solid dark blue line) and MAPR (solid black line) during 11 stratiform cases. Cases 11a, 18a and 18b are excluded from this averaging due to their differences in wind speed and structure. One standard deviation variance off the mean is shown for VAD (light blue bars) and MAPR (grey bars). Both profiles are smoothed with a 5 point running mean. Dashed gray line marks the transition from radial inflow (negative values) to radial outflow (positive values).

Figure 3.6 also supports the hypothesis of the MAPR overestimating horizontal wind speeds as suggested in Figure 2.6. The grey (MAPR) and light blue (VAD) bars shown in Figure 3.6 represent one standard deviation off the mean of the average profiles. Although there is some overlap in variance between the two instruments, it is often minimal, with the MAPR consistently observing higher values. This issue is not seen in the radial wind profile comparison in Figure 3.4 because the radial wind component is much smaller than the tangential wind component.

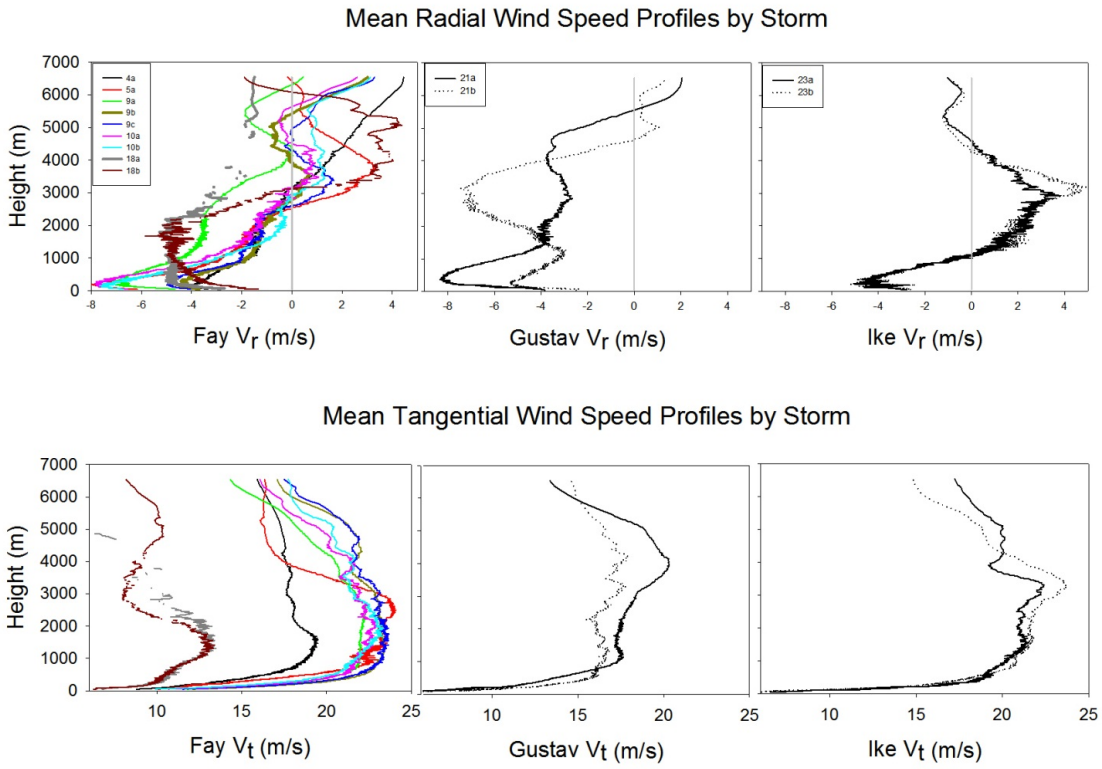

Figure 3.5: Upper panels: Mean VAD radial wind profiles with height by storm. Light gray line marks transition from radial inflow (negative values) to outflow (positive values). Lower panels: Mean VAD tangential wind profiles with height by storm. Band 11a is excluded from this plot as it lies outside the bounds of one standard deviation of the mean.

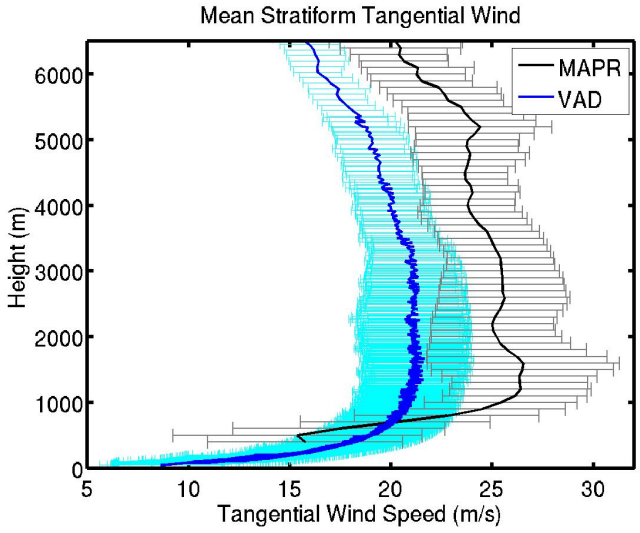

Figure 3.6: As in Figure 3.4, but for tangential wind.

3.4. Temporal Variability

Previously this study focused on mean profiles of wind components averaged over the 6-165 minutes of stratiform rainband occurrence. In this section, the temporal variability in the profiles is examined, first within the longest stratiform period, and then by presenting a case study of the profiles before, during, and after Bands 4a and 5a to understand how radial and tangential wind profiles vary with rainband passage.

3.4.1 Time Series of Band 21

Time-height images of SNR and vertical velocity of Band 21 were shown in Figure 2.7. Band 21 is broken down into two stratiform regions, Band 21a, which represents the longest period of stratiform conditions, followed by an hour gap where conditions are more convective than stratiform, and then a second short stratiform period (Band 21b). Figure 3.7 uses averaged half hour VAD profiles to illustrate the changes in mean, radial, and tangential wind over four hours. Mean wind speed profiles (left panel) show that while winds in the log-wind regime remained relatively constant over the time period, the wind speeds near the low-level (1000 m) wind maximum increased steadily, becoming a distinct jetlike feature around 0400 UTC. An ascending and strengthening low-level wind maximum was also seen during an hour time progression of stratiform conditions during TS Gabrielle (2001) by Knupp et al. (2006). During the half hour gap between Bands 21a and 21b this wind maximum disappears and the wind speed drops to just below the initial wind speed at the start of Band 21a. The wind maximum between 3000-5000 meters AGL exists for all time periods during Band 21a, but has also disappeared by Band 21b. The third panel of Figure 3.7 shows the consistent nature of the

secondary wind maximum near the melting level during Band 21a in the tangential winds, and the wind speeds at this height generally increase with time. This upper wind maximum was seen in many rainbands in profiles of V_h discussed in Section 3.2, and it is worth noting that it also shows up in MAPR profiles (not shown), so it is not just due to an artifact of the VAD technique. The time progression of radial wind speed is displayed in the middle panel of Figure 3.7, and shows a decreasing strength in low-level radial inflow with time during 21a, with a drastic drop in radial inflow with Band 21b. Although the height of reversal from radial inflow to outflow shows no trend throughout Band 21a, it is about 500 meters in altitude lower in Band 21b. The third panel of Figure 3.7 shows the time progression of the tangential wind component. The patterns seen here mimic those of the mean wind temporal variability, as the tangential wind component is significantly larger than the radial wind component. One difference of note is that the depth of the log-wind regime decreases over time in the tangential winds, but not in the mean winds. A careful study of WSR-88D loops during and after Bands 21a and 21b indicates that while there are no distinct changes in the structural appearance of the rainband, as the rainband moves NNW over the CSTARS location, the tail end of the band is approached. Shortly after the end of Band 21b, the entire rainband begins to dissipate, and the line structure of the rainband weakens. This post-band environment could potentially begin affecting the rainband conditions during Band 21b, which could explain the sharp changes in profiles seen between the two stratiform cases.

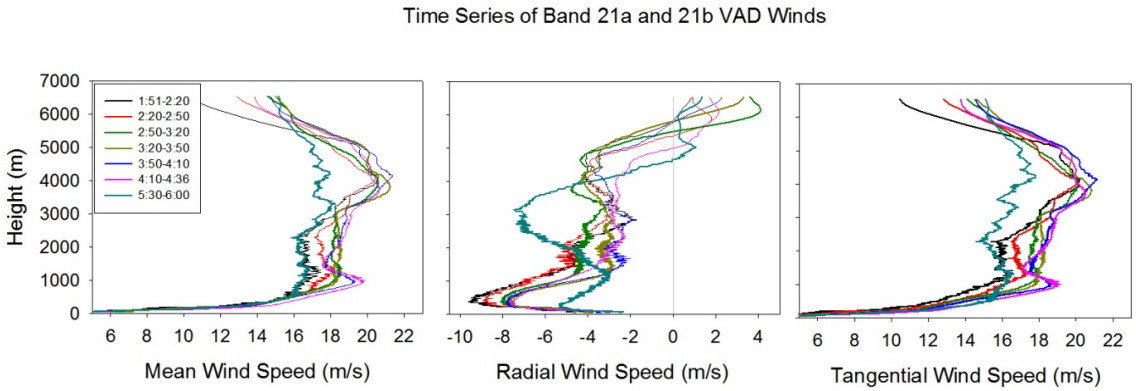

Figure 3.7: Averaged half hour VAD profiles of mean wind speed (left), radial wind (middle) and tangential wind (right) during Bands 21a and 21b.

3.4.2 Change in Wind Profiles Before, During and After Rainband Passage

Winds during non-precipitating periods before and after rainband passages were analyzed using 5-minute consensus MAPR winds. Winds during these non-precipitating periods can be compared with the wind speed structure from VAD analysis during stratiform rainbands to give wind profiles before, during, and after a rainband passage. Soundings made at the field site and at the National Hurricane Center (NHC/KMIA, 13.8 miles from the field site) can also be included in this analysis. Figure 3.8 shows a case example of such an analysis using radial (upper panel) and tangential (lower panel) profiles to illustrate changes during Bands 4a and 5a. In this figure, the 'MAPR Before 4a' profile is a 15 minute non-precipitating time period before the approach of the rainband that contained stratiform Bands 4a and 5a, and the 'MAPR After 5a' profile another 15 minute average during non-precipitating conditions after the entire rainband has passed over the site. Soundings from KMIA before the rainband approach (1200 UTC on August 18th) and after rainband passage (0000 UTC on August 19th) are also shown, along with a CSTARS sounding before the rainband approach at 1400 UTC. The upper panel of Figure 3.8 shows that the depth of the radial inflow layer deepens during the rainband,

and then drops in height after the rainband passage to a more shallow height than before the rainband approach. The strength of the radial inflow is variable, and an overall trend in inflow strength is not apparent.

The lower panel of Figure 3.8 shows that the tangential wind speeds were weakest before the rainband, and increased from Band 4a to Band 5a, and then even further after the rainband passage. A large part of this tangential wind speed increase is most likely due to the fact that the center of Tropical Storm Fay was moving closer to the field site during this time period. Evidence of a small wind maximum around 1000 meters altitude appears in each profile, although it is not the height of the strongest winds either before the rainband or during Band 5a. It appears that the low-level wind maximum has risen in height and broadened after the rainband passage. There is also some evidence of an upper level wind maximum developing around 3000 meters as the rainband progresses, and lingering after the rainband has passed, as seen in the 0000 UTC KMIA sounding. If this upper-level feature is related to the wind maximum seen during Bands 23a and 23b in Hurricane Ike (Figure 3.1), then strong secondary jets may not just be limited to stronger storm systems.

The value of the VAD technique is apparent in Figure 3.8, as the high-resolution observations (~7 meters in the vertical) are able to capture small-scale features due to the close location to the Miami WSR-88D. The VAD profiles are more efficient at showing the strength of the radial inflow, as the profiles are approximately point profiles rather than moving with the winds as the rawindsondes do. In the tangential profiles, the VAD show more structure in the log-wind layer and wind maximums at levels all the way up to

the melting layer, while the MAPR profiles only extend up to just over 2000 meters at a much lower resolution.

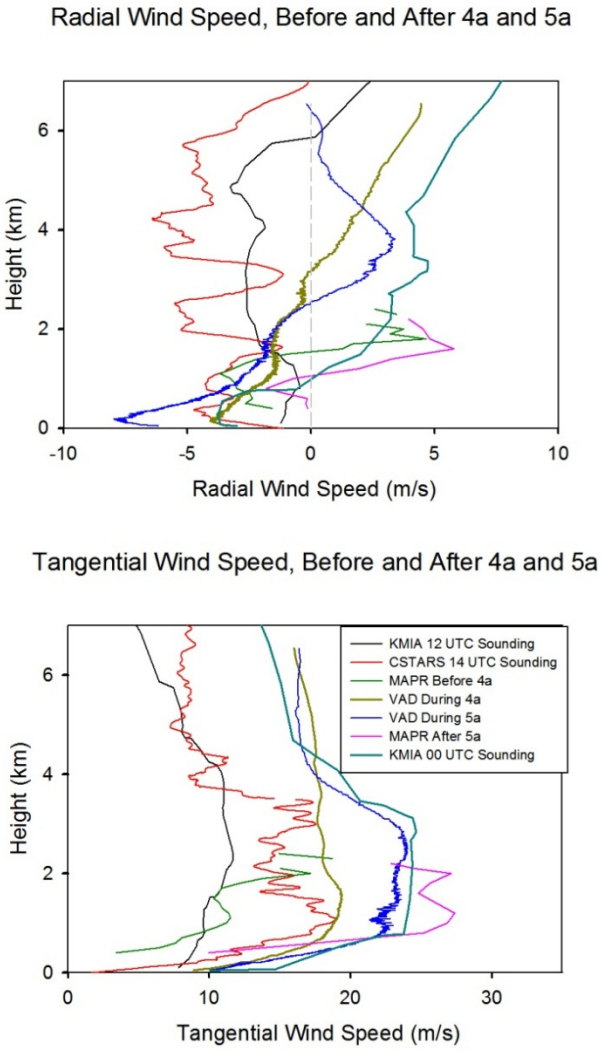

Figure 3.8: Before, during and after radial (upper panel) and tangential (lower panel) wind profiles for Bands 4a and 5a. Before and after profiles are made using 5 minute-consensus MAPR data smoothed with a 5 point running mean, and during profiles are from VAD, also smoothed with a 5 point running mean. In this example, the 'MAPR Before 4a' is a 15 minute non-precipitating time period before the approach of the rainband that contained stratiform cases 4a and 5a, and the 'MAPR After 5a' is after the entire rainband has passed over the site and is another 15 minute average during non-precipitating conditions. Soundings from KMIA before the rainband approach (12 UTC on August 18th, black line) and after rainband passage (00 UTC on August 19th, teal line) are also shown, along with a CSTARS sounding before the rainband approach at 1400 UTC (red).

3.5 Low- level Mean Wind

As seen in Figure 3.1, wind speeds decay exponentially within the HBL. The wind speeds and structures in this layer are critical, since they will have the largest impact on human life and property. This section examines the expected rate of logarithmic decay (Stull 1988) for each stratiform case, as well as the ratio between surface winds (3, 14.5 and 18 meters AGL) and mean horizontal HBL winds.

3.5.1 Log-wind Profiles

The individual plots of mean wind speed versus height for each stratiform rainband all show an exponential decrease in horizontal wind speed in the lowest 500 meters (see Figure 3.9 for Band 9c), similar to the typical logarithmic variation of wind speed with height in a neutral boundary layer (Stull 1988). To investigate this decay rate, statically neutral conditions were assumed (as expected by stratiform conditions of data set (Stull 1988), and shown in straight line of slope in Figure 3.10). For each stratiform case, wind speed was plotted against the logarithm of height minus a 6 meter displacement distance following Stull (1988, see Figure 3.10). If this plot remains linear without the profile becoming concave upward or downward, then the displacement distance is appropriate. The variables of the log-wind profile are calculated using Equation 3.1 (Stull 1988, Eq. (9.7.3a)).

$$\overline{U} = \left(\frac{u_*}{k}\right) \ln\left(\frac{(z-d)}{z_0}\right) \qquad \text{(Equation 3.1)}$$

Where $\overline{U}$ is the average rainband wind speed; u_* is the friction velocity (meters per second); k is the von Karman constant, chosen to be 0.35; d is the displacement distance

in meters (chosen to be 6 meters as approximate height of surrounding trees); z is the height above ground in meters; and z_0 is the aerodynamic roughness length, also in meters. Eq. 3.1 is in y=mx+b form in Equation 3.2 where ln(x-d) is the y axis, and wind speed is the x axis (as in Figure 3.10).

$$\ln(z-\mathrm{d}) = \left(\frac{k}{u_*}\right)\overline{\mathrm{U}} + \left(\frac{u_*}{k}\right)\ln(z_0) \qquad \text{(Equation 3.2)}$$

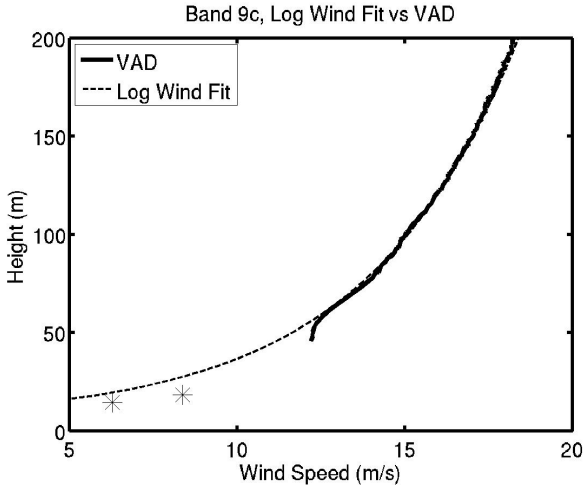

Figure 3.9: Close-up of lowest level of the hurricane boundary layer in Band 9c (thick line), along with Log-wind profile calculated using Stull (1988), extrapolated to lower levels (dashed line). Data points from the CSTARS tower at 18 and 14.5 meters are shown as black stars.

A best linear fit was made for each of the wind profiles using VAD values from 65 meters to 120 meters altitude to represent the surface layer. The slope and intercept of each line are used to solve for u_* and z_0 by case following Eq. 3.2. The results are shown in Table 3.1 and are fairly close in calculation of u_*, which should experience some variability due to the strength of the horizontal wind. However, there is a much wider range of calculated values in z_0 than expected, since it should not change with

wind speed, stability or stress for a particular surface (Stull 1988). From Stull's table of aerodynamic roughness lengths for typical terrains (1988, Fig 9.6), expected aerodynamic roughness lengths for the South Florida terrain should range from 0.7 meters for large towns and small cities to 2.5 meters for centers of large cities with tall buildings. With the environment around the field site consisting of trees and urban housing, Bands 11a, 21b, and 23a are well above the expected range for z_0, while Bands 4a and 21a are more representative of outskirts of towns. Band 5a is significantly lower and is on the scale of farmland roughness length. While the calculated z_0 values are on the right order of magnitude compared to oceans (~10^{-3}), unlike previous studies (e.g. Colin and Faivre, 2010; Powell et al. 2003; Vickery et al. 2009), there is no set value for z_0 based on the 14 stratiform cases. There is also not an obvious relationship between z_0 and fetch, wind speed or direction of rainband approach (not shown), though higher values of z_0 are associated with higher values of u_* and maximum wind speed in the lowest 2000 meters AGL. Overall the goodness of fit between the linear fit and log-wind wind speeds is extremely high. It appears that z_0 is highly dependent on the heights used in calculating the best-fit line, as a small shift in included heights can change z_0 significantly (see Figure 3.11). Thus, the fact that a consistent range of heights for the best-fit line was chosen in an attempt to calculate a constant z_0 factor rather than choosing ranges that would optimize the goodness of fit could influence the z_0 values. Additionally, fitting winds only up to 100 meters should help keep z_0 values lower, as including higher measurements has been shown to increase roughness length (Masters et al. 2010). If the

two cases with less than 91% correlation in linear fit (Bands 18a and 21b) are removed and z_0 and u_* are re-averaged, the new values are 1.54 and 0.982 respectively.

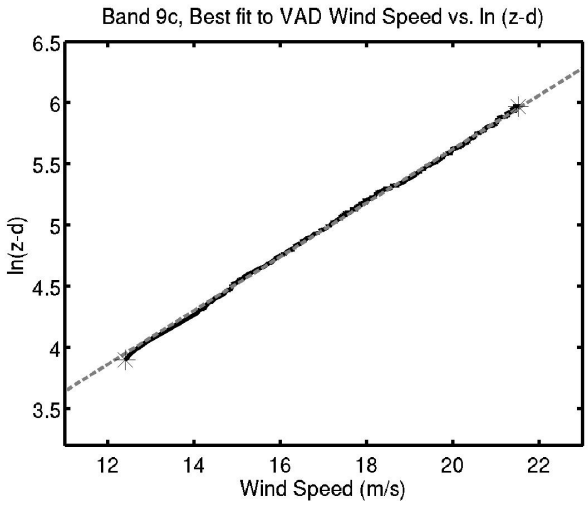

Figure 3.10: Low-level VAD winds from Band 9c plotted against natural log (height minus displacement distance) in black. The best fit line (gray dashes) is calculated using between 65 and 120 meters (black stars).

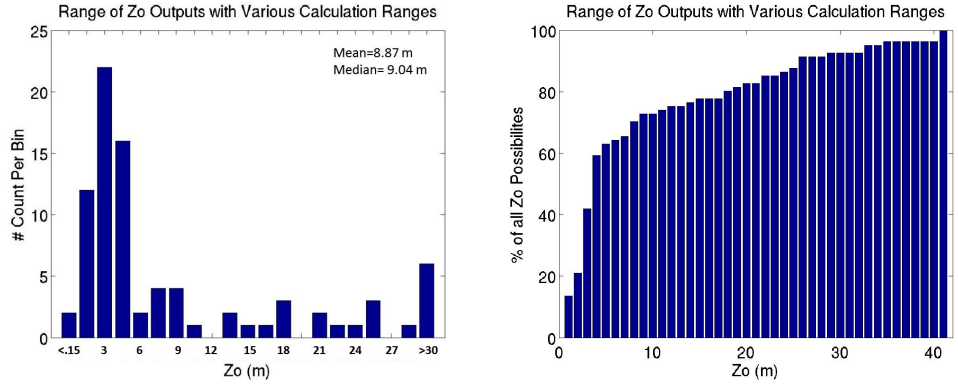

Figure 3.11: Histogram binning of z_0 for all stratiform rainbands using height ranges varying by 50 meters up to a height of 200 meters. Left panel shows number count per bin, with bins of 1.5 m. Right panel shows cumulative bins (CDF) of 1 m each. In CDF, 60% of all z_0 values are less than 4 meters. A total of 81 z_0 calculations are shown here, and while most z_0 values are less than 4 meters there is significant variability depending on the range used in the calculation.

When the calculated u_* and z_0 values by rainband are put back in Eq. 3.1 to solve for wind speed at each height, a good agreement is seen. The depth that the log-wind fit captures the wind speed profile in the surface layer extends from close to the surface up to heights varying from 129-249 meters, which is called the Top of the Surface (Sfc) Layer in Table 3.1. It is important to note the difference between the Inflection Point (IP) of the Surface Layer (V_h IP, Top of the Sfc Layer), IP of the Log-Wind Layer (V_h IP, Top of the Log-Wind Layer), and IP of the Radial Wind (V_r IP). The first (V_h IP, Top of the Sfc Layer) is the top of the region that was used to calculate the log-wind fit above, and represents the rate of wind speed increase with height in the lowest levels of the atmosphere. The second (V_h IP, Top of the Log-Wind Layer) is where the VAD profile transitions from a log-wind pattern to a wind maximum, but the log-wind slope is often different than the slope in the lower surface layer. For instance, in Band 9c the calculated log-wind fits the VAD curve well until just above 200 meters AGL, and then the profile remains logarithmic up to almost 500 meters AGL, but at a different rate of growth. The IP of the Radial Wind (V_r IP) is the depth where the radial wind reaches its peak inflow, and was found to be lower than the IP of the surface layer when the rainbands were observed close to storm center and higher than the IP of the surface layer when the rainbands are observed at greater distances from storm center. One final height worth mentioning is the Lifting Condensation Level (LCL), which is the height at which is the height at which saturation will occur. All four of these heights are listed by rainband in Table 3.1.

Table 3.1: Observed variability of friction velocity (u_*) and aerodynamic roughness length (z_0) by using a logarithmic best-fit line to each stratiform case. Goodness of linear fit to wind data is shown as r. Values in parenthesis under mean are average with Band 18a and Band 23b (r < .91) excluded. Inflection points (IP) are the height at which the calculated log-wind profile no longer fits well to observations and are described in the text. The lifting condensation level (LCL) is calculated using the 14.5 meter tower data. All heights are shown in height above ground level (AGL).

Band	Max Wind Speed (lowest 2 km)	u_* (ms^{-1})	z_0 (m)	Goodness of fit (r)	V_h IP, Top of Log-Wind Layer (m)	V_h IP, Top of Sfc Layer (m)	V_r IP (m)	LCL (m)
4a	19.9	0.724	0.436	0.992	950	244	164	277
5a	24.18	0.633	0.059	0.997	510	234	208	360
9a	22.69	1.182	1.041	0.988	502	249	207	480
9b	23.6	1.220	1.149	0.990	491	189	225	434
9c	24.0	1.305	1.683	0.989	472	222	199	416
10a	23.6	1.317	1.691	0.970	485	234	138	414
10b	23.9	1.189	1.337	0.983	510	173	138	427
11a	23.72	1.444	3.864	0.974	493	155	82	315
18a	15.12	0.660	1.020	0.891	553	145	284	1044
18b	15.2	0.653	1.475	0.947	788	134	341	1042
21a	18.59	0.399	0.235	0.971	765	141	385	499
21b	17.21	1.040	9.053	0.901	523	137	179	438
23a	22.08	0.978	3.205	0.957	485	134	255	301
23b	22.33	0.744	2.317	0.987	858	129	252	357
Mean	**21.15**	**0.963 (0.982)**	**2.04 (1.54)**	**0.967**	**599**	**180**	**213**	**507**
Stan-dard Devi-ation	**3.3**	**0.324**	**2.28**	**0.033**	**164**	**47**	**86**	**250**

Comparing the actual VAD wind speed with the calculated wind speed (using a different u_* and z_0 for each rainband) at 90 meters AGL shows excellent agreement (Figure 3.12, lower panel), which is expected since 90 meters is in the height range used to calculate each u_* and z_0. At a height above that included in the linear fit, the log-wind vs. VAD calculation at 300 meters still shows decent agreement (Figure 3.12, upper

panel); but the calculations underestimate wind speeds by 1-2 ms^{-1} for the tropical storm rainbands, and underestimate wind speeds by 4-6 $ms^{-1}$for the hurricane rainbands, although the site is over 425 km from the from the storm center during the latter. Comparing the calculated wind speed values with the 18 meter height CSTARS tower observed winds (not shown), the wind speed is again underestimated by 1-4 ms^{-1}, although this negative bias is more consistent across all cases. Overall, despite the observed variability in z_0, these values can be used to give an accurate estimation of wind speeds elsewhere in the surface layer. Even though this relationship breaks down extremely close to the surface, it gives a fairly good representation down to 45 meters, a location where wind speed knowledge is critical for tall buildings.

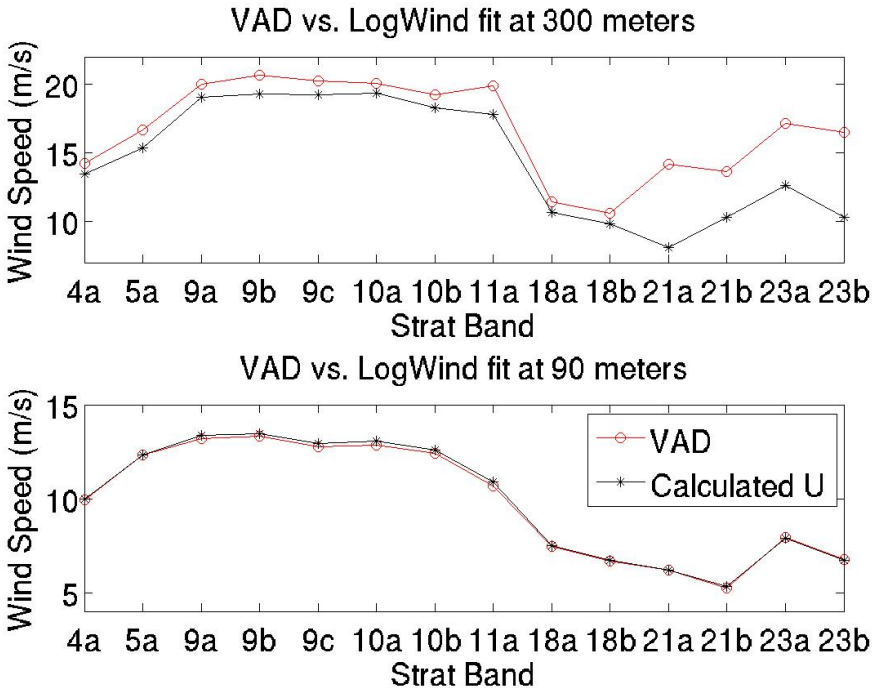

Figure 3.12: Comparison of true VAD winds (red circles) and calculated winds (black stars) at 300 meters (upper panel) and 90 meters (lower panel). Data points in red circles are true winds from the VAD, starred data points are calculated mean winds based on Stull Log-wind equation using u_* and z_0 for each rainband case.

Rather than using individual values for z_0 for each rainband as in Figure 3.12, Figure 3.13 shows a comparison of true VAD winds to calculated wind speeds (U) using the mean z_0 value of 2.04 m (left panel) and the mean z_0 value without the outliers (r < .91) of Bands 18a and 23b (1.54 m, right panel). In this figure, both mean z_0 values provide U values that are within 6 ms^{-1} of the VAD wind speed at 90 meters (left panel). There is not a consistent trend in whether the U value over- or under-estimates the actual wind speed, but in terms of building codes, using a mean z_0 is an acceptable option for estimating wind speeds near the tops of tall buildings (200-400 feet) if wind speed values in that range are used for the z_0 calculation. Alternatively, using a mean z_0 value from 200-400 feet to assess wind speeds at 18 meters underestimates the winds by 2-6 ms^{-1}, even for weak (< 10 ms^{-1}) wind speeds. This suggests that using a mean z_0 is not an effective way to calculate near-surface wind speeds from winds aloft (and vice versa). If this is a challenge even under the low wind speeds observed during the stratiform rainbands, it is likely to be even less possible under high wind conditions, so a mean z_0 does not seem to be valuable for determining building wind codes during rainband conditions, at least not based on this data set.

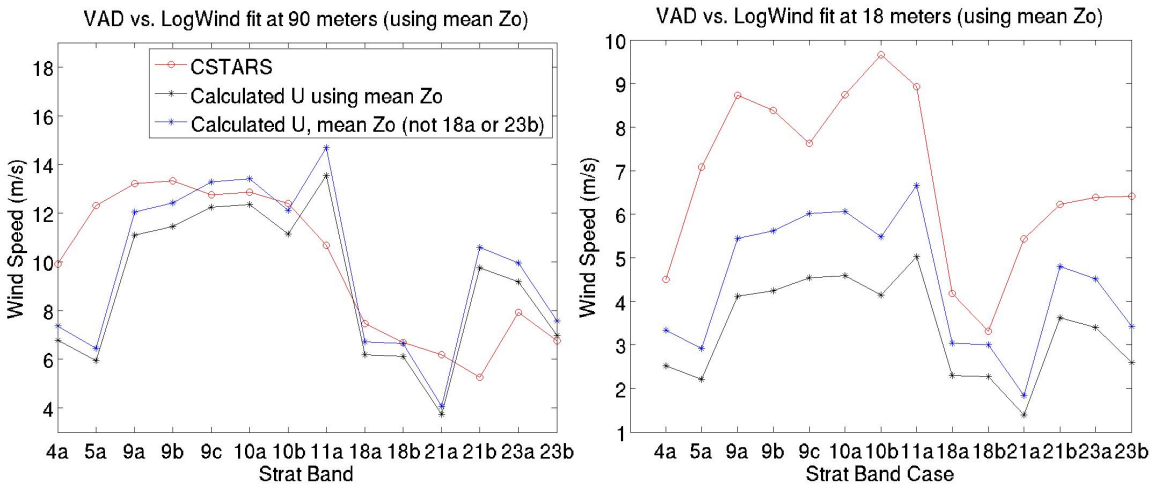

Figure 3.13: Comparison of true VAD winds (red circles) and calculated winds using mean z_0 value of 2.04 m (black stars) and 1.54 m (blue stars) at 90 meters (left panel) and 18 meters (right panel). Data points in circles are true winds from the VAD, starred data points are calculated mean winds based on Stull Log-wind equation using u_* for each rainband case with a mean value of z_0.

3.5.2 Ratio of Hurricane Boundary Layer Winds to Winds Aloft

Mean winds speeds from the VAD profiles can be used to compare the speeds at the top of the log-wind regime to lower levels in the HBL. For each of the profiles the top of the HBL was defined as the inflection point of the log-wind layer (V_h IP, Top of the Log-Wind Layer, as shown in Table 3.1) where the wind speeds transition from a log-wind profile to a wind maximum (similar to the distinction made by Franklin et al. 2003). The height of this level and the maximum wind at the inflection point was obtained for each wind profile (Table 3.2). For wind observations within the HBL, the mean winds from the CSTARS tower at 14.5 and 18 meters above the ground are used, along with mean winds from the 3 meter NCAR tower. Table 3.2 lists all of the wind speeds at the top of the HBL (mean from inflection point to 30 meters above inflection point) and the ratios of these winds to those in the near-surface (3, 14.5 and 18 meters AGL) HBL. The average ratio of the 18 meter winds to the inflection point winds is 0.36, and the average

ratio at 14.5 meters is 0.26. At the 3 meter level from the NCAR tower, the mean ratio drops to 0.17. Following this trend, the ratio decreases with height as the near-surface wind speed decreases. All three of these ratios are significantly lower than those previously reported, even though the near-surface ratios were calculated to the inflection point wind speed, which was lower than the maximum wind speed found in the VAD profiles at heights between 1300-3300 meters AGL. Powell and Black (1990) found that 10 meter surface winds from ocean buoys were within 55-85%, with a mean ratio of 0.67, of winds measured by aircraft at 500 meters AGL, 1500 meters AGL and 3000 meters AGL. Blackwell (2000) reported that on the eastern side of Hurricane Danny (1997) surface winds at landfall over flat terrain were 64% of 850 hectopascal (hPa) flight level winds. The previously accepted 90% rule (Franklin et al. 2003) is also supported by Powell, Uhlhorn and Kepert (2009), who found a mean ratio of 0.89 between sonde 10-meter maximum winds to the maximum 700 hPa flight-level speed near the eyewall over water, and by Dunion et al. (2003) whose ratio of 10-meter sonde data to a 29 ms^{-1} wind mean HBL wind over the ocean is 0.9. The much lower ratios calculated here may partially be due to the friction effects of being over land, the high trees surrounding the field site and thus limiting the 10 meter wind, and the fact that the observations are located far from the storm center, as Franklin et al. (2003) reported that the adjustment factor between 850 hPa and the surface drops to 0.75 in the outer vortex. Additionally, the mean inflection point wind speeds are on average 10 ms^{-1} lower than those measured by Dunion et al. (2003), though Dunion suggests that as the mean HBL wind speed increases, the ratio should decrease. If wind gust data from the 14.5 meter CSTARS tower sensor are used to approximate the maximum 10 meter maximum wind speed

(similar to Powell et al. 2009), the mean ratio increases to 0.53, which is just below the low end of the range suggested by Powell and Black (1990).

Table 3.2: Mean inflection point (IP) wind speeds from VAD compared to average wind speed from CSTARS towers instruments (18 meters and 14.5 meters) and surface (3 meters) wind speeds. Surface data are missing for Bands 21a and 21b.

Band	Mean V_h at the IP (Top of the Log-Wind Layer) from VAD (ms^{-1})	CSTARS 18 meter Wind Speed (ms^{-1})	Ratio of 18 m wind speed to IP Wind	CSTARS 14.5 meter Wind Speed (ms^{-1})	Ratio of 14.5 m wind speed to IP Wind	CSTARS 14.5 m wind gusts (ms^{-1})	Ratio of 14.5 m gusts to IP wind	3 m Wind Speed (ms^{-1})	Ratio of 3 m wind speed to IP Wind
4a	18.79	4.50	0.24	2.63	0.14	6.84	0.36	4.55	0.24
5a	19.73	7.08	0.36	5.45	0.28	10.83	0.55	2.62	0.13
9a	21.97	8.72	0.40	7.16	0.33	12.45	0.57	3.51	0.16
9b	22.33	8.38	0.38	6.29	0.28	11.28	0.51	3.14	0.14
9c	21.93	7.63	0.35	5.91	0.27	11.46	0.52	3.79	0.17
10a	21.48	8.74	0.41	6.80	0.32	12.40	0.58	3.88	0.18
10b	21.10	9.66	0.46	7.92	0.38	12.60	0.60	3.83	0.18
11a	21.69	8.93	0.41	6.63	0.31	12.20	0.56	3.35	0.15
18a	11.70	4.18	0.36	3.19	0.27	7.72	0.66	2.57	0.22
18b	12.18	3.31	0.27	2.13	0.18	6.44	0.53	2.03	0.17
21a	17.56	5.43	0.31	3.56	0.20	8.05	0.46	N/A	N/A
21b	16.03	6.23	0.39	4.64	0.29	9.27	0.58	N/A	N/A
23a	19.28	6.38	0.33	4.38	0.23	9.30	0.48	3.45	0.18
23b	20.72	6.41	0.31	4.43	0.21	9.44	0.46	2.95	0.14
Mean	**19.04**	**6.83**	**0.36**	**5.08**	**0.26**	**10.02**	**0.53**	**3.30**	**0.17**

3.6 Summary

Fourteen cases from stratiform periods in outer rainbands of three tropical systems in August and September 2008 in South Florida are analyzed to study rainband wind structure. These cases are chosen due to their constant reflectivity profile with time, presence of a bright band located around 4.5 km, and light to moderate rainfall rate. Time periods during the 14 rainbands are evaluated using a VAD technique with Level 2

KAMX radar data to study wind structure in high resolution. Results show that the maximum horizontal wind speed in the rainbands is typically between 1000-1500 meters in height, and remains nearly constant up to 3000 meters AGL, then decreases between 3000 and 4000 meters AGL. Several cases show evidence of a secondary horizontal wind maximum around 3500-5000 meters AGL. This secondary wind maximum is found to be stronger than the low level wind maximum in the four cases from stronger storms observed at further distances from storm center. Wind direction profiles show a general veering with height of 20^{o}-30^{o} over the lowest 1000-1500 meters AGL, or up to the height of the wind maximum.

Radial and tangential wind components are also analyzed and show a mean transition from radial inflow at low levels to radial outflow around 2500-3000 meters AGL. The radial inflow maximum is around a height of 500 meters, though maximum outflow is much more variable in height. The strength of the maximum radial inflow is on average 2-3 ms^{-1} higher than the strength of the maximum radial outflow. The majority of the VAD profiles show evidence of a second radial inflow between 4500-5500 meters AGL. Tangential wind profiles are all positive, with a peak between 1000-3000 meters AGL, where values are close to constant with height. Although most tangential profiles decrease in speed with height above 3000 meters AGL, a few of the cases do show evidence of a small tangential wind maximum around 3000-4000 meters AGL, especially during the stronger storms Gustav and Ike, though there is also some evidence of it occurring during some of the rainbands from Tropical Storm Fay as well. Tangential wind profiles by rainband closely match the mean horizontal wind in strength and structure, as they make up the largest component of total horizontal winds, although

changes in wind directions appear to be associated with changes in the radial wind. These findings on radial and tangential wind profiles are in agreement with those found during previous studies, both over water and over land.

Temporal variability within Band 21 is examined with half hour averaged profiles during Band 21a and Band 21b to illustrate changes over a four hour period. Two striking features seen during this analysis are an ascending and strengthening low-level wind maximum during Band 21a that is gone an hour later by Band 21b, and a decrease in the low-level radial inflow over time. Analysis of plan position indicator (PPI) radar imagery showed that Band 21a is a diagonal cross-section through the early part of the rainband, and then an hour-long gap of more convection conditions occurs before the shorter Band 21b at the end of the band. The drastic differences in wind structure between the 30 minute averages during Band 21a and 21b further helps to illustrate that while both scenarios are stratiform rainbands, the location of the rainband sampled can cause the observed conditions to vary widely.

Radial and tangential VAD profiles during stratiform periods are compared to clear periods before and after rainbands using MAPR data and rawindsondes. In the case study presented, an increase in V_t is apparent over time that is related to the storm center moving towards the site. A low-level wind maximum is present around 1000 meters AGL, and it appears to rise in height and broaden with rainband passage. The depth of the radial inflow layer is shown to deepen during the rainband case study, and then return to a more shallow level after rainband passage.

All rainbands show a logarithmic wind speed decrease below 500 meters AGL, though it often changes slope in the lowest part of the surface layer (lowest 200 meters

AGL). These winds are plotted against a logarithm of height using the log-wind profile (Equation 3.1) from Stull (1988) and are each solved for the various components of the equation. The goodness of fit to the linear plot is very high, and the calculated friction velocity is reasonable based on the rainband conditions. While the aerodynamic roughness length is found to be much more variable than previous observations, using the calculated components allows for the estimation of winds from 65-500 meters AGL with decent accuracy. However, a constant value for extrapolating wind speeds near the surface in future storms appears unrealistic based on this data set. While there is a correlation between higher values of aerodynamic roughness length and higher values of friction velocity and maximum wind speed, there does seem to be a high dependency of z_0 on the heights used in the calculation of logarithmic fit which could easily influence the values of the calculated variables.

A comparison between surface winds and HBL winds found a mean ratio of 0.36 between 18 meter mean wind speeds and the mean wind speed at the top of the HBL. This ratio is lower than even the lowest bound of 0.55 found by Powell and Black (1990) between ocean buoys and flight-level winds, and much lower than the 0.67 ratio found by Blackwell (2000) over land to flight-level winds. The much lower ratios could partially be due to the friction effects of being over land, the fact that these observations are located far from the storm center, and the fact that the mean HBL wind speeds are lower than those measured by previous studies. Using 2-minute wind gust data from the 14.5 meters CSTARS tower sensor to approximate the maximum 10 meter maximum wind speed causes the mean ratio increases to 0.53, which closer to the low end of the range suggested by Powell and Black (1990).

Rainband characteristics can change drastically depending on storm intensity, storm-relative location, and rainband stage, so it is important to remember that even with several case profiles, these observations are still only point profiles in a much larger tropical system. While many of the VAD observed wind structure components agree with previous observations, the high resolution of this data set and wider variability in observing instruments allows for the study the variability in structure in greater depth. Though not all of these observations agree with previously published work, having several cases for analysis helps to solidify the belief that the differences seen could be partially due to the location over land, which makes this data a valuable comparison to data collected over the ocean. A major benefit of this field site location is that due to the close proximity to the KAMX WSR-88D, high-resolution (~ 7 meter) VAD data was obtained from 65 meters above ground level up to 6550 meters above ground level and compared to co-located vertically pointing data sets. This was especially useful in studying the logarithmic wind profile in great detail, which is something that is challenging to do with aircraft observations. It is important to study and understand the layer of the atmosphere closest to the surface in order to better be able to predict storm conditions and their impact on life and property. This study has provided further evidence in the location and strength of wind speed maximums in tropical cyclone rainbands over land. Even in conditions that are thought of as stratiform, wind speed maxima are evident and understanding where they are located and how they change is important current and ongoing work.

Chapter 4: Case Studies of Stratiform Variability

4.1 Background

The work in Chapter 3 of this dissertation shows profiles of wind speed that are averaged over certain stratiform periods ranging from 6 minutes to 165 minutes. These profiles give a good representation of the mean characteristics of the vertical structure of these rainbands, but the question of how much vertical and horizontal variability exists in these seemingly stratiform conditions is still unanswered. This is important in terms of evaluating the presence and impact of hurricane boundary layer (HBL) rolls, which have been found to exist in the lowest 400-1000 meters of the atmosphere on wavelengths of about 1000-2000 meters (e.g. Lorsolo et al. 2008, Morrison et al. 2005) and variability due to small spiral bands (e.g. Gall et al. 1998) which have wavelengths of about 10 km and can exist up to depths of 6000 meters. While the time series of vertical profiles during Band 21a (Figure 3.7) helps showcase the longer-scale (> 30 minute) changes in the rainband with time, to observe the shorter-scale (< 5 minute) variability it is important to look at two-dimensional images of variables plotted in time and height. This chapter presents an in-depth look at the four stratiform periods lasting 30 minutes or longer-Bands 9a, 4a, 21a and 21b. The majority of the data presented in this chapter comes from the wind profiler, which has a resolution of 30 seconds spatially and 200 meters vertically from 400-8000 meters, which means that any turbulent features on longer scales than these can be observed.

The moments (reflectivity and vertical velocity) for the four cases are presented in Section 4.2, with a more detailed analysis of the variability within the stratiform parts of the rainbands presented later in the chapter. The variability seen in the residual vertical

velocity and radial and tangential winds are showcased and related to possible forcings in Section 4.3. Section 4.4 combines vertical and horizontal variability to look at fluxes in the rainbands, and Section 4.5 compares the turbulent kinetic energy of the rainbands. Two potential forcings behind the fluxes shown are described in Section 4.6 with supporting evidence. The chapter concludes with a discussion of all the variability seen in the four case studies in Section 4.7, along with an attempt to explain the causes of the variability.

4.2 Four Case Studies

The four case studies used for this chapter come from stratiform rainbands lasting 30 minutes or longer so that 60 or more 30-second temporal observations are available to examine the variability. The first case comes from Band 9. It was one of the rainbands that was observed at a closer distance (156 km) to the center of Tropical Storm Fay, and was observed along-band. Figure 4.1 shows X-band and wind profiler (MAPR) moments from Band 9 on August 19, 2008. This rainband began with several equally spaced convective elements before the mostly stratiform remainder of the rainband passed overhead for the next 2.5 hours. During the three stratiform periods from 2:06-3:36 UTC (Band 9a), 3:53-4:11 UTC (Band 9b), and 4:18-4:30 UTC (Band 9c) the melting layer is prominent as an increase in both reflectivity and vertical velocity. Figure 4.1 also shows evidence of variability in vertical motions, even in the regions considered to be stratiform. This variability appears to be on similar time scales to the equally spaced convective elements in the beginning of the rainband and may be induced by gravity waves or HBL

rolls. It is important to note that the signal to noise ratio shown in the top of both plots is uncalibrated, and is shown only as a representation of the storm structure.

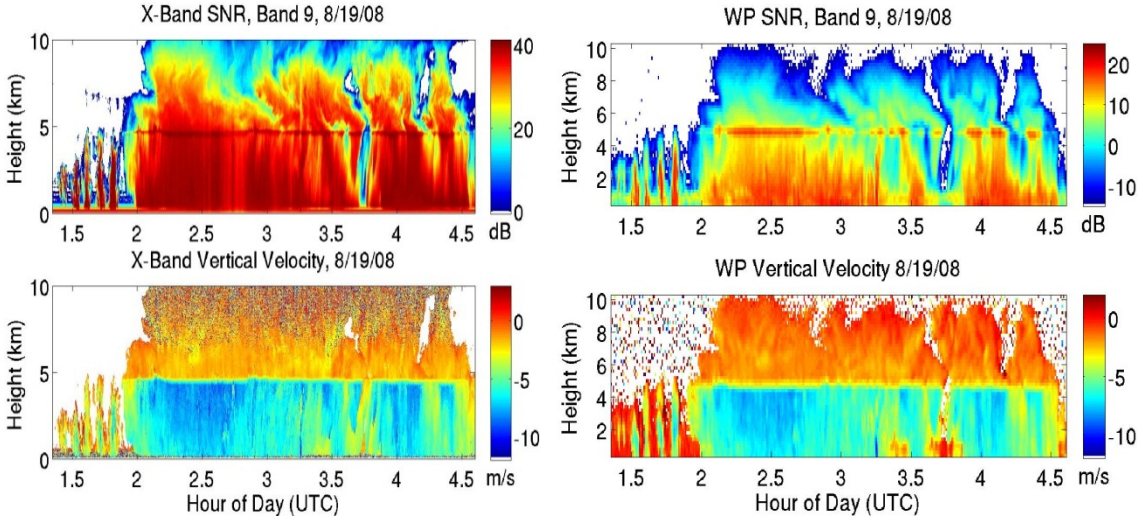

Figure 4.1: Radar observations of Band 9, which has both a convective portion and three stratiform regions. Two moments from the X-band are shown on the left and from the wind profiler on the right: reflectivity (uncalibrated, top) and Doppler velocity (bottom, where negative values represent motion towards the radar and are a combination of vertical air motion and drop fall speed).

The MAPR winds are used to examine the *u* and *v* components of the horizontal winds, which are shown in Figure 4.2 for Band 9. Winds below the melting level were mostly from the east, with a small weak westward component just below the melting level. The north-south wind component shows winds from the south throughout the lowest 10 km, which is the direction from which the rainband was approaching.

The moments from the remaining three stratiform cases are shown in Figure 4.3. Band 4a was an entirely stratiform rainband which occurred on August 18, 2008 and was an early leading rainband of Tropical Storm Fay as it approached South Florida. As seen in the MAPR moments in the left panel of Figure 4.3, Band 4a did have some variability in SNR (top panel) and vertical air motions (bottom panel), but the melting level remained close to constant throughout the band. Band 21 occurred on August 31, 2008

and was the longest of the observed rainbands, lasting over 5 hours as it streamed northward over the field site. Band 21 was also from the strongest storm, Hurricane Gustav, which was a Category 4 system at the time of observation. Due to the large distance from storm center (452 km), conditions sampled at the field site were not extreme. Band 21 was broken into two stratiform areas, Band 21a, which lasted over 2.5 hours, and Band 21b which occurred after an hour-long more convective period in the rainband and only lasted 30 minutes. As seen in the MAPR moments in the middle panel of Figure 4.3, Band 21a did have some variability in SNR (top panel) and vertical air motions (bottom panel), especially early in the time period, but the melting level remained present and close to a constant height throughout the band. The SNR (upper panel) and vertical motions (lower panel) for Band 21b are shown in the right panel of Figure 4.3, and show remarkable consistency in conditions, with observations that are more uniform than those observed in Band 21a.

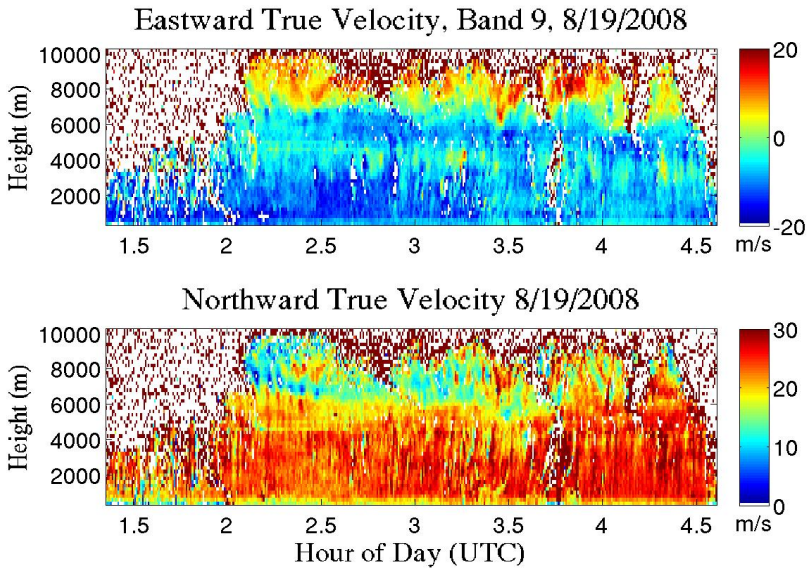

Figure 4.2: True wind motions from the MAPR during Fay Band 9. The top image shows the eastward velocity with positive values representing winds from the west and negative values representing winds from the east. The lower image represents the northward velocity component, with positive values representing winds from the south.

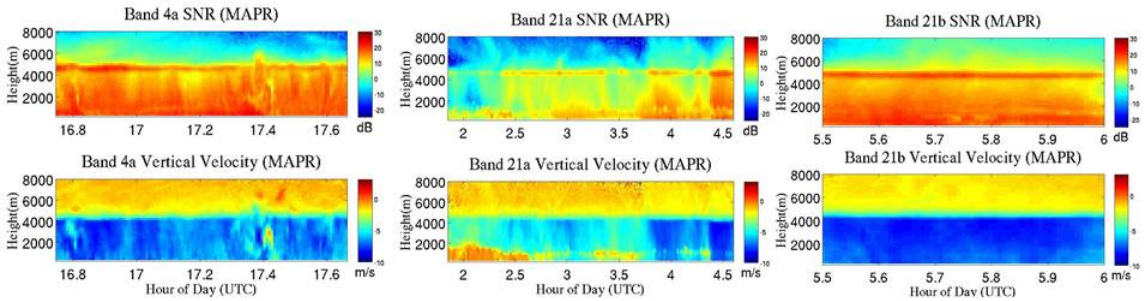

Figure 4.3: MAPR SNR (top panels) and vertical velocity (bottom panels) for Bands 4a (left), 21a (middle) and 21b (right).

4.3 Variability

4.3.1 Residual Vertical Velocity

The three stratiform periods shown in Figure 4.3 can be used along with Band 9a to showcase the vertical variability in the stratiform conditions. One complication in interpreting the vertical velocity observations (as mentioned in Section 2.3.3) is that they are the sum of both the rainfall velocity and the vertical air motions. If it is assumed that the rain fall velocity is fairly constant during stratiform rain, then the mean vertical velocity on 30 minute averages can be removed at each radar gate to remove the mean rain drop velocities to examine the scales of vertical motion perturbations. In this case, the velocity fluctuation (w') still represents the combination of both the vertical air motion and changes in fall speeds due to larger raindrops. Figure 4.4 shows w' from the X-band for a Band 9a, the largest stratiform region of Band 9, where the rainrate was light and constant (<10 millimeters per hour). This figure shows small scale vertical velocity perturbations extending from the surface up to, and even above, the melting layer.

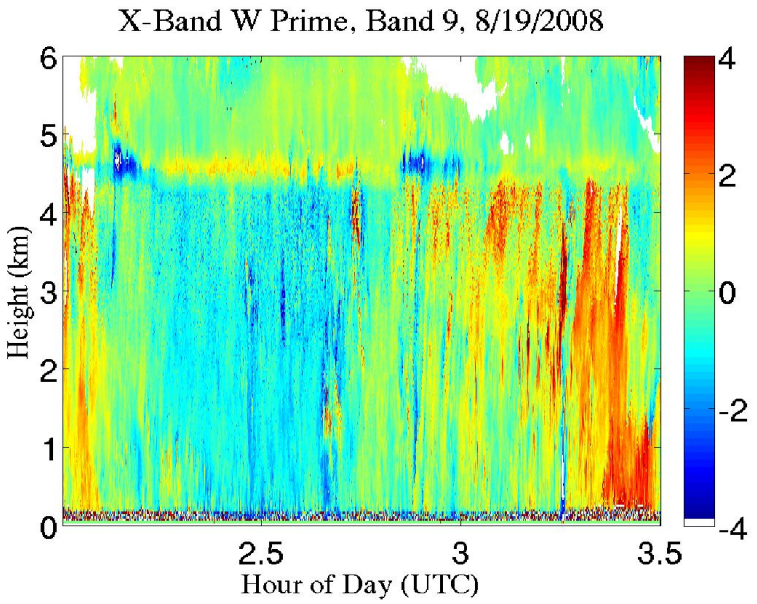

Figure 4.4: w' prime from the X-band radar during Band 9a. The removal of $\overline{w}$ on 30 minute averages simulates removing the fall velocity of the rain, leaving w' to represent air motions and drop size differences. Negative values represent motion towards the radar.

Perturbation w values were also estimated for Band 9a using the MAPR data. A comparison of the w' from the MAPR with the X-band values calculated at a height of 2000 meters is shown in Figure 4.5 where the blue line is w' from the X-band and the red line is w' from the MAPR. Due to the higher temporal resolution of the X-band than MAPR (1 second vs. 30 second), the fine-scale variability (30-60 seconds temporally) in wind motions is much better defined by the X-band. However, even the MAPR data (red line) shows small-scale variability (2-3 minutes temporally) along with larger scale motions during the time period. The fine scale variability is on the order of ~ 4 ms^{-1}. The variability in DSD at the surface during this time period from the WXT instrument (Figure 4.6) show that the majority of drops are between 1.0-2.5 mm. As larger drops have higher terminal velocities, the larger bin sizes can be compared, even though there are very few drops in the 3 mm and 5 mm bins. Using the drop size fall speed chart from

Foote and DuToit (1969, Figure A9 in Appendix 9), the 3 mm drops have a terminal fall speed of ~ 9 ms^{-1} while the 5 mm drops have a terminal fall speed of just over 10 ms^{-1}. The velocity variations seen in Figure 4.5 are too large to be solely due to drop size variability, which implies that w' is a function of both w' of the drops and w' of the air.

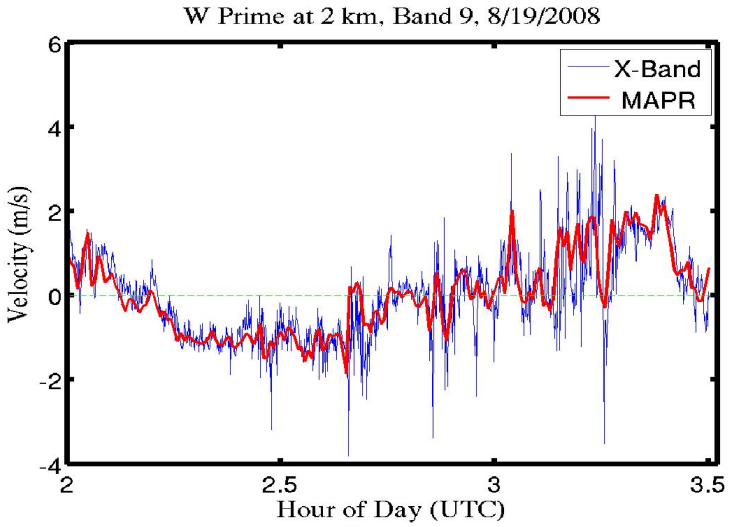

Figure 4.5: Vertical velocity perturbations w' at 2 km height from the X-band (blue) and wind profiler (red) during Band 9a. The dashed green line shows zero velocity. Negative values represent downward motion. The resolution of the MAPR is 30 seconds while the X-band is higher at 1 sample per second.

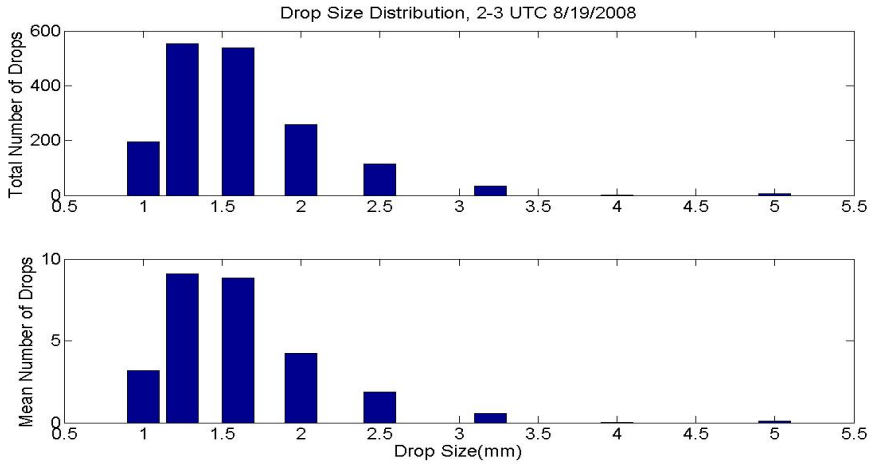

Figure 4.6: Surface total (upper panel) and mean (lower panel) DSD from the WXT for an hour (200-300 UTC) of Band 9a.

The vertical velocity perturbations from the remaining three cases are shown in Figure 4.7, and consist of alternating areas of upward and downward motion extending from the surface to the melting level at 4500 meters for Band 4a (left panel) and Band 21a (middle panel). The vertical features in these two cases are similar to what was seen in Band 9a (Figure 4.4). However, during Band 21b (Figure 4.7, right panel) the strength of these vertical features has weakened, although some evidence of weak upward and downward motion extending from the surface to the melting level is still present.

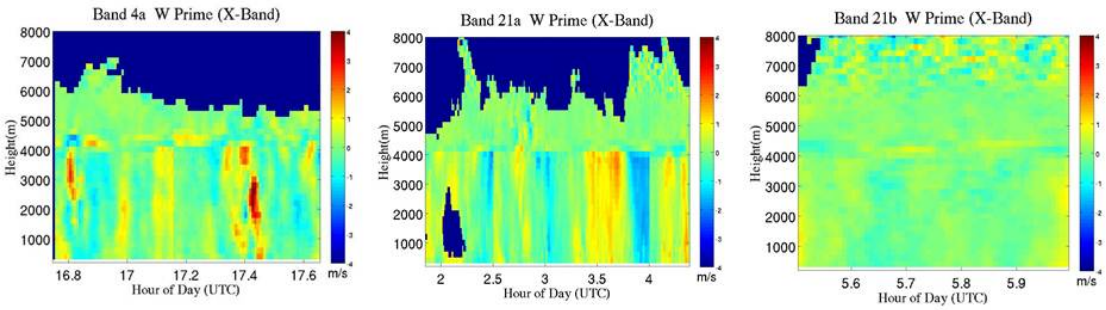

Figure 4.7: As in Figure 4.4, but for Bands 4a (left), 21a (middle), and 21b (right).

4.3.2 Surface Connections to Velocity Perturbations

In an attempt to deconvolve the potential causes of the velocity variations seen in Figure 4.4, the observed variability in w' is compared to variations in reflectivity, surface drop size, and rainrate with time. Values of w' at 1000 meters are compared with these three variables for Band 9a in Figure 4.8. The top panel shows w' along with scaled signal to noise ratio (SNR) at 1000 meters. Since larger raindrops have a higher reflectivity and also fall at a faster rate, a high level of negative correlation between these two variables would suggest that most of the vertical variability is due to differences in drop size. As seen in this figure, there is some agreement between stronger downward

motion and increased reflectivity, but with a correlation coefficient of -0.59, only a moderate correlation exists.

The second panel in Figure 4.8 shows the volume-weighted mean drop diameter (D_m) from the Parsivel disdrometer. Some of the Parsivel data were removed during post-processing during the early part of this rainband, but again it is expected that larger surface drops would be related to more downward motion. although there is some agreement between w' and D_m, the correlation coefficient of -0.63 suggests that there is slightly more agreement than w' with SNR, although it still does not explain all of the variability. The third panel in Figure 4.8 shows the surface rainrate from the Parsivel disdrometer. This correlation is more difficult to interpret, since as both larger drops and stronger downdrafts could increase the surface rainrate, explaining why a higher correlation coefficient with w' could exist. Although there is likely some evaporation of the rain occurring between 1000 meters and the surface, the surface rainrate should represent the combination of both effects on vertical variability. However, the correlation here is lower at -0.34, signifying that there is not a clear and consistent connection between the two variables. Finally, the bottom panel of Figure 4.8 shows the three largest drop size bins from the WXT- 3.2 mm, 4 mm, and 5 mm- with time. The rainrate from this instrument does have a strong correlation with the Parsivel rainrate (correlation coefficient of 0.84, figure not shown), but the low correlation of 0.18 between the sum of the three largest WXT bins and w' suggests that again there is not a clear answer to explain the observed variability. An additional point to note in Figure 4.8 is the spike in D_m just after 0312 UTC (3.2 UTC). This large value of D_m suggests that a few large drops are contributing to a heavier rainrate and higher drop variability. This is supported

by the increase seen in 3.2 mm (and larger) surface drops seen with the WXT at the same time period.

A similar comparison between w' and variations in reflectivity, surface drop size, and rainrate with time is done for Bands 4a (Figure 4.9), 21a (Figure 4.10), and 21b (Figure 4.11). A slice through w' along 1000 meters is compared with these three variables for Band 4a in Figure 4.9. The top panel shows w' along with a scaled SNR at 1000 meters. The correlation here is lower than in Band 9a at 0.16. The second panel in Figure 4.9 shows volume-weighted mean drop diameter (D_m) from the Parsivel disdrometer. Again it is expected that larger surface drops would be related to more downward motion. Although there is some agreement between these, the correlation coefficient of 0.44 suggests while there is more agreement than with SNR, it still does not explain all of the variability. The third panel in Figure 4.9 shows the surface rainrate from the Parsivel disdrometer. The correlation here is still low at 0.19, signifying that there is not a clear and consistent connection between the two variables. Finally, the bottom panel of Figure 4.9 shows the three largest drop size bins from the WXT- 3.2 mm, 4 mm, and 5 mm- with time. The low correlation of 0.13 between the sum of the three largest WXT bins and w' suggests that again there is not a clear answer to explain the forcing mechanisms behind the observed variability. In Figure 4.9, a large median volume diameter (D_m) is again seen at 1724 UTC (17.6 UTC), that corresponds with a peak in 3.2 mm surface drops, suggesting that a few big drops make up the D_m spike.

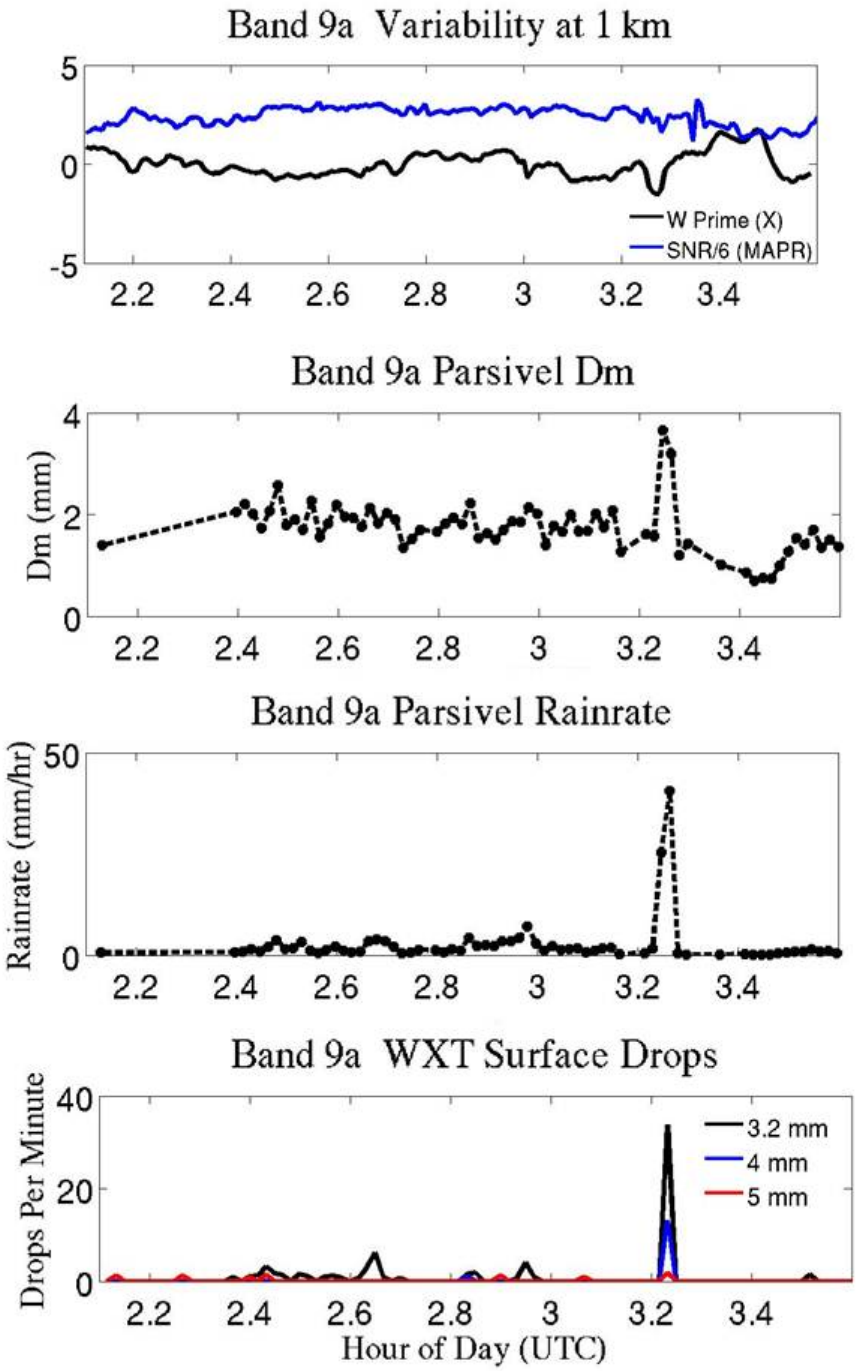

Figure 4.8: Time series during Band 9a of *w'* (top panel) from the X-band (black) and SNR from the MAPR (blue) at 1000 meters; surface Dm (mm) from the Parsivel (second panel). Third panel: surface rainrate (millimeters per hour) from the Parsivel. Bottom panel: surface distribution of three largest WXT drop size bins- 3.2 millimeters (black), 4.0 millimeters (blue) and 5.0 millimeters (red).

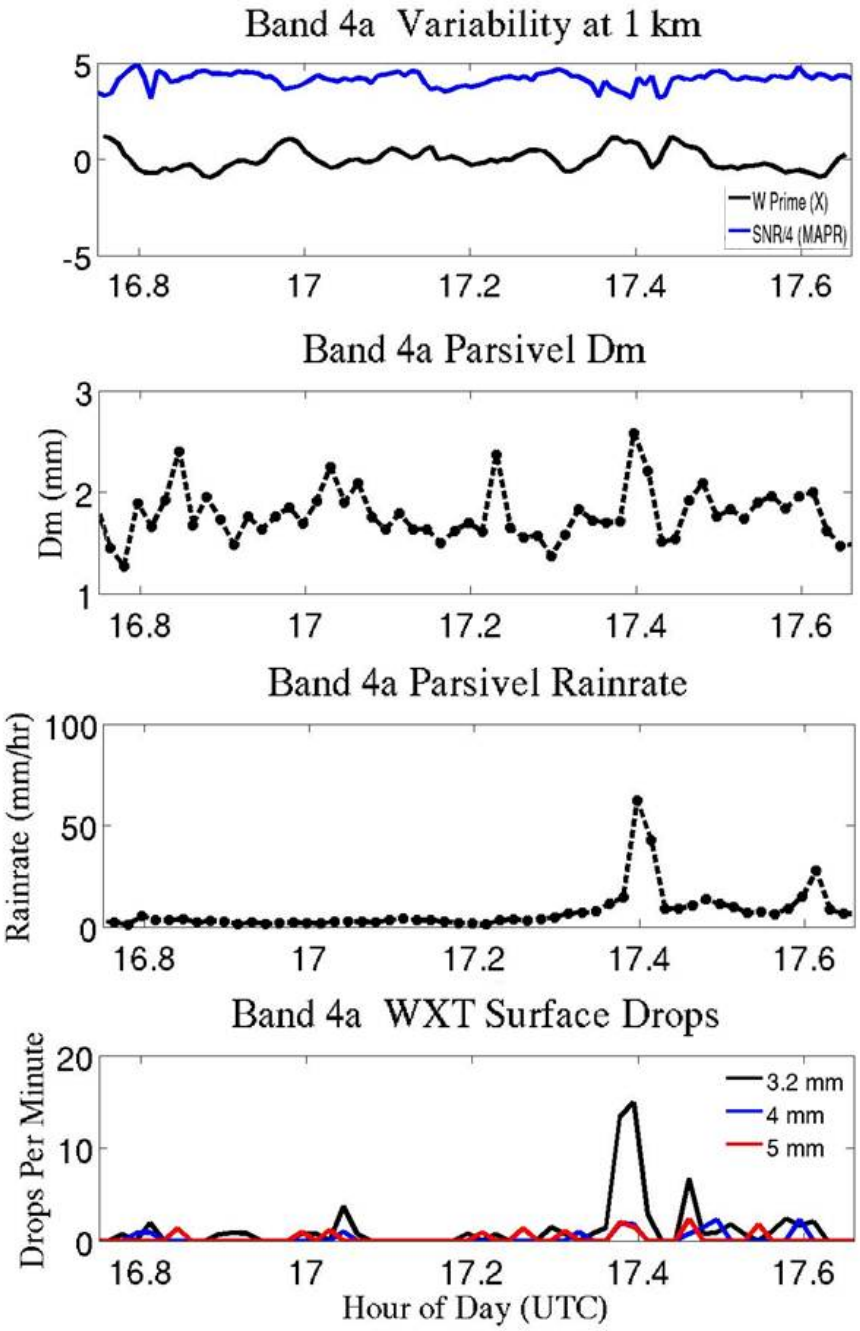

Figure 4.9: As in Figure 4.8 except for Band 4a.

A slice through w' along 1000 meters is compared to reflectivity and surface drop size and rainrate variability during Band 21a in Figure 4.10. The top panel shows w'

along with a scaled SNR at 1000 meters. The correlation here seems to be stronger visually, but actually is lower than in Bands 4a and 9a at -0.02. The second panel in Figure 4.10 shows volume-weighted mean drop diameter (D_m) from the Parsivel disdrometer. The Parsivel data from the first half of the rainband period was removed by NC State during post processing, making any correlations calculated less valuable. Again it is expected that larger surface drops would be related to more downward motion. Although there is some agreement between these, the correlation coefficient of -0.25 suggests while there is more agreement than with SNR, it still does not explain all of the variability. The third panel in Figure 4.10 shows the surface rainrate from the Parsivel disdrometer. The correlation here is still very low at -0.06, signifying that once again there is not a clear and consistent connection between the two variables. There is no WXT data available for Bands 21a or 21b, so a time series plot of surface drop size bins is not shown.

Finally, comparisons between w' and reflectivity at 1000 meters and surface variables are shown for Band 21b in Figure 4.11. The top panel shows w' along with a scaled SNR at 1000 meters. Unlike the previous three cases, the variation in both variables has decreased, and the correlation is moderate at -0.57. The second panel in Figure 4.11 shows volume-weighted mean drop diameter (D_m) from the Parsivel disdrometer, which has the highest correlation of the 4 cases at -0.50. The third panel in Figure 4.11 shows the surface rainrate from the Parsivel disdrometer, which also has a moderate correlation of -0.57. Although this correlation is higher than any of the three previous cases, it is more difficult to interpret, as both larger drops and stronger downdrafts could increase the surface rainrate, explaining why a higher correlation with

w' could exist. The Parsivel data for Band 21b shows a variability of 2-3 minutes between rain peaks, which is on a similar temporal scale as the radar observed variability seen in the w' data in the far right panel of Figure 4.7. Once again, this case suggests that there is not a clear and consistent connection between variables, and no way to completely deconvolve the relative impact of vertical air motions and drop size variability.

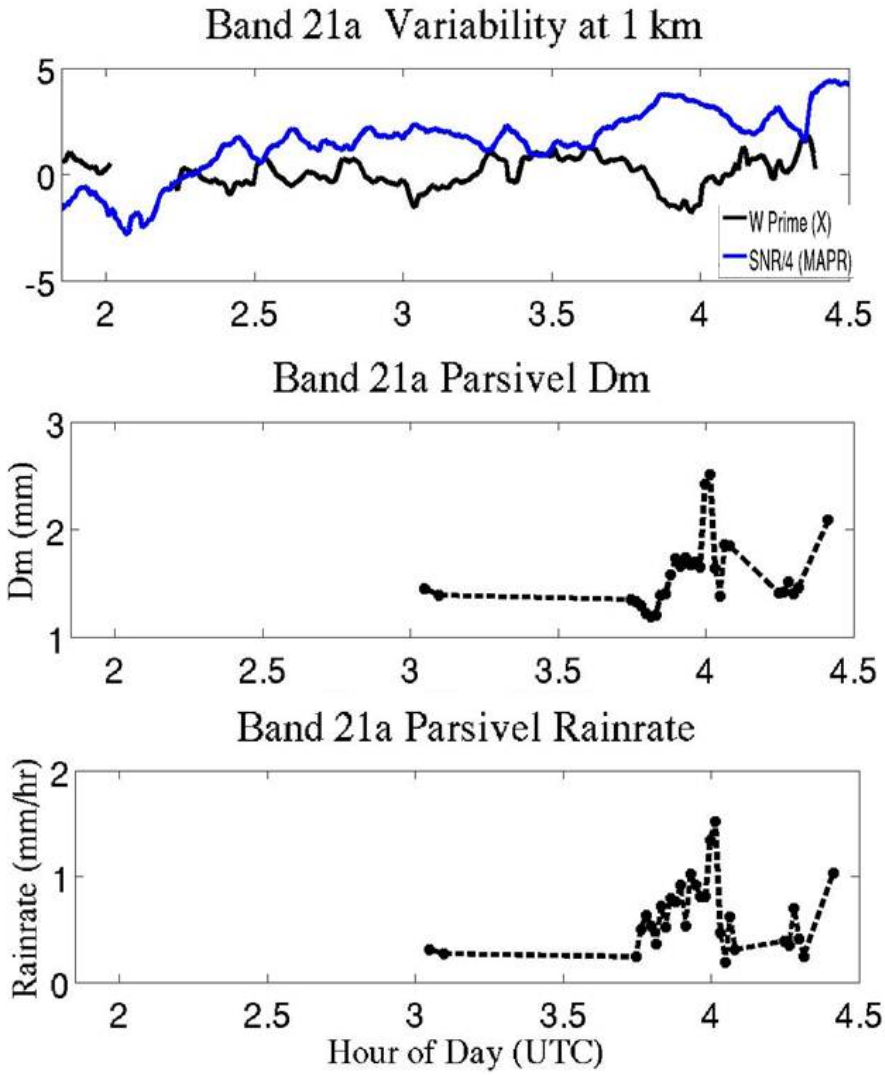

Figure 4.10: As in Figure 4.8 except for Band 21a. There is no available WXT drop size data during this time period.

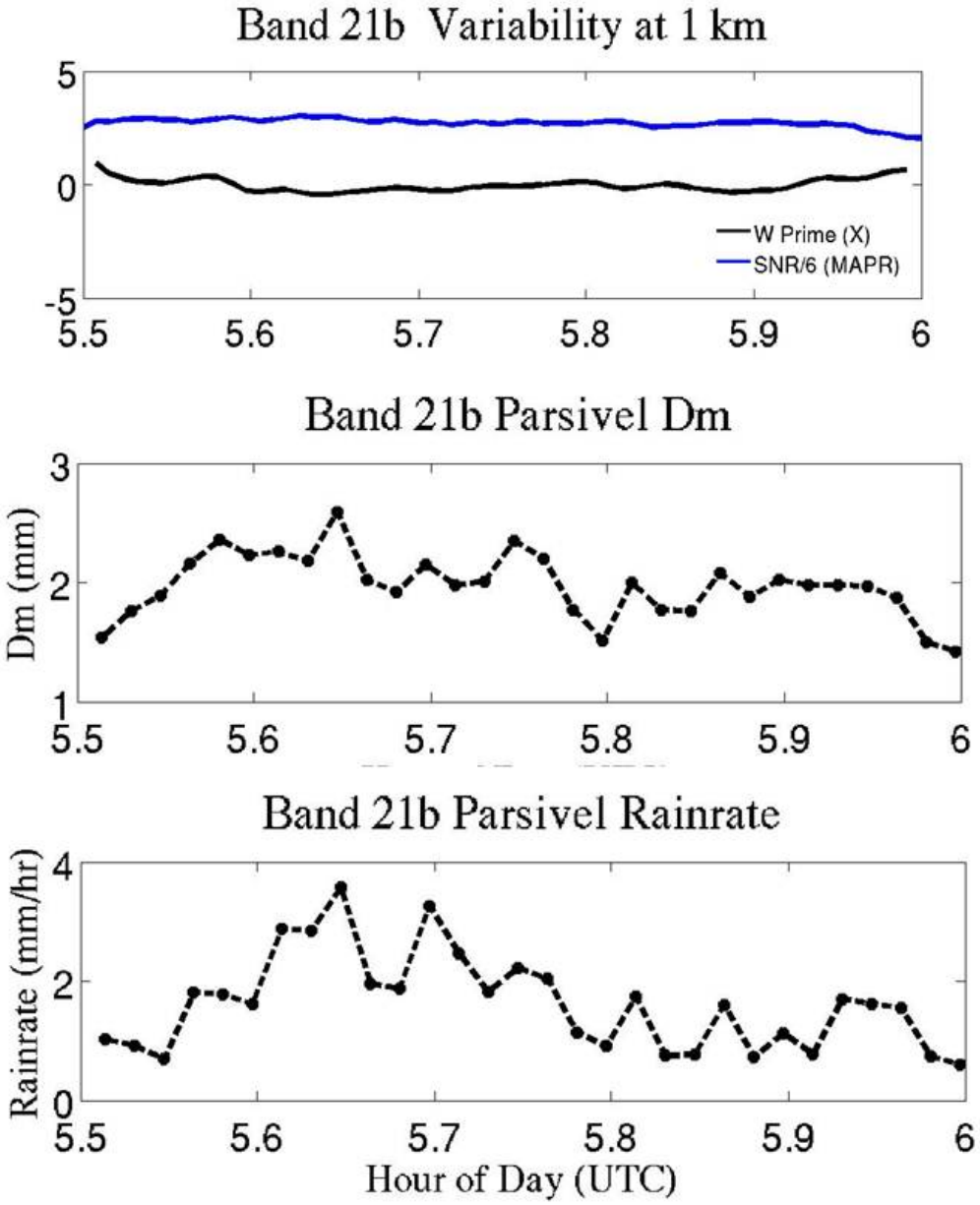

Figure 4.11: As in Figure 4.8 except for Band 21b. There is no available WXT drop size data during this time period.

4.3.3 Radial and Tangential Wind Perturbations

This section shows how the radial (V_r) and tangential (V_t) winds and the perturbations of these (V_r' and V_t', respectively) look for Band 9. Only one of the four cases is shown here, but the residual wind components are combined with vertical air

perturbations to examine the fluxes in Section 4.4, so it is important to include an example of how they appear for at least one case. The radial and tangential winds were estimated from the MAPR winds using the closest center position as described in Section 3.3. The time/height sections of these wind components for Band 9 are shown in Figure 4.12. Below the melting level, radial winds show flow towards the eye at low levels and flow away from the eye above 3500 meters. Tangential winds are positive (cyclonic) at all levels, with the peak values occurring between 1000-3000 meters and decreasing with height. Both of these results are in agreement with those observed during Hurricane Floyd (1981) by Barnes et al. (1983), with radial inflow below 3000-4000 meters and peak tangential winds between 1000-2000 meters.

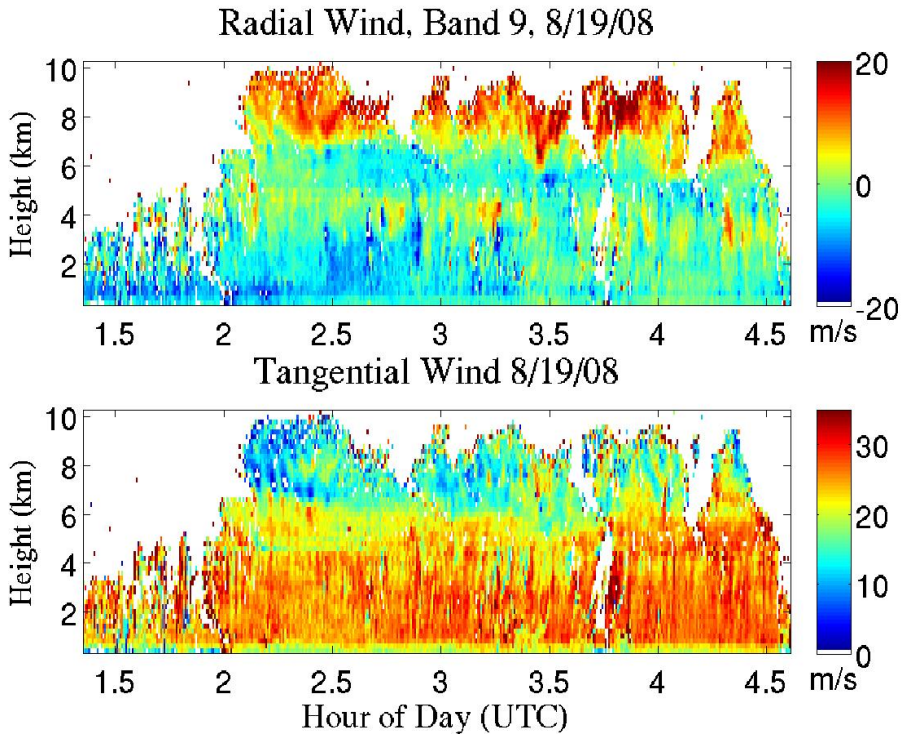

Figure 4.12: MAPR radial (top) and tangential (bottom) winds during Band 9. Radial winds are positive away from the eye and tangential winds are positive cyclonic.

The wind variability was further characterized by examining the perturbations of the wind components relative to the mean. These perturbations--V_r' and V_t' -- were obtained by removing the mean values in half hour increments at each height and are shown in Figure 4.13. Here it can be seen that the residual radial velocity contains small regions of variability that exist from the surface up to the melting level (such as the streak seen just before 300 UTC.) These streaks last for about 4-5 minutes, which puts them on length scales of 6.0-7.5 km when multiplied by the mean wind of 25 ms^{-1}. One theory is that these variations may be related to HBL rolls. At first glance there does not seem to be a direct connection between the two, as HBL rolls are generally only seen in the lowest 1000 meters of the BL, and on wavelengths from 500 meters up to 3000 m (Morrison et al. 2005). However, it is possible that HBL rolls are just the generating mechanism for these perturbations, and there is enough moist instability, even in the stratiform rainbands, to allow these perturbations to be carried up to the melting level. It is also possible that the larger scales of rolls are triggering the features seen above the HBL since a spectrum of roll scales exists.

A supporting factor to this theory is that HBL rolls are more likely in the direction of the wind shear, and the variations show up more prominently the radial image than in the tangential one. Rolls have also been seen in modeling studies (e.g. Nolan 2005) with wavelengths of 3000-5000 meters. These roll instabilities are theorized to gain some of their energy from the vertical shear associated with the reversal of the radial flow at the top of the HBL. Vertical transports could then help to carry this energy up to the melting level.

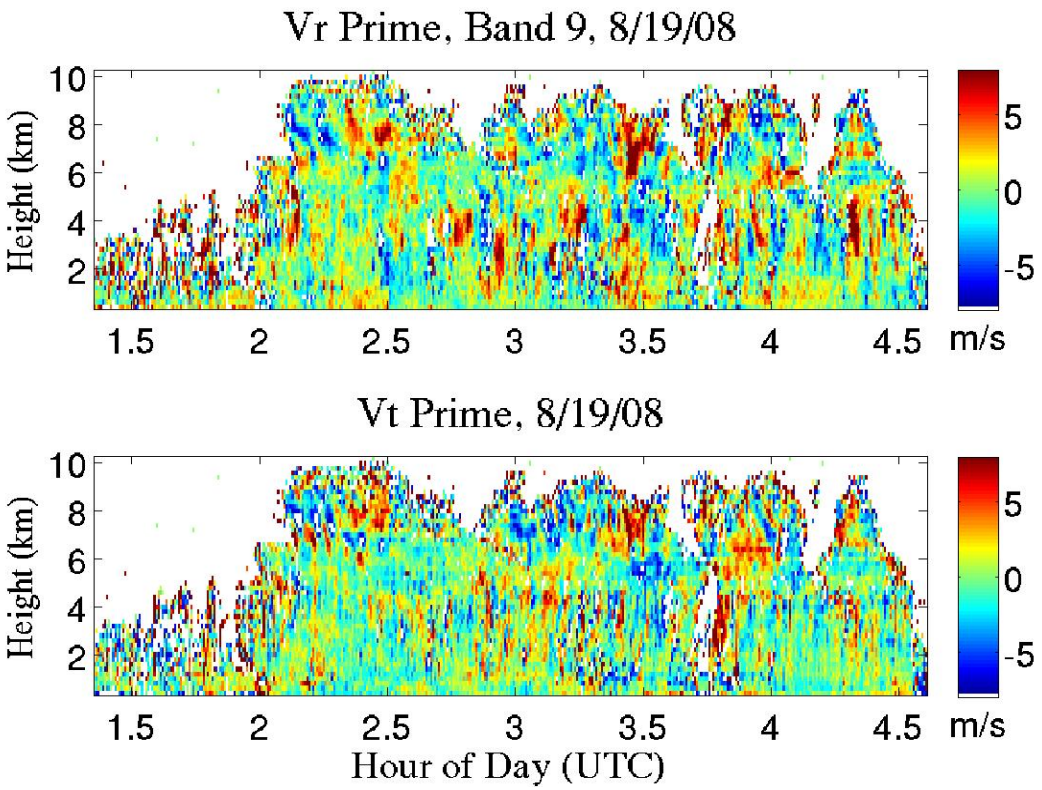

Figure 4.13: V_r' (upper panel) and V_t' (lower panel) from Band 9. These values are calculated by removing the mean V_r and V_t on 30 minute intervals from the MAPR V_r and V_t. For the radial winds, negative value represent winds towards the storm center, while for V_t', positive values represent cyclonic motion.

The perturbations of the wind components relative to the mean shown in this section are combined with w' from Section 4.3.1 in the following section to represent the fluxes occurring in each of the four stratiform cases.

4.4 Fluxes

Further insight into the processes responsible for the variability observed in the rainbands can be examined using the co-variances between the perturbation vertical velocities and the perturbation radial and tangential wind components— $w'V_r'$ and $w'V_t'$. These quantities are estimated using w' from the X-Band and V_r' from the

MAPR in order to avoid introducing instrument bias. The temporal resolution of the X-Band was degraded from 1 second to 30 seconds and the vertical resolution from 60 meters to 200 meters to match up observations from the X-Band and the MAPR. These collocated observations were then used to calculate $w'V_r'$ and $w'V_t'$ for each of the four stratiform cases.

For Band 9a, $w'V_r'$ and $w'V_t'$ are shown in Figures 4.14 and 4.15 respectively. These covariances are not time-averaged, and can be interpreted as local momentum fluxes, if the perturbations are due only to air velocity perturbations and not due to perturbations in the drop size distribution (DSD) than can also affect w'. However, even though it is likely that these figures do show a combination of variability due to fall velocities and air velocities, the correlation is still important and can still be used to represent fluxes as long as it is kept in mind that the sign of the features seen is more significant than the exact magnitude. Figure 4.14 again shows vertical features that extend from about 1000 meters up to the melting level (e.g. the red streak just before 300 UTC). These features are spaced about 15 minutes apart, which equates to a 15.9 km spacing between elements with the rainband moving at 63 $kmhr^{-1}$ due north. These features are also on a similar time scale as the features seen in in Figure 4.13, with a duration of about 5 minutes, corresponding to spatial scale of about 5.3 km.

The wavelengths of these features are significantly larger than those seen in HBL rolls, suggesting that they might have more in common with finescale bands, such as those seen by Gall et al. (1998). These finescale bands were found to exist within the inner 100 km of 3 intense hurricanes, and have scales of 10 km across the rainband and 100 km outwards. They move close to the tangential wind speed of the storm, and are

regions of enhanced updrafts and strong wind variations (~8 ms^{-1}). Gall et al. (1998) theorize that these bands are similar to HBL rolls, although theirs were found to extend up to 5000-6000 meters. However, they state that they do not have enough data to fully describe the finescale rainband features. Although there is not enough data to completely explain the existence of this variability, one possibility is that it is being triggered at low levels (<500 meters), and the instability in the atmosphere is carrying the features up to the melting level. Alternatively, these features could be driven at the melting level, as Gall et al. (1998) defined their finescale bands based on reflectivity data, and variations in dBZ suggest melting or drop size variability that could be occurring well above the HBL.

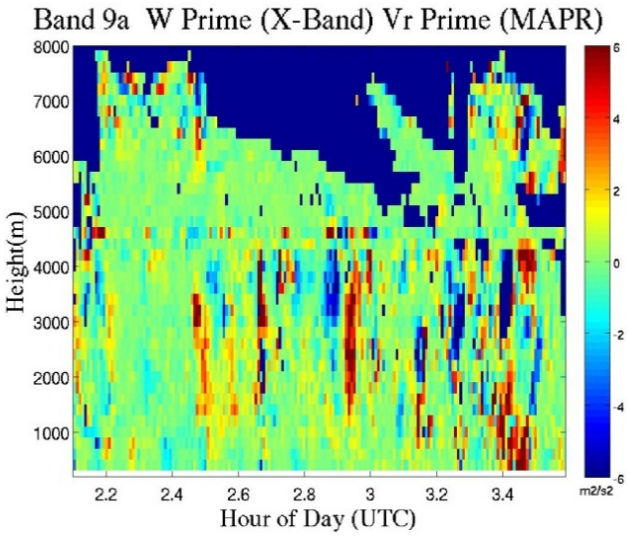

Figure 4.14: $w'V_r'$ **with height for Band 9a.**

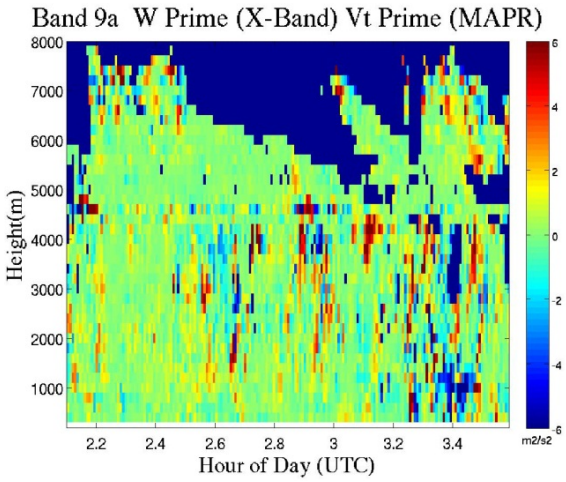

Figure 4.15: As in Figure 4.14, but for $w'V_t'$.

Similarly to the fluxes shown for Band 9a, the covariances $w'V_r'$ and $w'V_t'$ are shown for Bands 4a, 21a and 21b in Figures 4.16, 4.17 and 4.18 respectively. During Band 4a (Figure 4.16), the vertical features extending from the surface to the melting level in $w'V_r'$ (left panel) are still present, but are less obvious than those seen in Figure 4.14 for Band 9a. These features are again spaced about 15 minutes apart, which equates to a 10.2 km spacing between elements with the rainband moving at 46 kilometers per hour ($kmhr^{-1}$) at 338^o. Their duration is again about 5 minutes, which equates to a wavelength of 3.6 km. This is shorter than the 5.3 km wavelength seen in Band 9a, but still longer than typical wavelengths associated with HBL rolls.

For Band 21a (Figure 4.17), the vertical features extending from the surface to the melting level in $w'V_r'$ (left panel) are similar to those observed during Band 9a (Figure 4.14). These features are again spaced about 15 minutes apart, which equates to about an 11 km spacing between elements for the rainband moving at 60 $kmhr^{-1}$ at 315^o. Again, the duration of these elements is about 5 minutes, corresponding to a wavelength of 3.56 km. This is shorter than the 5.3 km wavelength seen in Band 9a and similar to the 3.6 km

wavelength seen in Band 4a, but still longer than typical wavelengths associated with HBL rolls.

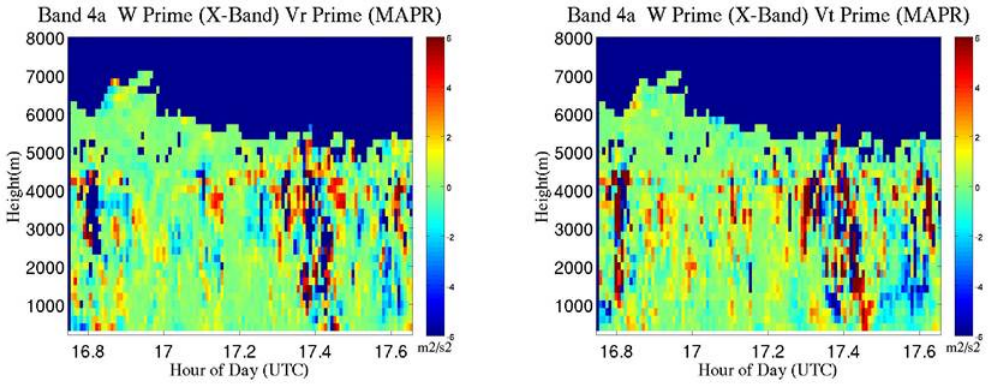

Figure 4.16: $w'V_r'$ **(left) and** $w'V_t'$**(right) during Band 4a. In these plots,** V_r'**and** V_t' **come from the MAPR, while** w'**comes from the X-band radar.**

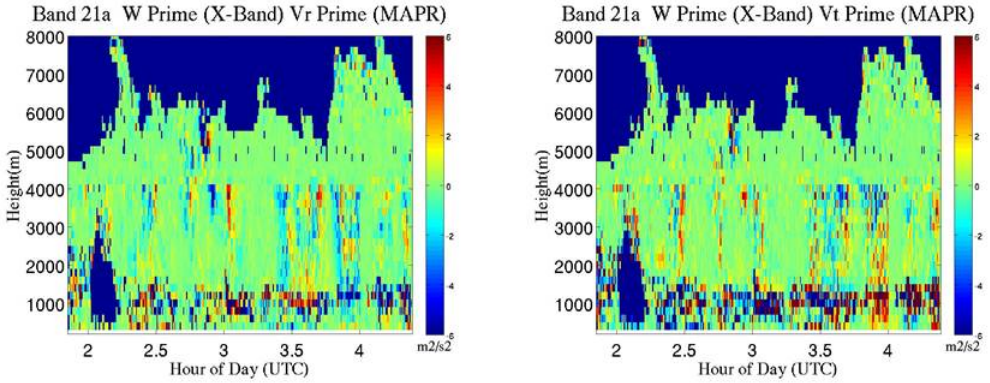

Figure 4.17: Similar to Figure 4.16 but for Band 21a.

In contrast to the previous three cases, the vertical structure of the features has changed during Band 21. In Figure 4.18 there is very little evidence of any vertical features seen previously, which suggests that the dynamics behind Band 21b are somehow different than the other three cases. As shown in Section 3.4.1, Band 21b is most likely influenced by environmental conditions rather than rainband conditions. The fact that this rainband does not contain the vertical turbulence features seen in Band 21

further supports that hypothesis. However, since Band 21b does not contain these features and the previous three cases do, it helps to support the theory that it is something in the rainbands themselves triggering these air motions, and not something in the general storm environment. This is discussed further in Section 4.7.

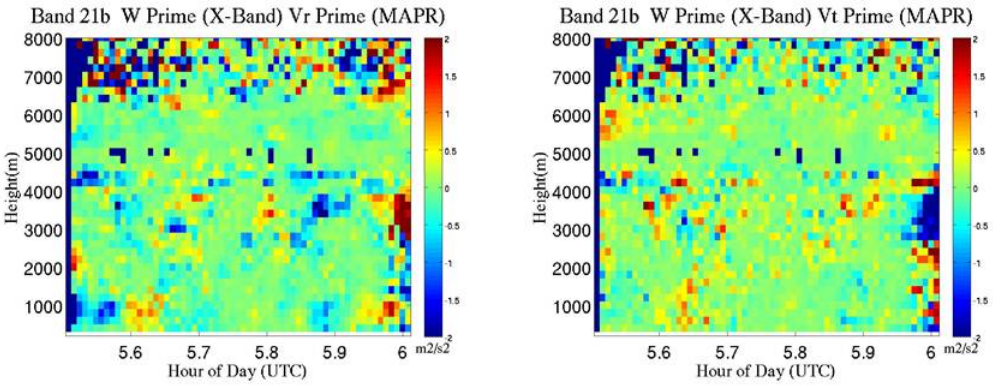

Figure 4.18: Similar to Band 4.16 but for Band 21b. Note the difference in scale for this case.

Time-mean eddy fluxes such as $\overline{w'V_r'}$ can also be computed which consist of the average of the previously shown covariances of $w'V_r'$. An average profile of $\overline{w'V_r'}$ for the stratiform period of Band 9a is shown in Figure 4.19 (left panel). If this figure represents fluxes, one can assume that the fluxes are mostly constant from the surface up to 2500 meters. From 2500 meters to 3500 meters there is a shift in fluxes, which occurs at the same height as the shift in $\overline{V_r}$ (right panel, from MAPR) from towards the eye of the storm to away from the eye. There is also a peak in $\overline{w'V_r'}$ near the height of the radial wind reversal. One possible explanation for this is that the eddy flux divergence is acting to smooth out the radial reversal at this height.

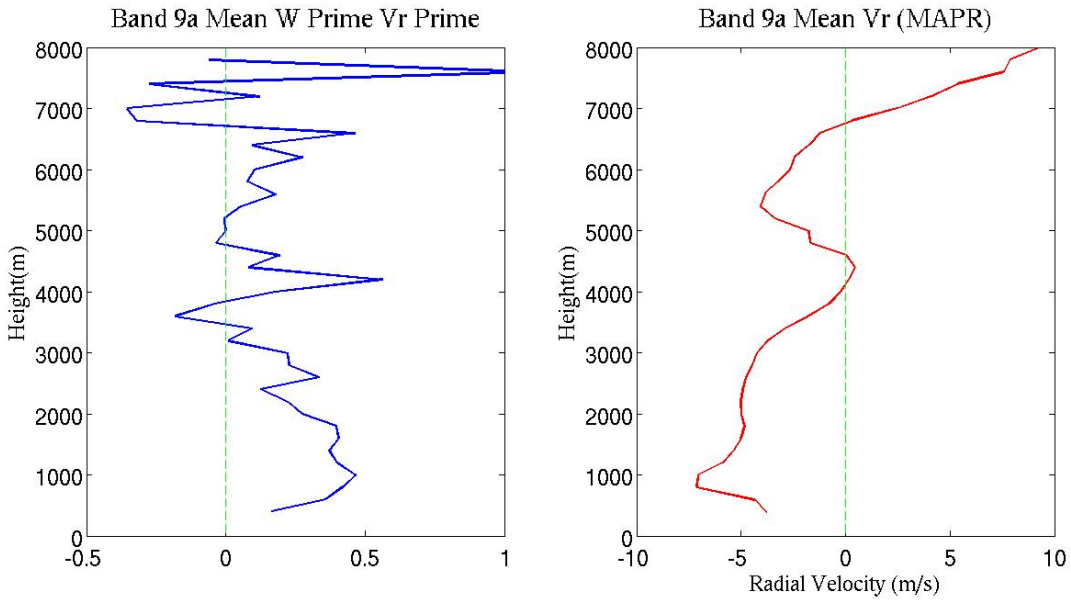

Figure 4.19: The time-mean covariance $\overline{w'V_r'}$ during the stratiform time period of Band 9a (left panel), which is representative of fluxes. The right panel shows $\overline{V_r}$ for the same time period.

An average profile of $\overline{w'V_r'}$ for the stratiform period of Band 4a is shown in Figure 4.20 (left panel). The fluxes do change sign but are weak up to 3000 meters. They strengthen around 4000 meters, which is where the shift in $\overline{V_r}$ (right panel) from towards the eye of the storm to away from the eye occurs. This is similar to what was seen in Band 9a (Figure 4.19) and helps support the theory that the eddy flux divergence is acting to smooth out the radial reversal at this height.

An average profile of $\overline{w'V_r'}$ for the stratiform period of Band 21a is shown in Figure 4.21 (left panel). There is no consistent trend in $\overline{w'V_r'}$, and unlike the previous two cases it does not seem to change much in strength around the height of radial reversal.

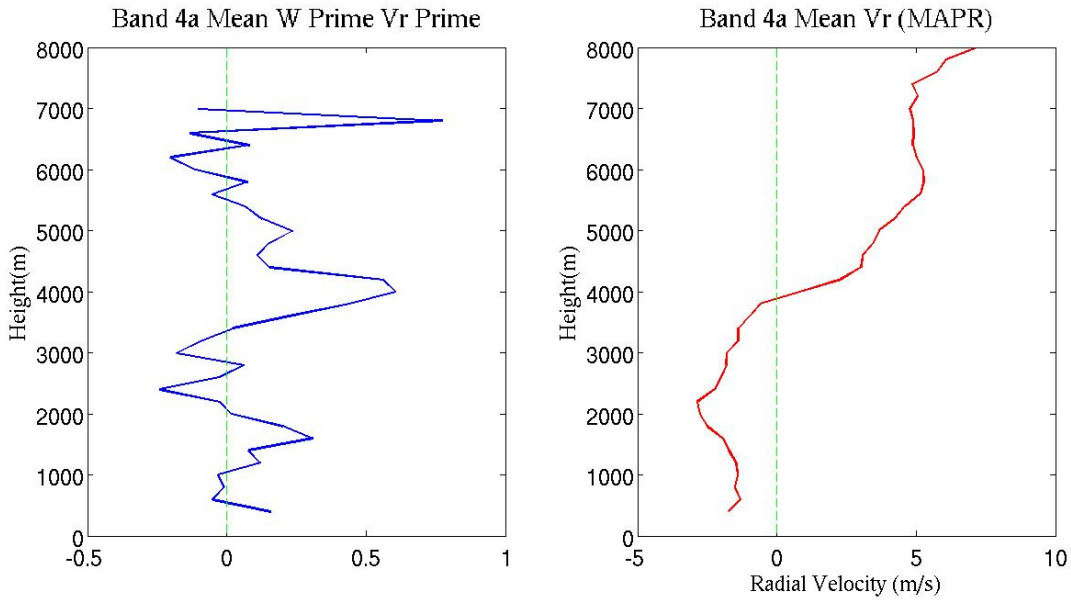

Figure 4.20: As in Figure 4.19 except for Band 4a.

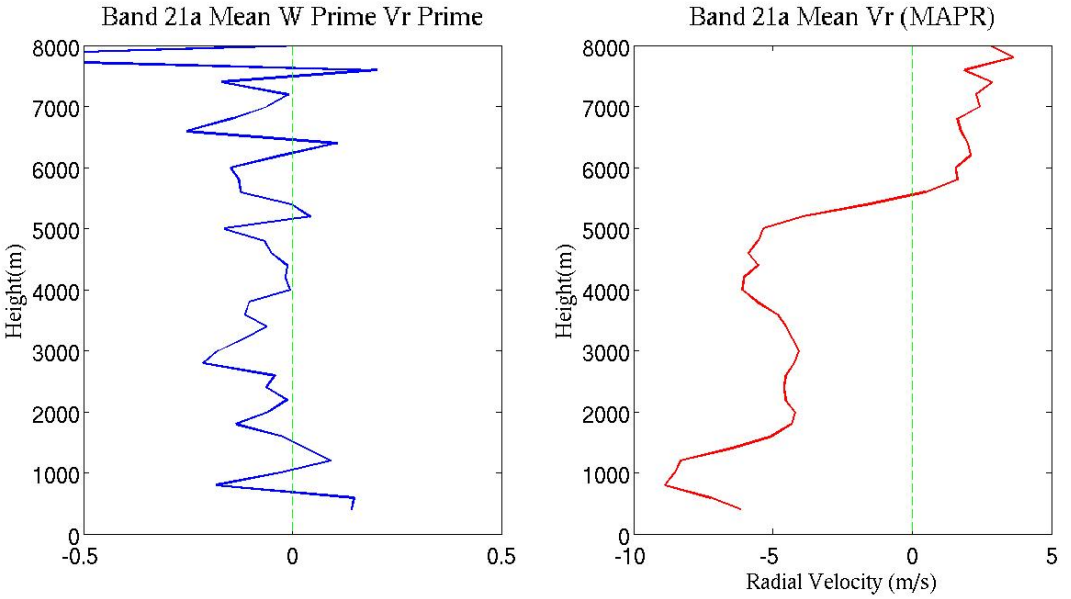

Figure 4.21: As in Figure 4.19 except for Band 21a.

Interestingly, a comparison of $\overline{w'V_r'}$ with $\overline{V_r}$ for Band 21b (Figure 4.22) reveals a similarity between Bands 4a (Figure 4.20) and 9a (Figure 4.19), and is less like Band 21a (Figure 4.21). Again a peak in fluxes at the height of the radial wind reversal is seen, which suggests that these eddy features are working to smooth out the radial reversal

even in the environmental conditions of the storm, and these dynamics are not limited to only occurring in rainbands. However, the eddy fluxes are negative at this height in Band 21b, while they are positive in Band 4a and Band 9a.

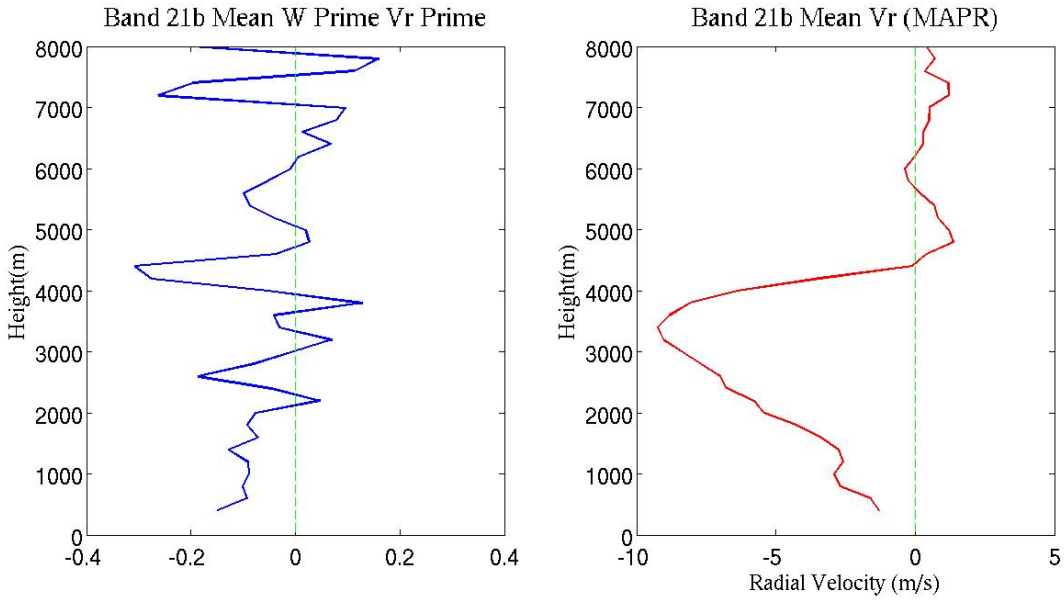

Figure 4.22: As in Figure 4.19 except for Band 21b.

4.5 Turbulent Kinetic Energy

This section examines the turbulent kinetic energy (TKE) of the 4 stratiform rainband cases to determine where in the atmosphere these rainbands contain the most turbulent energy and how the TKE varies between the cases. Figure 4.23 shows TKE with height for each of the four cases. In this figure, the TKE is derived using MAPR V_r' values, with all V_r' values > 6 ms^{-1} or < -6 ms^{-1} thresholded out. Since the mean TKE is defined as $TKE = 0.5(\overline{u'^2} + \overline{v'^2} + \overline{w'^2})$, and V_r' is a combination of the turbulent components of the wind, it is hypothesized that the mean squared perturbation ($\overline{Vr'^2}$) is a good approximation of the TKE (Lorsolo et al. 2010). As seen in Figure 4.23, the TKE values are relatively low (2-10 m2s-2) throughout the lowest 7000 meters. In Band 4a

and Band 5a, the TKE is highest below and at the height of the melting level (4500 meters AGL), and decreases in the HBL. In Band 21a and Band 21b, the TKE is highest near the top of the HBL (~1000 meters AGL) and decreases to values lower than Bands 4a and 9a above the HBL but below the melting level. The differences seen in the TKE profiles may suggest that different mechanisms could be acting in these bands. For instance, Bands 4a and 9a could be driven more my melting layer, or thermodynamic, processes, while Bands 21a and 21b could be driven more by low-level dynamic processes. A detailed discussion of these different processes and their connection to the vertical features seen in Section 4.3.1 and Section 4.4 is given in Section 4.6.

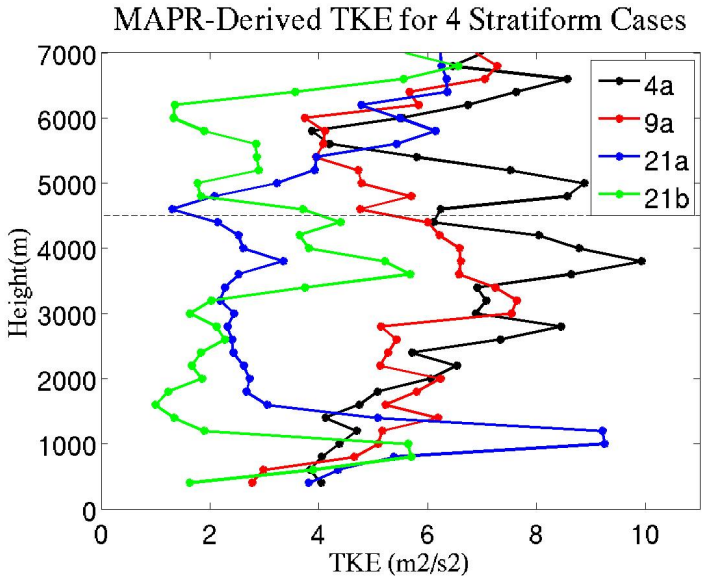

Figure 4.23: Turbulent kinetic energy (TKE) with height for Bands 4a (black), 9a (red), 21a (blue), and 21b (green).

4.6 Forcing Mechanisms

This section focuses on two possible forcing mechanisms that give the vertical features seen in the previous sections. The first forcing mechanism is hurricane boundary layer rolls, which begin near ground level and could carry features vertically if the

atmosphere is unstable enough. The second forcing mechanism is negative buoyancy generated at the melting level due to evaporation.

4.6.1 Hurricane Boundary Layer Rolls

One feature that has been shown to trigger the low-level HBL rolls is low-level vertical wind shear (Nolan 2005). To examine this possibility, Figure 4.24 shows the vertical wind shear between 400 and 800 meters from the MAPR along with $w'V_r'$ at 1000 meters and 4000 meters AGL for Band 9a. The radial wind perturbation is used here as that is where the vertical wind shear is most evident. During this case, neither height of $w'V_r'$shows a strong correlation with the shear (-.0.36 and .002 for 1 km and 4 km, respectively), although there is some evidence that increased vertical wind shear does lead to more negative eddy fluxes, which represents either downward motion and increased radial wind or upward motion and decreased radial wind. Correlations of $w'V_r'$ with the radial (V_r) shear between 400 and 800 meters (not shown) were also calculated and are also low at -0.14 for 1 km and 0.14 for 4 km.

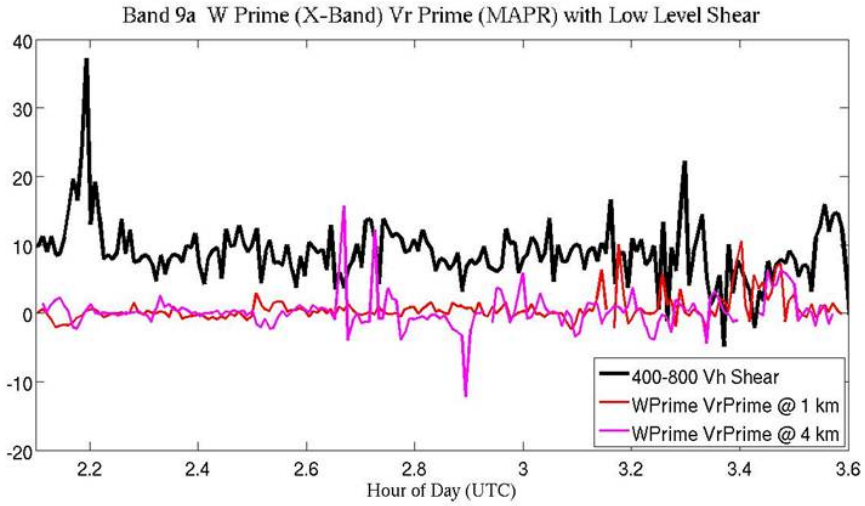

Figure 4.24: Time series of V_h shear between 400-800 meters from MAPR (black line), and $\overline{w'V_r'}$ at 1000 meters (red line) and 4000 meters (pink line) for Band 9a.

Figure 4.25 shows the vertical wind shear and $w'V_r'$ for Band 4a. As in Band 9a (Figure 4.24) neither variable has much correlation with the shear (-0.16 and -0.08 at 1 km and 4 km, respectively). Correlations of $w'V_r'$ with the radial (V_r) shear between 400 and 800 meters (not shown) were also calculated and are also low at -0.003 for 1 km and 0.02 for 4 km. Figure 4.26 shows the vertical wind shear and $w'V_r'$ for Band 21a There is a lot of noise in the data set below 1.5 km, making any interpretations hard, but it appears that as with Bands 4a and 9a neither level has much of a correlation with the shear (correlations of -0.15 and 0.003 at 1 km and 4km, respectively). Correlations of $w'V_r'$ with the radial (V_r) shear (not shown) are also very low at 0.06 and 0.01 for 1 km and 4 km, respectively. Figure 4.27 shows the vertical wind shear between 400 and 800 meters from the MAPR along with $w'V_r'$ at 1000 meters and 4000 meters for Band 21b. Like the three previous cases, some fluctuation in the shear is evident, but there is very little correlation between the eddy fluxes and the shear (correlation of 0.14 at 1 km and 0.22 at 4 km). Correlations of $w'V_r'$ with the radial (V_r) shear between 400 and 800 meters (not shown) were also calculated and are higher than the three previous cases, but still low-to-moderate at 0.51 for 1 km and -0.38 for 4 km.

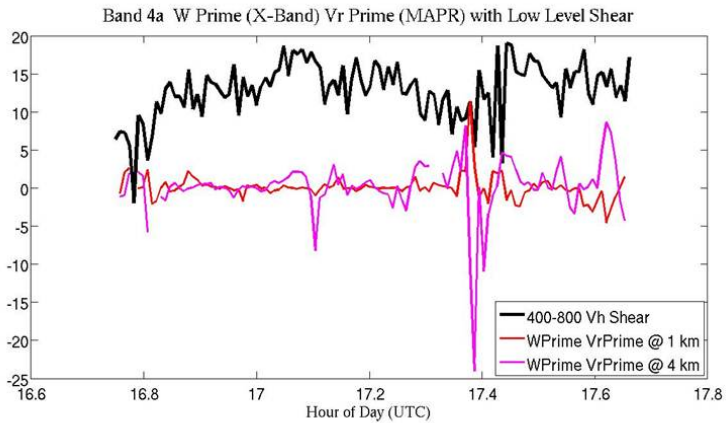

Figure 4.25: As in Figure 4.24 except for Band 4a.

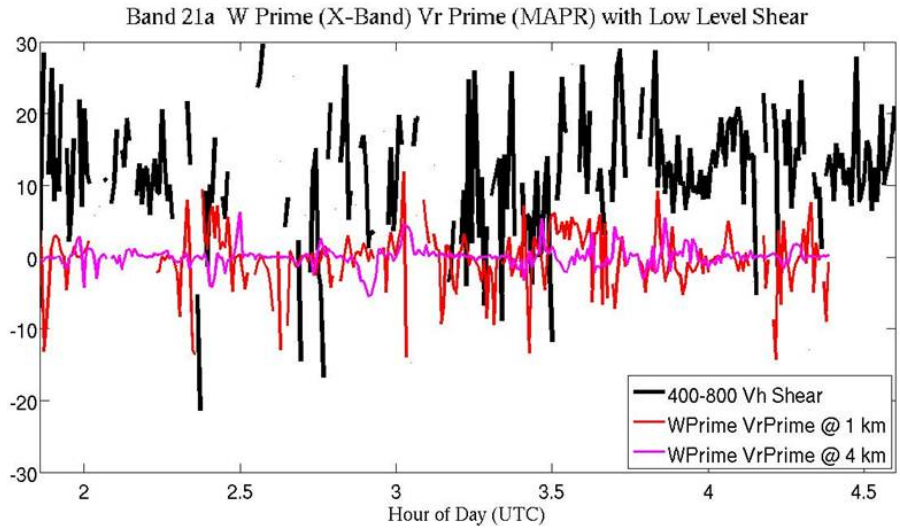

Figure 4.26: As in Figure 4.24 except for Band 21a.

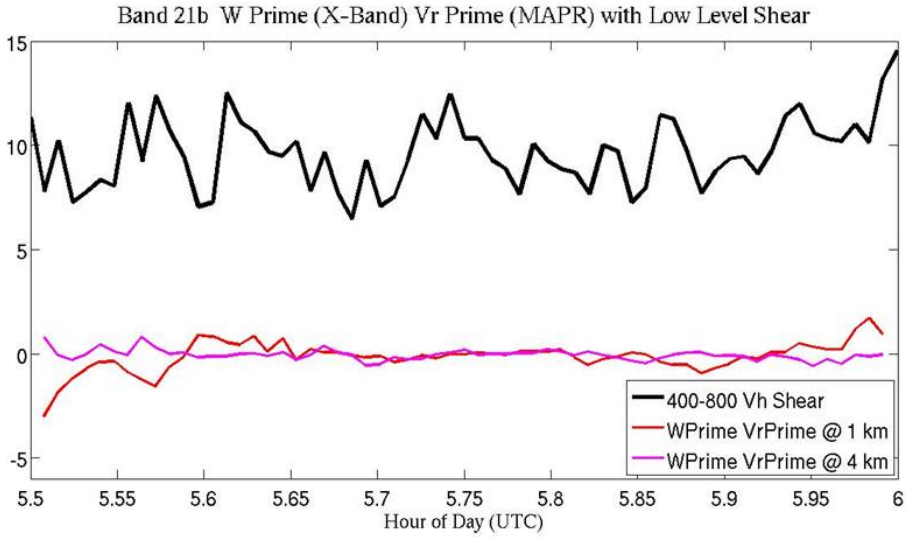

Figure 4.27: As in Figure 4.24 except for Band 21b.

4.6.2 Melting Layer Processes

Alternatively, it is possible that rather than being dynamically forced by HBL rolls at low levels, the eddies are driven thermodynamically from the melting level,

where melting and evaporation have been shown to generate negative buoyancy (Frank 1977). Figure 4.28 shows the residual SNR from the MAPR for all four of the stratiform case studies. For each of these subplots, the mean SNR for the entire stratiform period is removed at each height gate. Again the data shown in this plot are not calibrated and are only intended to show a qualitative picture of the residual reflectivity structure as the mean is removed in linear space rather than logarithmic space.

Figure 4.28a shows the residual SNR from Band 9a. This figure appears to show a mixture of mechanisms, where early in the rainband the filaments appear to be primarily in the rain, while later in the rainband (after 230 UTC) they are driven by features above the melting level. In this case there is little evidence of evaporation through the HBL, but some is present around 330 UTC. The majority of the variability in Band 4a (Figure 4.28b) appears to be driven by features starting just above the melting level, especially after 1720 UTC. There is also a larger amount of evaporation evident in this case between 2000 meters and the ground level. This is seen in the lower values of SNR' at these levels, which represent smaller (or less) droplets below 2000 meters. During Band 21a (Figure 4.28c), a mixture of forcing mechanisms that closely resemble Band 9a (Figure 4.28a) are evident. Early in the rainband the vertical features appear to be primarily in the rain, with significant evaporation below 2500 meters, while later in the rainband (especially after 330 UTC) they are driven by features above the melting level.

However, unlike the previous three cases, the image of residual SNR with height for Band 21b (Figure 4.28d) suggests that the vertical structure is completely melting layer driven, with some clear indication of evaporation effects. Again this suggests that the dynamics behind Band 21b are somehow different than the other three cases. Since

the strong positive $\overline{w'V_r'}$ vertical features were not seen in in Band 21b and it appears to be mostly melting level driven, the data suggest that the cases with vertical features are most likely influenced by a combination of HBL rolls and melting level features, while Band 21b is only influenced by melting layer processes and evaporation and not HBL rolls.

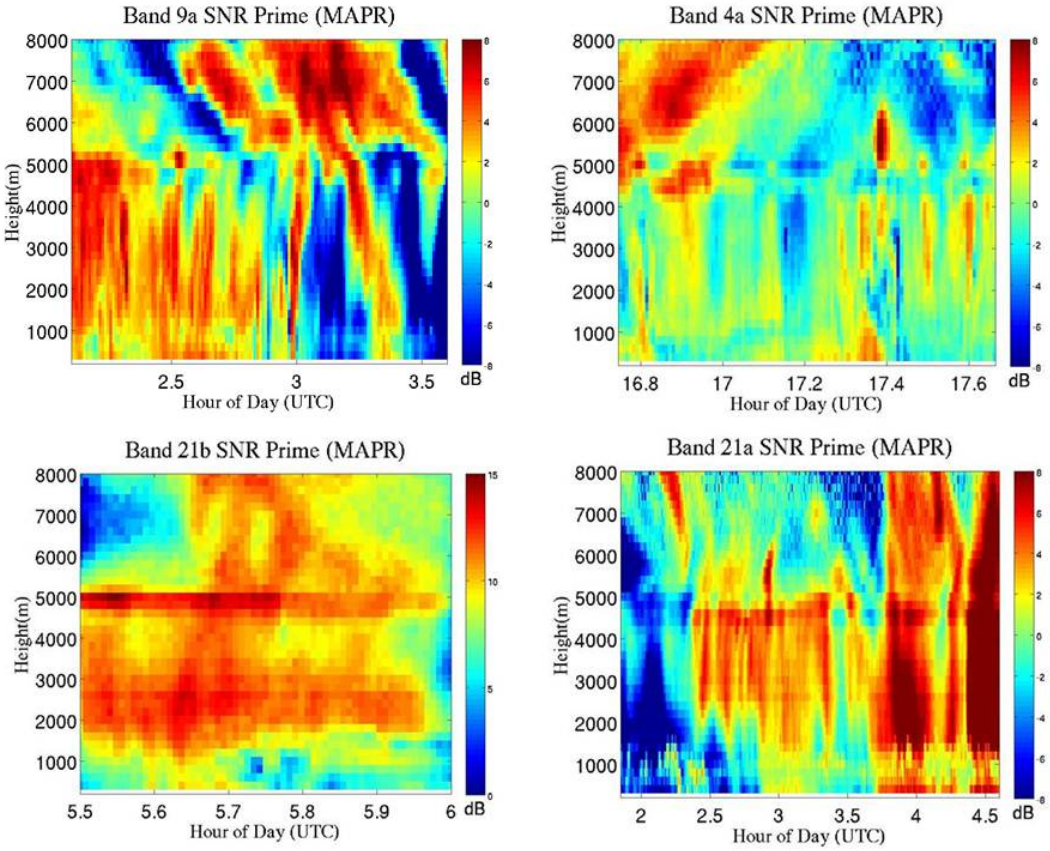

Figure 4.28: SNR' with height from the MAPR. The mean SNR from each stratiform rainband is removed at each height gate. Clockwise from top left: (a) Band 9a; (b) Band 4a; (c) Band 21a; (d) Band 21b.

4.7 Discussion

For stratiform-type rainbands and conditions, the four cases presented here show a lot of variability. Even with a constant melting level height and similar rain rates, vertical fluctuations are present in the majority of the cases. The vertical velocity perturbations

(w') are due to a combination of updraft and downdraft features and drop size variability. Attempts to deconvolve these two influences do not indicate that one is more dominant than the other consistently. Even if it was possible to determine the influence of both, strong downdrafts could still contain larger raindrops or vice versa. Without a way to quantify the changes in drop size between the melting level and the surface, there does not seem to be a way to remove effects of rainrate and drop size variability to see the true vertical wind motions.

Eddy fluxes are shown for the four cases to represent vertical variability. Three of these cases (Bands 4a, 9a, and 21a) show vertical features extending from about 1000 meters up to the melting level that are on wavelengths of 3.5-5.3 km and are spaced about 15 minutes apart (10-15 km depending on rainband motion). The wavelengths of these features are shorter than those seen in finescale bands (10 km, Gall et al. 1998) but longer than those seen in HBL rolls. Previous observations of HBL rolls find them to be anywhere from 500-3000 m in wavelength (Morrison et al. 2005), with the higher wavelengths more likely outside the radius of maximum winds (Foster 2005). Previous observations of HBL rolls also have found them to be shallow and usually existing only below 660 meters, but can extend up to 1000 m with increasing radial distance (Morrison et al. 2005). The features seen in this chapter extend up to the melting level (4500 meters) but are located at large distances beyond the radius of maximum wind. Thus, while it is possible that the depth of the rolls could increase, it does not seem likely they would extend to such high levels. It is possible that the rolls are being triggered at low levels (<500 meters), and the instability in the atmosphere is carrying the features associated with them up to the melting level.

Another possible explanation for the variability is that the vertical features could be forced thermodynamically from the melting level. Residual SNR is shown for each case as a way to qualitatively express where larger drops exist. The first three cases suggest that a combination of forcing mechanisms are at work, with some of the filaments being generated above the melting level, and some just existing in the rain. It is likely that a combination of surface forcing and melting level/evaporation forcing are acting on these three cases, which can explain why the resulting length scales do not solely fit into the theory of any forcing mechanism. A blend of two or more mechanisms acting in conjunction could superimpose a new wavelength on the signal through constructive interference, making it impossible to determine which mechanism is more dominant. However, the fact that Band 21b does not have vertical features in w' or $w'V_r'$ and also is completely melting layer forced suggests that the other three cases that do have vertical features are most likely influenced by a combination of HBL rolls and melting level features, and that the HBL rolls may play a larger role in the vertical transport to create the vertical features. This means that HBL rolls or a similar dynamic mechanism are most likely responsible for the vertical features seen in w' and $w'V_r'$.

The fourth case presented in the chapter, Band 21b, provides an interesting perspective of the differences between environmental conditions in the HBL and in stratiform rainbands. The fact that large vertical variability and the turbulent features are only seen in Bands 4a, 9a, and 21a suggest that these are features related to band-specific dynamics. However, Band 21b does show a strengthened eddy flux at the height of V_r reversal, suggesting that the storm dynamics themselves are still working to counteract the radial reversal above the HBL, even at large distances from storm center.

Unfortunately, vertical profiles of TKE with height do not support the previous conclusions, as they suggest that Bands 4a and 9a are gaining the most energy from turbulence above the HBL and near the melting layer, while both cases from Band 21 have the highest TKE near the surface, making them more likely to contain HBL rolls. This apparent disconnect between potential forcing mechanisms makes it difficult to determine the exact cause of the vertical features seen in the four cases presented in this chapter.

In conclusion, it is uncertain whether the features presented in this chapter are related to HBL rolls, since the characteristics are at odds with those observed previously. Modeling work by Foster (2005) suggests that while the hurricane boundary layer is predisposed to form rolls, HBL rolls do not form in hurricane rainbands or are at least not the dominant structures. Foster suggests that in convective rainbands, local vertical motions would disrupt the rolls. On the other hand, Lorsolo et al. (2008) found HBL rolls present in all of the inspected radar data from Hurricane Frances (2004) and Hurricane Isabel (2003), both in stratiform and convective conditions. They state that HBL rolls themselves would not cause much surface damage since their perturbation is small, but that they could combine with larger scale variability to transport significant energy, which could be what is seen in this data set. Overall it seems most likely that a combination of HBL roll forcing and melting layer forcing is acting on these rainbands, though it is hard to deconvolve the relative importance of each forcing with only four cases. Either way, these new features are observed on a very high spatial and vertical resolution, so while there is not enough data to draw concrete conclusions, they provide a

very valuable addition to previous research done on small-scale variability in hurricane rainbands.

Chapter 5: Educational Applications of the Rainband Data Set

5.1 Motivation

Many times meteorologists wish to use the data that they have collected in the field in the classroom. This could range from using observations to explain how a particular instrument collects data to a class of meteorology majors, or to support science content teaching in a secondary science classroom. As such, data collected during this field project was used to determine the most effective way of using a scientific data set in an upper-level meteorology classroom. The purpose of this study was to test two laboratory approaches using a real-world data set to see if one improved student learning outcomes and/or attitude towards science more than the other.

This work involved designing a weeklong study conducted with a group of 53 senior meteorology majors at the University of Oklahoma to test whether a traditional laboratory approach or an inquiry laboratory approach changed attitudes about science and content knowledge growth and retention about hurricane rainbands. The particular research questions to be addressed were:

I. Does an inquiry-based learning approach using real-world data enhance students' understanding about the nature of science or improve their attitude towards science?
II. Is this approach effective at conveying content knowledge in an undergraduate meteorology classroom?
III. Is this approach more or less effective at improving content knowledge growth and retention and/or attitude towards science than a traditional approach?
IV. What are the challenges associated with an inquiry approach and a traditional approach and how can they be overcome?

This study fills in important gaps in the literature that have often ignored learning approaches in higher education. It not only provides two examples of ways that real-world data can be used in an undergraduate meteorology classroom to effectively convey content knowledge, it also compares two learning approaches and their impact on student learning outcomes and attitude towards science. The benefits of using each approach are highlighted, and suggestions are made of ways to overcome the challenges associated with each approach in order to improve classroom teaching.

This chapter begins with a review of previous science education studies involving using inquiry in higher education classrooms in Section 5.2. A description of the laboratory approaches used in this study is given in Section 5.3, and results comparing the two groups' attitudes about science, content growth, and content retention on stratiform hurricane rainbands are shown in Section 5.5. This chapter concludes with a review of the key findings related to the research questions in Section 5.6. The contributions of this work to the education literature and the field of teaching are discussed, and suggestions for future research are given.

5.2 Background

5.2.1 Inquiry-based Learning

Inquiry-based learning involves a student-centered approach, where the teacher acts as a facilitator of learning rather then a disseminator of information. Inquiry is an inductive approach to teaching, where learning is driven through the student's need for facts, procedures and guiding principles to explore possible answers. This is in contrast to

deductive approaches in which the teacher presents theories and principles and connects them directly to applications (Spronken-Smith et al. 2008).

The use of inquiry in science classrooms has received much attention in the education literature since Joseph Schwab's curriculum work on enquiry in 1962 (Chiappetta 2008). Schwab believed that students should be taught about the manner in which a certain community of scientists viewed a major idea and the ways they investigate that idea. This led to inquiry becoming a popular approach in the science education community and a promotion of inquiry in high schools, especially through laboratory work. With the release of the *National Science Education Standards* (National Research Council (NRC) 1996) and the companion work *Inquiry and the National Science Education Standards* (NRC 2000), inquiry use in K-12 sciences become a big focus of science reform (Chiappetta 2008).

Inquiry in the classroom can be broken into three areas- science as inquiry, learning as inquiry, and teaching as inquiry (Anderson 2002). The central concern in the literature is with teaching in an inquiry-based method to improve content knowledge and understanding of the nature of science. Inquiry as a teaching methodology includes developing learners who can (a) engage in scientifically oriented questions; (b) give priority to evidence; (c) formulate explanations from evidence that address scientifically oriented questions; (d) evaluate their explanations in light of alternative explanations, particularly those reflecting scientific understanding; and (e) communicate and justify their proposed explanations (NRC 2000).

There is also a distinction in the literature between "full inquiry" and "partial inquiry", where some teachers, especially at the college level, don't believe that inquiry is

being accomplished unless the 5 main components listed above are all included and there is little to no teacher guidance. This makes it challenging to generalize inquiry as a concept when every publishing author has a different perspective on it.

Education literature provides very few examples of inquiry-based learning in higher education Earth science courses. Those that exist often include examples of curriculum reform to include inquiry but do not provide a comparison between inquiry and other learning styles, so it is difficult to determine if the inquiry aspect itself creates beneficial student learning outcomes.

5.2.2 Inquiry in Higher Education

The majority of colleges and universities offer one or more Earth science specialties as undergraduate or graduate degree programs, so though much of the focus on inquiry use in Earth sciences in the literature is from elementary, middle and high school courses (e.g.. Mao & Chang 1998; Qingchao, Xiufang, and Guangyan 2008; Agne and Blick 1972; Chang 1999; Chang, Hsiao and Barufaldi 2006; Gardner, Simmons and Simpson 1992), research on inquiry in higher education is important as well. If incoming college students already have experience with scientific inquiry, they will expect to continue learning in the same ways in college. Additionally, college is where students begin to develop their own identities as future scientists, so training them to be independent thinkers is crucial. This means that professors will be expected to deviate from traditional textbook teaching and "cookbook" labs to more student-centered approaches. Without training, designing a learner-centered classroom with inquiry-based instruction is a challenge for college professors because it means revising current

curriculum and teaching strategies that have been formed through years of trial and error. One source for information on creating a student-centered learning experience can be science education literature, but since the majority of the research thus far has been on primary and secondary education it can be challenging for faculty members to make connections between the literature and their higher education classrooms. Further published work on inquiry use in higher education is needed for those connections to be made more easily.

The majority of the research on inquiry teaching in higher education Earth sciences relates to describing new teaching techniques, including reformed courses (Clayton and Gautier 2006; Gautier 2006; Krockover et al. 2002; Cohn, Hallett and Lewis, 2006; Simmons et al. 2008) or hands-on projects (Barrett and Woods 2012: Gautier and Solomon 2005; Illari et al. 2009; Spronken-Smith and Kingham 2009; Oh 2010) or modules (Spronken-Smith et al. 2008). Although a lot of these reformed and developed courses and projects are based on full or partial inquiry, others seem to highlight doing science, but not with any true inquiry aspects, which makes it challenging to relate any content growth that occurs directly to the teaching approach.

Two studies related to introductory meteorology courses display this difference well. The first, by Cutrim et al. 2006, describes purposeful course reform to address misconceptions, encourage engagement, and promote inquiry-based learning. However, the four new techniques used- including flashcards to gauge student understanding, daily teacher presentations on weather from an integrated data viewer, and assigned reflection questions- are quite far from what most education researchers would consider actual inquiry-based teaching. Only one of the approaches, which had the students working in

groups of three to answer open-ended writing questions for each chapter, shares a resemblance with inquiry activities. This approach is still far from achieving student knowledge about the nature of science, as most of the questions they were answering were still regurgitating previously lectured classroom content.

On the other hand, the Yarger et al. (2000) study shows how using a forecasting activity in an introductory meteorology classroom could be applied to inquiry-based teaching. Unlike the Cutrim et al. (2006) study, where the professor goes through the making of the forecast each day, this study engages students in doing what practicing meteorologists do through making frequent individual weather forecasts throughout the semester. This required classroom component was designed based on constructivist learning theory, and showed that after overcoming initial challenges, students were all able to increase their mean forecasting scores with practice. In the Yarger et al. (2000) study, a student-centered approach using real-world data was shown to be effective at conveying content knowledge. However, a need for a wider range of inquiry research in higher education still exists.

5.2.3 Inquiry and Ideas about Science

Introducing students to how scientific data collection, analysis, interpretation, and communication take place in their own field can develop their view of the nature of science. Parker et al. (2008) surveyed an introductory undergraduate atmospheric science class about their ideas regarding the nature of science (NOS) and found that most students saw science as a discipline based on data, where experiments tested or confirmed scientific ideas. The students appeared to appreciate the importance of data collection in

science, but with a "right-vs.-wrong" approach, rather than grasping the continuum of possibilities. The majority of students saw that creativity was used in doing science, and those that did not were less likely to pursue careers in science. This study concluded that ideas about the nature of science could be developed- even at the undergraduate level- that would be useful in the future scientific careers of the students.

As more students become exposed to inquiry-based learning, there is a need to ensure that they aren't just doing inquiry for the sake of performing activities, but doing inquiry as a means to gather skills that will serve them in their future careers. This requires the students to be engaged with the inquiry process, something that is challenging the first time they experience it in higher-level college courses. Studies involving student engagement vary from those including full inquiry (e.g. Apedoe 2007), to those with partial inquiry (e.g. Spronken-Smith and Kingham 2009). Results show that although students enjoy and value the hands-on projects they may not grasp the full range of inquiry skills that they have learned. For example, students tend to be overly concerned about the data quality and the need to get good results, and don't seem to appreciate that problems of data collection and quality control are universal in scientific research. Spronken-Smith and Kingham (2009) suggest that in order for students to reap the most benefits from inquiry-based teaching, they should be told that they are doing inquiry at the start of the project. This way, the students can relate their challenges to those of scientists, and not just feel like they are doing a class project.

Overall, inquiry use in higher education has been shown to have a positive effect on enhancing students' ideas about how science is done, which is important in developing future scientists. By participating in the scientific process, students have increased levels

of engagement with their courses, and still receive comparable or improved course grades. It is also beneficial if the students are aware that they are participating in inquiry, as that can help them to make the connection between classroom and real-world science. However, research on whether or not student-centered learning improves student's attitudes toward science at the college level still needs to be conducted.

5.2.4 Comparisons of Inquiry and Traditional Approaches

Much of the inquiry literature simply describes a new teaching technique or hands-on course, but a few of the studies are designed with a specific goal of comparing the inquiry technique with a more traditional one. One such study, which is similar to the Yarger et al. (2000) work, tests a new severe weather laboratory exercise in an introductory weather and climate class. This work was done by Grundstein et al. (2011), and also involves non-science majors working in teams to identify atmospheric conditions, in this case those that promote severe weather. The instructor of this class randomly assigned class sections to the comparison or experimental groups. The comparison group was taught using a severe weather laboratory exercise provided in a commonly used laboratory manual, while the experimental group solved the problem of where severe weather was likely to form on their own. The 40 students in the comparison class and 51 students in the experimental class were compared on engagement with the lab and content knowledge about severe weather. The results of this study indicate that the experimental group enjoyed the lab significantly more, but that there was no statistically significant difference in content growth between the groups. The outcome of this study supports inquiry use, especially in a lab setting, as it promotes interest among

non-scientists without sacrificing content knowledge. However, much more research on using inquiry with atmospheric science students is needed, especially at more advanced levels in their degree programs.

5.2.5 Challenges Associated with Inquiry

Although much of the previously described work shows the value of including inquiry in higher education, there are many challenges associated with inquiry use that still must be overcome. These include ensuring that faculty members understand how to enact both full and partial inquiry-based activities correctly and preparing students to take on more responsibility in their classroom learning through student-centered learning.

Most college science faculty view inquiry from an "all-or-nothing approach" (Chang and Chang 2010), where students have to be involved in the development of a scientific question, data collection, data analysis, and communication about their scientific ideas. With this extreme approach, inquiry requires a large time commitment both in preparation and in implementation. However, much of the published work in the literature shows that in addition to a complex full inquiry practice, partial versions of inquiry can also take place in just one activity or small course project. For example, Rogers and Abell (2008) suggest that: (1) inquiry teaching can be a part of all class components, not just laboratories; (2) inquiry teaching can illustrate the social and interdisciplinary nature of scientific knowledge; and (3) modeling laboratories from scientific papers can help to illustrate how science is done while giving students an opportunity to control their own learning. Future studies on partial inquiry are needed, especially those where students do not participate in hands-on data collection.

Some of the other challenges for professors involving inquiry teaching in higher education include prior textbook dependence, fears about lack of student content knowledge, challenges of assessment with group work, working with large introductory lectures, and inadequate teacher preparation. It is also often a large challenge for students to appreciate the goals of inquiry, especially if they do not encounter the teaching style frequently. However, if students can appreciate an inquiry-based teaching method then they can become better scientists, an advantage which is crucial with the current state of the job market.

A challenge for both students and faculty associated with initial exposure to inquiry is the amount of faculty guidance during the project. There is a fine line in inquiry-based teaching between the professor guiding the students too much (where the learning becomes more teacher-centered) and the professor leaving the students completely to their own devices (where they can become frustrated with the lack of direction and may not learn the intended content appropriately). Creating a balance between what the teachers and students both feel is an acceptable level of guidance is often a challenge in inquiry activities (Apedoe 2007).

5.2.6 Areas for Future Inquiry Research

Inquiry-based learning has been shown to have positive effects on student attitudes about the nature of science, both in grades K-12 and in higher education. Although many inquiry studies do show science content growth using inquiry, much of the research highlights the limited and often superficial use of inquiry in higher education

of Earth science topics. This points to a need for systematic comparisons between inquiry and traditional teaching approaches related to content growth and retention.

The Earth sciences, including meteorology, lend themselves well to inquiry activities because of the opportunity to use real-world experiences and data for learning. For instance, weather observations can be made from the classroom or home, and compared with other locations freely through the Internet. This helps to reduce some of the time and financial obstacles encountered with lab work, and allows students to easily experience what they are learning about and construct their own ideas. Future studies of effective ways of using real-world data in college classrooms are needed.

This study presents an example of how to use real-world (but not real-time) data in an undergraduate classroom through a student-centered approach for effective student learning. It quantitatively compares the student-centered approach to a traditional approach, and discusses the benefits and challenges associated with each approach and their implications for student learning.

5.3 Methodology

5.3.1 Data Set

The goal of this study was to examine whether an inquiry-based or traditional laboratory approach was a more effective way to use meteorological data from a field campaign in an upper-level undergraduate meteorology classroom. Since the field project had already been completed, the students would not be able to participate in the data collection part of inquiry, which meant that the data they were using in the lab had to be chosen for them. After careful analysis of the stratiform wind profiles shown in

Sections 3.2 and 3.3, three cases were chosen for use in the lab. These cases were 4a, 9b, and 23a, all of which contained the main content information intended to be conveyed during the lab with enough differences to show the variability in stratiform rainband wind profiles. Topics covered during the lab consisted of the location of wind maximums in horizontal, radial, and tangential wind profiles; how wind speeds vary near the surface; how moisture profiles fluctuate with height; and how wind speeds and moisture change with rainband passage based on the three cases analyzed.

5.3.2 Experimental Design

This study was conducted using 53 senior undergraduate meteorology majors in METR 4424, a synoptic meteorology laboratory at the University of Oklahoma. This investigation involved spending four 105-minute class periods with the students. Days 1 and 4 involved the entire class, and half of the class participated in each of the different treatments that took place on Day 2 (Inquiry) and Day 3 (Traditional).

On Day 1, each student randomly drew a number from 1-53 out of a bag, to be assigned as an ID Number to use on all lab and assessment materials for anonymity. Seven students registered for the course were absent, so only the first 47 numbers were used. Students who drew an odd number were placed into the Inquiry Group (known to them only as "Group 1") and students who drew even numbers were placed into the Traditional Group (known to them only as "Group 2"). Students in Group 1 were told to come to class the second day but not the third, and students in Group 2 were told to come on the third day but not the second. At that point, a pretest (shown in Appendix B1) was given to test content knowledge about stratiform tropical cyclone rainbands as well as

evaluate the students' attitude towards various lab styles. Students had as long as they needed to complete the pretest, which took most of them 20-30 minutes. The pretest consisted of 10 Likert Scale questions related to attitude towards science labs (Questions 1-8) and opinions about content knowledge (Questions 9-10). Questions 1-8 were designed to be either inquiry-positive (e.g. "*Being able to design and conduct a scientific investigation improves my understanding of the material*") or traditional-positive (e.g. "*I like working on my own during labs*"), so that a choice of *Strongly Agree (5)* represented student preference for either inquiry or traditional lab activities. Once the pretests were collected, an interactive lecture was given to describe the field campaign and instrumentation used, as well as make sure that prerequisite knowledge needed for the lab was reviewed. Background information reviewed consisted of radar operations, VAD technique, basics of tropical cyclones, and radial and tangential winds. The lecture ended with a brief discussion of the data that both groups would be seeing during the labs.

On Days 2 and 3, the laboratory component of the study took place, with both groups given the exact same data files, computer tools, and time to complete the lab, but with varying laboratory approaches. Group 1 students participated in the lab on Day 2 and after they received the data files they took on more active roles in the investigation by designing experimental procedures and looking for key scientific discoveries. With this group concepts were presented as scientific questions and the students were responsible for deciding how to use the data files to answer those questions. During this inquiry-based lab, classroom collaboration and discussion was utilized to check for understanding and lead students toward developing a valid understanding of scientific ideas. On Day 3, Group 2 students participated in a traditional lab approach, with step-

by-step instructions on how to use the data files to make figures, as well as directions about which figures to analyze to reach scientific conclusions. In this approach, content topics were grouped and introduced in sections along with the relevant data. Group 2 students worked on the lab individually and were allowed to ask the lab instructor for help with technical issues such as loading and plotting data, but were not lead towards specific answers. It is important to note that five of the seven students absent on Day 1 showed up on Day 2 and were allowed to participate in the inquiry lab approach. These students received ID Numbers 60-64, and they were analyzed in the results section both with the rest of the Inquiry Group and as their own group (Inquiry without Lecture). A more detailed description of the inquiry approach and traditional approach are given in Sections 5.3.3.1 and 5.3.3.2, respectively.

On Day 4, the entire group convened again (minus 1 student) and took the posttest (Appendix B5), which was identical in content knowledge to the pretest, but asked them to respond to the attitude survey questions based on the experience with the lab approach they participated in. Again, students had as long as needed to complete the posttest, most taking 15-20 minutes. Once the posttest was collected, students were finally told what the other lab approach was, and a group discussion with student feedback took place.

A month after the initial weeklong investigation, a retention test (Appendix B6) was given to the entire class to assess content retention. The retention test consisted of 9 questions, 6 short answer (of which 4 were taken directly from the pre/posttest) and 3 multiple choice questions where students had to select a representative profile and explain their reasoning.

5.3.3 Two Laboratory Approaches

5.3.3.1 Inquiry Approach

As described in Section 5.2, pure inquiry labs involve all aspects of the nature of science, from discovery of a scientific question to planning how to solve it, collecting and analyzing data, and communicating scientific results. During an inquiry lab, students should learn about how scientists do science in addition to learning the content knowledge. They should invoke their own creativity and collaborate with their classmates to reach conclusions. The inquiry approach used in this project is considered to be guided inquiry, since the students were already presented with the data set and a broad suggestion of what scientific problems they should work towards solving. Additionally, throughout this lab, their learning path was partially directed by the lab teacher (myself) in order to stay on a reasonable timeline. A total of 27 students participated in the inquiry lab, 22 from Day 1 and 5 who were missing on Day 1 and thus missed the lecture but did take the pretest before the lab began on Day 2.

The inquiry lab began with students being told that the lab would be voice recorded, but that their names or ID numbers would not be used for identification during the lab or in future presentations or publications. Once students signed their consent to be voice recorded, it was explained that they would be working with the data set as an entire class. They were instructed to visit their class website and download the 4 Excel spreadsheets, one with the mean wind with height and one for each of the sounding cases, along with the supplemental files (radar loops and still image Word documents for the 3 cases.) The class was asked to use Excel to plot all of the data to avoid any bias introduced by alternative data viewing software. The class was given the handout with

instructions for the inquiry lab (Appendix B2) and Supplemental Rainband Information (Appendix B4) and were told that they had 5 minutes to download everything and get familiar with the data, as stated in the quote below:

Teacher: *So I'm going to give you guys five minutes to kind of download everything, get familiar with the data and then what we're going to do is work as a class going through our scenario at the bottom, investigating the rainbands. We're going to pretend to be scientists. Or PhD students (in my case) and we're going to work through this as a class. So I'm going to ask you to discuss this a lot, we're all going to work together. No one has to hand in any lab paperwork other than your ID number but if you want to make notes for yourself on the side you're welcome to. But you won't be graded on any of this, you're just going to get credit for coming today. Any questions so far? [silence] So go ahead and take your 5 minutes.*

There was some difficulty accessing the data online, so several students used a portable drive to share the data. Every student but one had their own laptop, but he looked on with the person next to him. Once students were familiar with the data sets, the lab officially began at 2:50 pm. The instructions of the lab were designed to present the main scientific question as a real-life scenario to enhance the students' connection to the learning. The students were told the following:

Teacher: *Your research lab collects the above observations during Tropical Storm Fay and Hurricane Ike. Your job as a scientist is to determine what features are observed in the wind and moisture profiles during the stratiform rainbands. You should determine if these features are real and robust, if they can be tied to scientific explanations, and whether you can make any broad statements about stratiform*

rainbands based on your data set. And as a hint/reminder of what your boss wants you to focus on "study all three wind components, and also to look at how wind speed and moisture profiles change with band passage"

Students discussed amongst themselves what data set they wanted to work with and how they wanted to plot the data to reach conclusions. They started by looking at the mean wind components with height using the VAD data, and reached a consensus on the main features they observed. When they asked questions, I would first ask if other students could explain topics in more detail (e.g. why winds speeds slow near the surface (friction)), and if no one could then I would explain. Once students were satisfied with their mean wind analysis, they moved on to radial and tangential components with the VAD data, and then chose to use two of the sounding cases to compare a before and after case to determine the influence of rainband passage. During the lab, 6-8 students took charge in leading the discussion, but several others spoke up occasionally. An open learning community was encouraged by soliciting questions and ideas from students regularly. During this lab, when students asked questions other students answered them. For example, one student asked *"why is the wind jet where it is?"* and another responded that "*warm core systems are different then cold core systems since they have winds that decrease with height."* Several students, especially those seated in the back of the classroom, seemed to struggle with plotting the data in Excel, and they were encouraged to share plotting techniques among themselves while I also walked around helping students who seemed confused. Each student tackled plotting in their own way, some plotting one case at a time while others plotted all three. Some students plotted the wind speeds vs. number of data points rather than vs. height. Since the figures made during the

lab were not collected, I allowed the students to plot to their preference. Overall, Excel seemed to provide a major challenge to the majority of the class, and it took a learning process before all students felt comfortable with the plotting. In addition, some students had issues with their Excel programs crashing, especially towards the end of the lab, which caused them to get off track with the rest of the class.

The inquiry lab took about an hour and 10 minutes to complete once students were ready to work on it as a group. Although students were not told what data to work on explicitly, I did have an idea of what main content knowledge I wanted to expose them to (based on the traditional lab and shown in Table 5.1), and encouraged them to move on to a new topic once they had adequately explored the current topic in detail. Once the students had successfully analyzed the horizontal and radial wind components by making the plots on their own, they were encouraged to collaborate on the tangential wind and sounding plots for the sake of time. Some students plotted wind speed, while others plotted wind direction, and the remainder plotted moisture between before and after cases. Some discussion between groups took place around this time about the significance of before/after changes, and the students seemed unsure of how to proceed with a disagreement in conclusions when one group saw a big change and one didn't. They were encouraged to have other people plot it and come to a consensus, and after some additional effort they decided that there is a little more moistening after rainband passage, but nothing drastic.

Overall, students seemed to have a mostly positive experience during the inquiry lab. The majority of the class seemed frustrated at first, which is a common response when experiencing inquiry for the first time. Once students gained confidence in their

ability to plot the data, they seemed to enjoy deciding what data sets to use to answer their scientific questions. Frustration with Excel was common theme throughout the lab, and these occurrences were used as opportunities to connect the work the students were doing with what scientists go through in their own careers, thus enhancing an understanding of the nature of science.

Table 5.1: Topics emphasized by instructor during inquiry lab.

Topics Emphasized During Inquiry Lab
-friction near surface -location of jets in horizontal wind -radial inflow vs. outflow -cyclonic rotation is dominant wind component (tangential wind) -if soundings could be compared to VAD -the influence of stratiform rainband on atmosphere (before/after) -why someone might care about the surface layer

5.3.3.2 Traditional Approach

The traditional lab approach was designed to be the "control" in this investigation, as the majority of college students have participated in labs in this manner before. These labs are known as "cookbook" labs, where students work through the lab in prescribed steps, and are told what data to use and what results they should be looking for in each step. A total of 24 students participated in the traditional lab, all of which were present for the pretest and lecture on Day 1.

Similarly to the inquiry lab, the students were instructed to download the files from the class website. This time the downloading went smoothly and there was no need to use a hard drive to share the data. Once again, every student had their own laptop and was asked to use Excel to plot all of the data to avoid any bias introduced by alternative data viewing software. The lab instructions were handed out (Appendix B3) and students

were told to write the ID number on the top and fill out their lab questions, but that they didn't have to hand in the graphs they made during the lab. Students were told to work independently and quietly and to not use any other sources. The teacher (myself) offered to come around and help anyone with data or plotting issues at any time. Once everyone had downloaded the files, the lab began at 2:10 PM. Shortly after the start of the lab, 5 students asked for help with plotting. Students worked on the lab quietly, with occasional short whispers or glances between students during the lab, but no real discussion. I tried to interrupt the class twice to explain where the surface data was and the direction of radial inflow, but even after stating it to the entire class, several students asked the question again, making it clear that interrupting the class while they were working on the lab obviously did not get the information across effectively.

It took the students a varying amount of time to complete the traditional lab, as they could work at their own pace. The first student was done in 50 minutes, 5 were done in a hour an 10 minutes (the length of the inquiry lab), 13 students were done within an hour and a half, 22 were done by the time the class period ended at 3:50 pm, and 2 did not finish. The labs were collected from this group to make sure content was understood correctly, knowing that the main content points had been discussed aloud during the inquiry lab.

5.4 Pre/Post/Retention Tests

5.4.1 Question Purpose

As stated in Section 5.3.2, students were given a pretest (Appendix B1), posttest (Appendix B5), and retention test (Appendix B6). The pre and post-tests were nearly

identical, except for the focus of the attitude questions. These tests were given to test content knowledge about stratiform tropical cyclone rainbands as well as evaluate the students' attitude towards various lab styles.

The attitude questions were designed to address research questions II and III stated in Section 5.1 by assessing each group's ideas about science labs before the study and seeing if they had changed after the study. This section consisted of 10 Likert Scale questions related to attitude towards science labs (Questions 1-8) and opinions about content knowledge (Questions 9-10). Questions 1-8 were designed to be either inquiry-positive (Questions 1,3,5,7,8) or traditional-positive (Questions 2 and 4). These questions were evaluated both individually and in groups as either inquiry-positive or traditional-positive. These questions were chosen to be on a quantitative scale for ease of evaluating the responses.

The content knowledge questions (Questions 11-21) were mainly short answer questions and were designed to address research questions I and III by determining if an inquiry approach provided effective content knowledge learning (I) and by comparing it to a traditional approach (III). Although the open-ended nature of these questions made evaluating the student responses more challenging, the questions were chosen to be in this form to avoid introducing any suggestions on possible topics students could work on during the inquiry lab approach. Examples of how student responses on these open-ended questions were made into quantitative values are shown in Appendix B7.

The retention test was designed to be a mix of short answer and multiple-choice questions, with the multiple-choice questions requiring an explanation of the choice along

with the letter selection. These questions were also evaluated in the same quantitative way as the pretest and posttest open-ended questions, which is described in Section 5.4.2.

5.4.2 Sample Responses and Rubrics

In order to assess changes in content growth, the content short answer questions had to be evaluated in a quantitative form. A 4-point rubric was designed for each of the questions to distinguish varying levels of quality in the content responses. The pretest, posttest, and retention tests were all evaluated using the same rubric. Every student response was hand graded by the author to avoid introducing a grader bias. For each question a full correct response was awarded a score of 3, a partial correct response a score of 2, an incorrect response or a correct response not related to the question a score of 1, and a blank answer or response of "I don't know" or "I forgot" was awarded a score of zero. Selected example responses to each question at various rubric scores are shown in Appendix B7 along with the student ID number each response originated from. Some students chose to draw sketches of their ideas instead of using words, and these drawings were accepted as responses.

5.5 Results

Once all of the pretest, posttest and retention test questions had been scored using the rubrics, a one-way analysis of variance (ANOVA) was calculated using MATLAB software to determine the statistical significance ($p<0.5$) from pre-lab to post-lab by group, and between the Inquiry Group (IG) and Traditional Group (TG) for posttests and retention tests. This section summarizes the results of these differences for attitude

change pre-to-post by group, content growth pre-to-post by group, content change post-to-post between groups, and content retention post-to-post between groups. The IG is also broken down into the 22 students who received the lecture (Inquiry With Lecture) and the 5 students who missed Day 1 and did not receive the lecture (Inquiry Without Lecture). Due to the wide range of student responses, question #20 from the pretest and posttest was removed from this evaluation and is not included in the results. Comments from the class discussion following the main portion of the study are presented in Section 5.5.4 to help suggests reasons why the results turned out the way they did.

5.5.1 Attitude Change

The change in attitudes about science labs was compared from the pretest to the posttest for the entire class (Table 5.2), for the IG (Table 5.3), and for the TG (Table 5.4). These results are shown for each of the 10 attitude questions, as well as by grouping the inquiry-positive questions and traditional-positive questions. When looking at the entire class, it can be seen that there was no statistically significant change from pre to post for any of the questions, except for questions 9 and 10, which were questions asking how much the students felt they knew about wind profiles and moisture profiles in a rainband. This indicates that as a whole, the rainband lab did not cause a major change to student opinions about science labs, but did cause them to feel that they had learned science content. Focusing on just the IG (Table 5.3), again no statistically significant changes from pre-to-post were found, except for questions 9 and 10. The TG (Table 5.4) also shows the same pre-to-post results with the only statistically significant changes

occurring in questions 9 and 10. These results can also be seen in visual form in Figures 5.1 (IG) and 5.2 (TG).

Table 5.2: Entire class pre-to-post responses to attitude questions.

Question	Mean Pre	Mean Post	Difference (Post-Pre)	STD Post	Statistically Significant (Y/N)
Inq Positive Attitude ?'s (1,3,5,7,8)	3.86	3.82	-0.04	0.55	N
Trad Positive Attitude ?'s (2,4)	3.36	3.47	0.11	0.59	N
1	3.69	3.60	-0.09	0.83	N
2	2.73	3.02	0.29	1.00	N
3	3.86	3.77	-0.09	0.67	N
4	3.94	3.90	-0.04	0.89	N
5	3.76	3.74	-0.02	0.72	N
6	3.41	3.66	0.25	0.82	N
7	4.00	4.16	0.16	0.84	N
8	4.00	3.84	-0.16	0.84	N
9	2.24	3.70	1.46	0.71	Y
10	1.98	3.30	1.32	0.91	Y

Table 5.3: Pre-to-post comparison of attitude questions for Inquiry Group.

Question	Inquiry Pre Mean	Inquiry Post Mean	Difference (post-pre)	Inquiry Pre STD	Inquiry Post STD	Statistically Significant (Y/N)
Inq ?'s	3.96	3.91	-.05	0.47	0.43	N
Trad ?'s	3.26	3.33	0.07	0.84	0.58	N
1	3.81	3.73	-0.08	0.74	.078	N
2	2.85	3.12	0.27	1.05	1.05	N
3	4.00	3.84	-0.16	0.92	0.75	N
4	3.67	3.54	-0.13	1.04	0.86	N
5	3.81	3.69	-0.12	0.79	0.55	N
6	3.48	3.81	0.33	0.85	0.69	N
7	4.07	4.31	0.24	0.92	0.79	N
8	4.11	3.96	-0.15	0.70	0.77	N
9	2.30	3.69	1.39	0.78	0.68	Y
10	1.93	3.27	1.34	0.73	0.87	Y

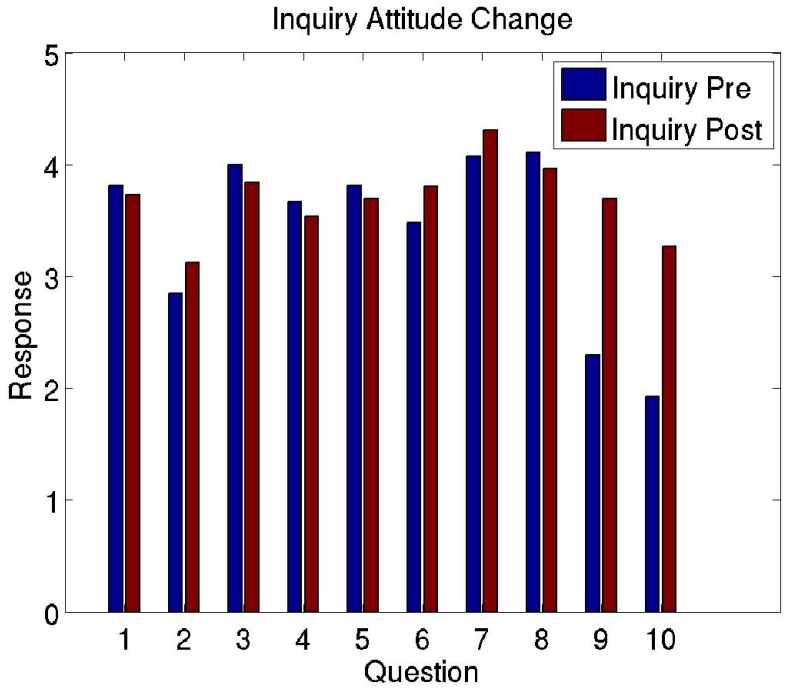

Figure 5.1: Pre (blue)-to-post (red) comparison of attitude questions for Inquiry Group.

Table 5.4: Pre-to-post comparison of attitude questions for Traditional Group.

Question	Traditional Pre Mean	Traditional Post Mean	Difference (post-pre)	Traditional Pre STD	Traditional Post STD	Statisti-cally Significant (Y/N)
Inq ?'s	3.74	3.71	-.03	0.47	0.64	N
Trad ?'s	3.48	3.63	0.15	0.63	0.58	N
1	3.54	3.46	-.08	0.83	0.88	N
2	2.61	2.91	0.30	0.99	0.95	N
3	3.68	3.68	0.00	0.64	0.57	N
4	4.25	4.29	0.04	0.68	0.75	N
5	3.71	3.79	0.08	0.95	0.88	N
6	3.33	3.50	0.17	0.76	0.93	N
7	3.92	4.00	0.08	0.78	0.88	N
8	3.88	3.71	-0.17	0.61	0.91	N
9	2.17	3.71	1.54	0.92	0.75	Y
10	2.04	3.33	1.29	0.91	0.96	Y

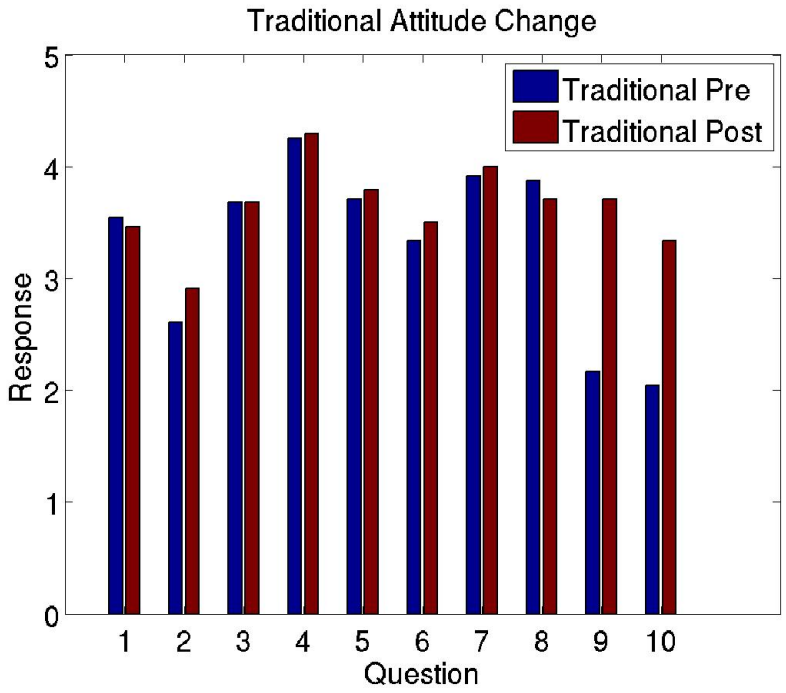

Figure 5.2: Pre (blue)-to-post (red) comparison of attitude questions for Traditional Group.

When comparing the attitude changes between the inquiry and traditional groups in the posttest only (Table 5.5), the only statistically significant difference between the groups was in Question 4, with the TG agreeing with the statement more. Question 4 was considered a traditional-positive question, since it asked about preference to following directions in a step-by-step manner. The fact that the TG responded more positively to this statement in the posttest might suggest that this group enjoyed this style of lab more. However, looking at the pretest responses to Question 4 (Figure 5.3), it can be seen that the TG also agreed with this statement more than the IG, which indicates that this is most likely not due to the lab treatment styles, but more due to the fact that even with random sampling the students placed in the TG had a predisposed preference towards traditional-style labs.

Table 5.5: Post-to-post comparison of Inquiry and Traditional responses to attitude questions.

Question	Inquiry Post Mean	Traditional Post Mean	Difference (IG-TG)	Inquiry Post STD	Traditional Post STD	Statistically Significant (Y/N)
Inq ?'s	3.91	3.71	0.20	0.43	0.64	N
Trad ?'s	3.33	3.63	-0.30	0.58	0.58	N
1	3.73	3.46	0.27	.078	0.88	N
2	3.12	2.91	0.21	1.05	0.95	N
3	3.84	3.68	0.16	0.75	0.57	N
4	3.54	4.29	-0.75	0.86	0.75	Y
5	3.69	3.79	-0.10	0.55	0.88	N
6	3.81	3.50	0.31	0.69	0.93	N
7	4.31	4.00	0.31	0.79	0.88	N
8	3.96	3.71	0.25	0.77	0.91	N
9	3.69	3.71	-0.02	0.68	0.75	N
10	3.27	3.33	-0.06	0.87	0.96	N

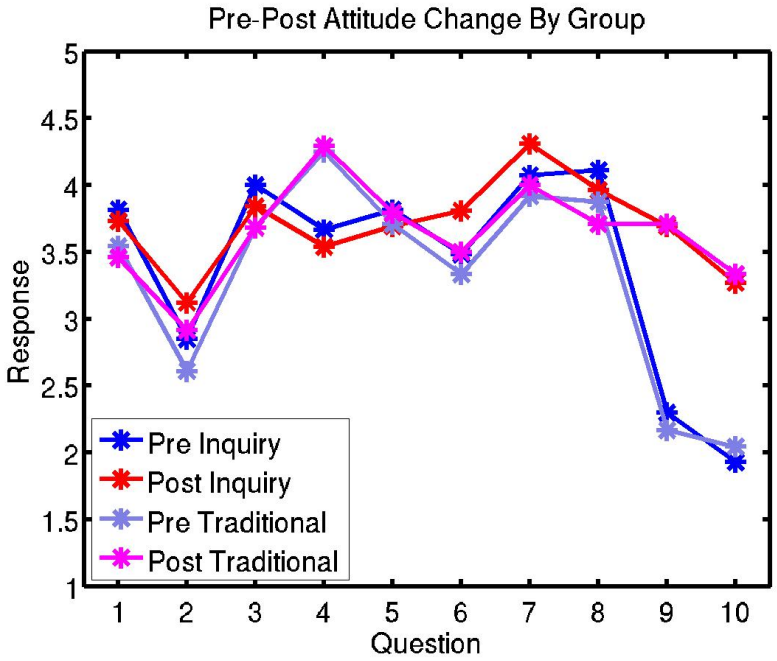

Figure 5.3: Pre (blue and purple, for IG and TG respectively) and post (red and pink, for IG and TG respectively) responses to attitude questions.

Finally, a comparison of post-to-post responses within the IG was done between those present on Day 1 who received the lecture, and those who joined the group on Day 2 and missed the lecture. The results of this comparison are shown in Table 5.6, and indicate a surprising statistically significant difference between the groups. The Inquiry without Lecture Group seemed to prefer the inquiry-positive questions more and the traditional-positive questions less than the Inquiry with Lecture Group. This result has two implications, the first of which is that being exposed to the review lecture probably did very little to change the students' ideas about the nature of science, and the second, which is supported by the results in Table 5.7, that suggests that the students in the Inquiry without Lecture group may also have been predisposed to enjoying inquiry-style activities. This second hypothesis is supported by the fact that the 5 students in this group missed class on Day 1 due to their own choice to go tornado chasing. These students clearly have a passion for experiencing meteorological phenomena, and since they were willing to ignore their original instructor's request for them to attend class, they also have shown themselves to be independent thinkers and were probably more comfortable doing the exploratory lab without guidance. Due to the very small sample size of the Inquiry without Lecture Group, the conclusions from the between group comparison are probably not significant, but are worth noting nonetheless.

Table 5.6: Post-to-post comparison in attitude between Inquiry with Lecture and Inquiry without Lecture groups.

Question	Inquiry w/Lecture Mean	Inquiry w/out Lecture Mean	Difference (with-without)	Inquiry w/Lecture STD	Inquiry w/out Lecture STD	Statistically Significant (Y/N)
Inq ?'s Post	3.83	4.26	-0.43	0.40	0.40	Y
Trad ?'s Post	3.48	2.70	0.78	0.54	0.28	Y

Table 5.7: Mean response by group for all pre and post attitude questions.

Question	Means Inquiry	Means Traditional	Means Inquiry with Lecture	Means Inquiry Without Lecture
Inq Pre (1,3,5,7,8)	3.96	3.74	3.88	4.32
Inq Post (1,3,5,7,8)	3.91	3.71	3.83	4.26
Trad Pre (2,4)	3.26	3.48	3.43	2.50
Trad Post (2,4)	3.33	3.63	3.48	2.70
1 Pre	3.81	3.54	3.68	4.40
1 Post	3.73	3.46	3.62	4.20
2 Pre	2.85	2.61	2.95	2.40
2 Post	3.12	2.91	3.25	2.60
3 Pre	4.00	3.68	3.95	4.20
3 Post	3.84	3.68	3.81	4.00
4 Pre	3.67	4.25	3.91	2.60
4 Post	3.54	4.29	3.71	2.80
5 Pre	3.81	3.71	3.77	4.00
5 Post	3.69	3.79	3.71	3.60
6 Pre	3.48	3.33	3.55	3.20
6 Post	3.81	3.50	3.67	4.40
7 Pre	4.07	3.92	4.05	4.20
7 Post	4.31	4.00	4.19	4.80
8 Pre	4.11	3.88	3.95	4.80
8 Post	3.96	3.71	3.81	4.60
9 Pre	2.30	2.17	2.18	2.80
9 Post	3.69	3.71	3.67	3.80
10 Pre	1.93	2.04	1.86	2.20
10 Post	3.27	3.33	3.19	3.60

5.5.2 Content Growth

The changes in content growth from the rubric scores were compared from the pretest to the posttest for the entire class (Table 5.8), for the IG (Table 5.9), and for the TG (Table 5.10). These results are shown for each of the 10 content short answer questions, excluding Question #20, with 21a being the multiple choice profile selection

and 21b being the explanation of the choice in 21a. When looking at the entire class, there was statistically significant growth from pre to post for all of the questions except for Question 19, which asked the students to describe changes in wind and moisture profiles before and after rainband passage. The most content growth is seen for Question 17, which asked students to compare the magnitude of the radial and tangential wind components on the mean wind. Focusing on just the IG (Table 5.9), statistically significant content growth can be seen in all questions except for #13 and #19. The TG (Table 5.10) has a similar outcome, except for a slight loss in content understanding on Question 19, though not significantly so.

When comparing the content knowledge between the inquiry and traditional groups in the posttest only (Table 5.11), it was found that although the IG did score slightly lower on 9 out of the 11 questions, the only statistically significant difference between the groups was in Question 15. Question 15 asked the students to describe a radial wind profile, and the results shown in Table 5.11 indicate that the TG had a deeper understanding of the features present in the radial wind in terms of inflow and outflow. These results can also be seen in visual form in Figure 5.4. Overall, both approaches to the rainband lab achieved content growth in almost every topic, with very little differences in significance of the amount of content growth between the two groups.

Table 5.8: Entire class pre-to-post content growth.

Question	Mean Pre	Mean Post	Difference (Post-Pre)	STD Post	Statistically Significant (Y/N)
11	0.86	1.90	1.04	1.27	Y
12	1.41	2.72	1.31	0.61	Y
13	2.35	2.64	0.29	0.63	Y
14	1.88	2.60	0.72	0.73	Y
15	0.75	2.02	1.27	1.08	Y
16	0.80	2.44	1.64	0.97	Y
17	1.33	2.32	0.99	0.87	Y
18	1.63	2.42	0.79	0.91	Y
19	2.16	2.40	0.24	0.99	N
21a	1.98	2.90	0.92	0.36	Y
21b	1.61	2.82	1.21	0.56	Y
Mean 11-21b	1.52	2.47	0.95	0.31	--
Mean 11-21, not 19	1.46	2.48	1.02	0.33	--

Table 5.9: Inquiry Group pre-to-post content growth.

Question	Inquiry Pre Mean	Inquiry Post Mean	Difference (post-pre)	Inquiry Pre STD	Inquiry Post STD	Statistically Significant (Y/N)
11	0.85	2.15	1.30	1.06	1.256	Y
12	1.48	2.65	1.17	0.89	0.69	Y
13	2.30	2.65	0.35	0.87	0.63	N
14	1.96	2.62	0.66	1.16	0.75	Y
15	0.74	1.65	0.91	0.86	1.06	Y
16	0.78	2.23	1.45	0.89	1.14	Y
17	1.26	2.19	0.93	1.20	0.98	Y
18	1.44	2.31	0.87	1.25	1.05	Y
19	2.00	2.54	0.54	1.14	0.90	N
21a	1.93	2.81	0.88	0.96	0.49	Y
21b	1.59	2.69	1.10	0.93	0.74	Y

Table 5.10: Traditional Group pre-to-post content growth.

Question	Traditional Pre Mean	Traditional Post Mean	Difference (post-pre)	Traditional Pre STD	Traditional Post STD	Statistically Significant (Y/N)
11	0.88	1.63	0.75	0.8999	1.2446	Y
12	1.33	2.79	1.46	0.8165	0.5090	Y
13	2.42	2.63	0.21	0.6539	0.6469	N
14	1.79	2.58	0.79	1.0206	0.7173	Y
15	0.75	2.42	1.67	0.7372	0.9743	Y
16	0.83	2.67	1.84	0.7614	0.7020	Y
17	1.42	2.46	1.04	1.0598	0.7211	Y
18	1.83	2.54	0.71	1.0495	0.7211	Y
19	2.33	2.25	-0.08	0.9168	1.0734	N
21a	2.04	3.00	0.96	0.9546	0	Y
21b	1.63	2.96	1.33	1.0555	0.2041	Y

Table 5.11: Post-to-post content knowledge comparison between IG and TG.

Question	Inquiry Post Mean	Traditional Post Mean	Difference (IG-TG)	Inquiry Post STD	Traditional Post STD	Statistically Significant (Y/N)
11	2.15	1.63	0.52	1.26	1.24	N
12	2.65	2.79	-0.14	0.69	0.51	N
13	2.65	2.63	0.02	0.63	0.65	N
14	2.62	2.58	0.04	0.75	0.72	N
15	1.65	2.42	-0.77	1.06	0.97	Y
16	2.23	2.67	-0.44	1.14	0.70	N
17	2.19	2.46	-0.27	0.98	0.72	N
18	2.31	2.54	-0.23	1.05	0.72	N
19	2.54	2.25	0.29	0.90	1.07	N
21a	2.81	3.00	-0.19	0.49	0	N
21b	2.69	2.96	-0.27	0.74	0.20	N

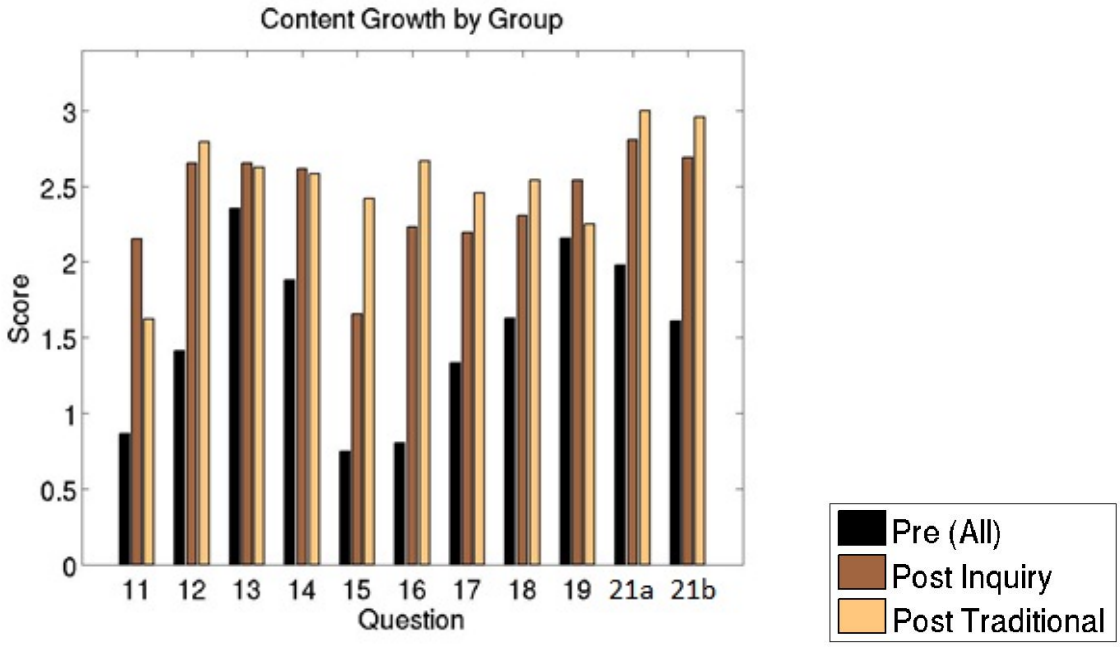

Figure 5.4: Content knowledge before for the whole class (black), post Inquiry (dark brown) and Post Traditional (light brown).

Finally, a comparison within the IG was done to determine if there were any significant differences in content growth between the inquiry students who were present on Day 1 and received the lecture and those who missed the lecture and joined the group on Day 2. The results of this comparison are shown in Table 5.12, and indicate that while most of the time (7 out of 11 questions) the group that received the lecture did score higher, only two of those times were statistically significant. The first of these, Question 13, asked whether all rainbands have the same mean horizontal wind profile. Although this topic wasn't covered in the lecture, several different cases of rainband radar loops were shown that might have helped the Inquiry with Lecture Group understand the variability in the observations better. The second question, Question 15, asked the students to describe a radial wind profile. Students who experienced the lecture scored a full rubric level higher on this question, but it was not covered at all during the lecture.

However, a description of what radial and tangential wind components represent in the mean wind was included, along with a description of how the profile data was collected, so the students may have been use that knowledge to make more meaningful connections during the lab. Although the sample size of the Inquiry without Lecture is too small to draw definite conclusions from, these results suggest that the information given in the lecture helped to enhance the conceptual understanding of the science content, indicating that a combination of lecture and lab work is most beneficial to student learning as the lecture provides necessary scaffolding to the inquiry work.

Table 5.12: Post-to-post comparison of content knowledge responses between Inquiry with Lecture and Inquiry without Lecture Groups.

Question	Inquiry with Lecture Post Means	Inquiry Without Lecture Post Means	Difference (With-Without Lecture)	Statistically Significant (Y/N)
11 Post	2.05	2.60	-0.55	N
12 Post	2.76	2.20	0.56	N
13 Post	2.81	2.00	0.81	Y
14 Post	2.67	2.40	0.27	N
15 Post	1.88	0.80	1.08	Y
16 Post	2.26	2.00	0.26	N
17 Post	2.19	2.20	-0.01	N
18 Post	2.38	2.00	0.38	N
19 Post	2.62	2.20	0.42	N
21a Post	2.76	3.00	-0.24	N
21b Post	2.62	3.00	-0.38	N

5.5.3 Content Retention

A retention test was given to the entire class one month after the initial investigation ended to test how well they remembered the main content covered in the lab and to see if there were any differences between the IG and TG in terms of content retention. The short answer retention questions were evaluated with a rubric similar to the

one described in Section 5.4.2, and the results comparing the responses between the IG and TG are shown in Table 5.13 and Figure 5.5. These results indicate that both groups were mostly even in content retention, with only moderate differences in Questions 3, 5, 7, and 8. Question 3 on the retention test was the same as Question 17 on the posttest, and on both tests the TG scored slightly higher. The concept referenced by this question involved comparing the magnitude of the radial and tangential wind components on the mean wind, and even though this topic was covered in the inquiry lab whole-class discussion it evidently did not make as significant of an impact on the group as it appeared to. Question 5 on the retention task asked students to state what dynamical force causes slowing in the mean wind speed near the earth surface (friction). This topic was also covered in some detail with the IG, and it appears that in this case, the conceptual understanding did take place for that group. The prior comments are mostly speculation, as the only significant difference in retention between the two groups was with Question 8, which required students to select a sample profile of the radial wind and explain their choice. As in Question 15 on the posttest, the TG scored higher on this topic again on the retention test, signifying that not only did they learn about the features during the lab more than the IG, but that their learning was meaningful enough to recognize the features a month later.

5.5.4 Student Input

The results shown in the previous sections indicate that only minimal differences in content growth and retention and no difference in attitude changes regarding science labs occurred between the groups. Some statements from the class discussion that took

place following the post-test suggest reasons why that may be the case based on this experiment.

Table 5.13: Content retention by IG and TG one month after the initial treatment.

Question	Mean IG	Mean TG	Difference (IG-TG)	STD IG	STD TG	Statistically Significant (Y/N)
1	1.92	1.96	-0.04	1.04	1.11	N
2	2.72	2.78	-0.06	0.68	0.52	N
3	2.00	2.26	-0.26	0.96	0.96	N
4	2.76	2.70	0.06	0.60	0.64	N
5	2.92	2.65	0.27	0.40	0.93	N
6	2.68	2.57	0.11	0.63	0.79	N
7	2.08	2.52	-0.44	0.81	0.79	N
8	1.52	2.04	-0.52	0.77	0.82	Y

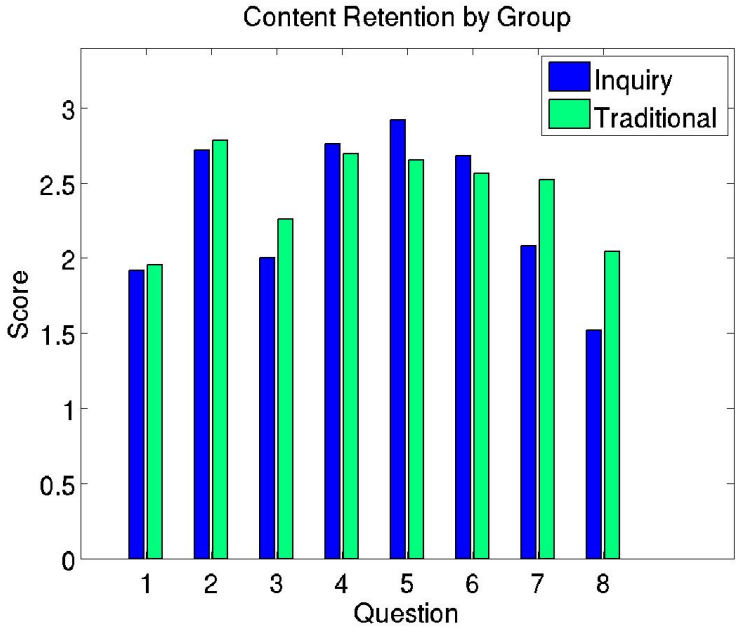

Figure 5.5: Content retention question responses between IG (blue) and TG (green).

Once the class handed in their posttests, they were told what both groups had done during their lab approach and asked for feedback on their experiences. The

discussion began with seven planned questions. First, the students were asked how many of them had done a lab with a similar style to their approach before. Although 16 out of the 24 students in the TG felt they had done traditional-style labs before, only 5 out of the 27 in the IG felt that they had previous experience with a similar inquiry lab.

Next, they were asked about the use of Excel as a plotting tool, as it had been a source of frustration for both groups. Both groups responded that they had used it before, but said they spent a lot of time figuring out how to graph. Both the IG and TG would have liked to see a projected example of plotting with Excel in front of the entire lab group to feel more comfortable with their plotting.

The third question asked about how much they enjoyed the lab. The IG commented that they felt it was a little short on learning, as there was too much emphasis on technology. Quite a few students from the IG said that they felt rushed to keep up with the rest of the group, but only 2 students from the TG (the two who did not finish the lab) agreed with the statement about feeling rushed. The TG did agree about there being too much focus on technology, but did not feel that it was short on learning.

The fourth question asked if the lab made the students feel like a scientist. Here, the IG said that it mostly did because it was *"like actual research since you have to decide what you need*". Another student in the IG commented that *"We had technology issues… but I guess scientists do too"*, showing some growth in their ideas about the NOS. The TG responded that they felt like scientists when doing the plotting only, but the fact that the rest of the instructions were spoon-fed made them feel more like students, not scientists.

The fifth question asked if they felt the lab was worthwhile. The students responded to this question by raising their hands to show that they felt it was worthwhile, with 18 students from the IG agreeing and 10 students from the TG agreeing.

The final two questions asked what the students liked about the lab and what they didn't like. Lots of students from both groups said they would have preferred a mix of both labs. The IG said their approach was confusing at first, and took a few minutes to get going, but once the ball was rolling they enjoyed it. They wanted a little more guidance in terms of what questions to answer at the start of the lab, but once they were guided to some scientific issues to explore they were more confident. Although there were several IG students who took charge during the lab and kept the pace moving forward who really enjoyed the approach, other students in that group commented that they felt left behind a lot, especially when they were struggling with Excel issues and had to focus on the software rather than the science content. Students in the TG complained that they didn't learn anything beyond making the graphs since there was no immediate feedback to know if they were plotting correctly in the first place. They also commented again that their approach was too repetitive on plotting tasks, and they wished the efficiency of getting to the content points were better so they didn't have to make so many plots.

After receiving responses to the seven planned questions, the discussion was opened up for any additional feedback. Most of the comments were related to the extremes of each approach. Many IG students commented that would have liked to start out in smaller groups to get used to the data, and then work as a class. A few students from the IG said they liked the big group, because more opinions could be shared.

Students in this group also commented that when they were plotting different things it was hard to share their plots on their laptops and it would have been nice to have a way to project the graphs so everybody could see them. Students in the TG said they also would have preferred working in smaller groups too, at least to discuss the plotting issues they were having.

One surprising result for the students was that a few people who said that they thought they preferred one type of lab were surprised to enjoy the other. An example of this was a student in the IG who was a leader during much of the inquiry lab who said that he usually preferred to work alone, but was surprised to really enjoy this approach. As a side note, this student said he had a high level of familiarity with Excel, so his enjoyment may have been influenced by not having as many plotting issues as other students. An alternative example to the lab style preference came from the one student in the IG who had to share a laptop with his neighbor. He said that although he normally enjoys group work, not being able to plot on his own made him wish he were working on the lab alone.

It appears that this lab pushed the boundaries on how the students thought they preferred to work, but it was surprising that when the students were told what the other group had done, a lot from the TG wished they had been in the IG, but a few from the IG also wished they had been in the TG. These preferences indicate that one lab approach does not fit all learning styles, which future instructors need to keep in mind when implementing any classroom activity. Overall, both groups seemed to agree that something in the middle of the two approached would be preferable, such as working in

smaller groups, having some broad questions to follow as instructions, not having to fill in the answers to the lab, and sharing the responsibility in making the plots.

5.6 Summary and Conclusions

5.6.1 Key Findings

Relating to the four research questions presented in Section 5.1, this study showed that

I. An inquiry-based learning approach using real-world data did not systematically change the student's attitudes toward science labs. However, comments from the class discussion in Section 5.5.4 indicate that many of the students in the inquiry group were able to vocalize an increased understanding about the nature of science, especially relating to data processing and analysis and collaboration.

II. The inquiry-based approach was effective at conveying content knowledge regarding wind and moisture profiles in hurricane rainbands.

III. This study suggests that there is no difference in attitude change depending on whether an inquiry or traditional teaching approach is used. The traditional approach did score significantly higher for content growth and retention related to the subject of radial wind profiles, but otherwise the difference in content growth and retention between approaches was minimal.

IV. One of the main challenges associated with an inquiry approach was adjusting to the inquiry process, as it was unfamiliar to the majority of the students. Technology presented a major challenge for both groups, but its effect was more pronounced with the inquiry approach due to the pressure to keep up with the rest

of the group. These challenges can be overcome by providing students with more opportunity to become familiar with the technology and providing teacher scaffolding as they build their inquiry skills. The traditional approach had specific challenges as well, mainly lack of collaboration and repetitiveness/boredom. A blend of the two extreme approaches tested in this study would be ideal for student learning.

5.6.2 Discussion

As the results shown in Section 5.5 indicate, in this case neither the traditional lab approach nor the inquiry lab approach was that different in terms of causing content growth or retention. The only significant difference between the groups favored the TG and was related to content involving the radial wind profiles. One hypothesis as to why a difference occurred with this subject is due to the technology. By the time the IG got to working with the radial wind data, the group of 6-8 students who were most vocal in the lab had become confident with their Excel skills, and were able to plot the data with more ease. Some of the other students were still struggling or had had their Excel programs crash and had to reboot their computers, causing a distraction from the learning. In order to keep up with the rest of the group, these students may have just vocalized agreement with what the leaders described without actually plotting and understanding the data themselves.

Additionally, in this study neither the inquiry approach nor the traditional approach had a significant effect on changing the students' attitudes toward science labs. Some statements from the discussion shed more light on why that may be the case based

on this experiment. The two approaches used in this lab are on the extreme ends of two lab styles, with the traditional lab being very rigid in instructions and individual work and the inquiry lab being very open-ended in instructions and conducted as a large group investigation.

During the planning stages, the traditional lab was designed first, and broad questions were developed from that as the guidelines for leading discussion during the inquiry lab. From there, the broad questions were transitioned into a scenario with guidelines, which was handed out as the instructions for the inquiry lab, as scenarios have previously been shown to increase student connection to the material (Howard and Miskowski 2005). The inquiry lab was conducted with half the group rather than small groups as it was both the students' and my first experience participating in a guided inquiry study, so one group was used to make sure it was done correctly. Additionally, the inquiry lab was conducted before the traditional lab in order to avoid introducing any bias of improving communication about topics learned during the traditional approach.

As both labs consisted of the extremes of their approaches, both labs had challenges. Some of the largest issues with the inquiry lab involved technology and adjustment to the inquiry process. As the majority of the IG was unfamiliar with this approach, there was class-wide hesitation about where to start. The issues with Excel caused some students to focus so much on plotting that they could not devote their time to learning. Students in the IG seemed afraid to admit that they were lost or could not plot, and found it hard to keep up with the 6-8 people leading the lab, even though the progression of the lab was often paused in an attempt to keep students on pace.

Although Excel was also a challenge for the TG, it wasn't so much of a stress because the students could work on the lab at their own pace and figure out how to plot on their own schedule. The main challenges with the traditional approach were the lack of interaction and the repetitiveness. The students in the TG expressed frustration at being unable to talk about how to plot except with the instructor. They wanted feedback that they were working with the right data set, making plots the correct way, and drawing acceptable conclusions, as they had no idea if the work they were doing was right or wrong. The fact that the instructions were explicitly laid out with the TG caused the lab to seem boring and repetitive with plotting and writing down answers, rather than being responsible for their learning trajectory as with the IG.

Overall, a blend of the two approaches described in this study is probably more effective than the extreme of either approach. The inquiry lab would work better if the students worked in smaller groups where they felt more welcome to speak up and explore their own ideas. Also, previous practice with Excel would have been helpful, as it was a major cause of issues in both groups. It is worth noting that the inquiry approach was practiced with a group of 5 junior meteorology majors at the University of Miami (UM) who volunteered their time prior to being done at the University of Oklahoma. The UM students worked together through the inquiry lab, and even though they also had the initial struggles found when deciding how to use the data, they seemed to struggle less with the technology side. These students, while a year earlier in their studies, had all taken a meteorological instrumentation course the previous year which required them to frequently use Excel to plot data. The UM students were not given any assessment tests, but vocalized enjoyment with the inquiry style more than the Oklahoma students seemed

to. A large portion of that could have been due to the fact that they were able to work in small groups and collaborate more effectively.

Based on this study, it appears that both the inquiry and traditional approaches are effective for student learning, though students do get a better understanding of how science is done with the guided inquiry approach. Although the inquiry approach does require a learning curve of deciding how to utilize the data which can cause frustration among the students, the students most comfortable with the technology seemed to get the most out of the inquiry experience. If the students were able to work in smaller groups and did not have to expend an effort keeping up with the whole class, it is likely that positive changes in attitude towards inquiry labs would be seen along with content growth, as in previous studies such as Yarger et al. (2000).

5.6.3 Contributions to the Literature

This study fills in valuable gaps in the literature related to inquiry use in higher education as it presents an example of how to use real-world (but not real-time) data in an undergraduate classroom through a student-centered approach for effective student learning.

This study not only presents an example of an effective inquiry lab, but also systematically compares the student-centered approach to a traditional approach to determine if the inquiry approach is better for content growth and understanding of the nature of science. This study suggests that for students that are not used to student-centered approaches, there is only a minimal difference in content knowledge growth between approaches. It also suggests that neither approach changes attitudes towards

science. Although this seems to imply that it doesn't matter which approach is used when using real-world data in an undergraduate meteorology lab, the comments from the class discussion indicate that several of the students in the inquiry group gained an increased understanding about the nature of science, while those in the traditional group just felt like they were completing a class assignment.

This study not only provides a quantitative comparison of the two approaches, but also a discussion of the benefits and challenges associated with each approach and their implications for student learning. This provides a useful insight for future faculty members to more effectively implement student-centered labs in their classrooms.

5.6.4 Implications for Teaching

This study also has several implications for classroom teaching using an inquiry-based approach. First, it shows that even students not familiar with inquiry-based learning are able to gain content knowledge using real-world data in this approach without having to physically take part in the data collection. This implies that faculty can use data sets found on line or from previous field projects to effectively convey content knowledge in the classroom without having to partake in expensive or time-consuming data collection (or re-collection). This also suggests that an inquiry technique would also be valuable with modeling projects or other theory-based classroom activities.

Second, this study shows that though not all students will appreciate an inquiry-based approach, those that are comfortable with it can gain an enhanced understanding about the nature of science. This implies that although there is very little difference in content growth between approaches, there are benefits to using an inquiry-based

approach over a traditional approach, provided that it is implemented and scaffolded correctly. Additionally, this study was based on a short intervention, and it is likely that a longer approach would produce even more positive inquiry experiences as students became used to the technique.

Finally, this study expands on previously seen challenges seen in the literature associated with inquiry-based learning. The two main challenges seen in this work are familiarity with the approach and competence with the technology. This study suggests some ways that classroom teachers at all levels can overcome these challenges to make inquiry-based learning more accessible, especially for faculty members who lack a strong knowledge of pedagogy.

5.6.5 Future Work

Although this study addressed many research questions related to using data in undergraduate classrooms through student-centered approaches, it also brings up three ideas for future research to enhance the understanding of the results found.

First, with this study in particular, it would be valuable to switch the groups in this class and conduct a similar study using another data set to evaluate attitude changes between groups with the alternative approach. This would help to ensure that the lack of attitude changes by group was not simply due to the random group placement, but to the different approaches themselves. Unfortunately, since this class has already concluded and the majority of the students have graduated, this work is not possible at this time. However, it should be kept in mind as an important study question for similar studies in the future.

It would also be interesting to conduct this exact same study at other universities to ensure that the results were not just due to the college where the study took place. Other universities may have students who are more familiar with Excel (as in the UM example) or are more familiar with student-centered approaches. It is possible that such students might see additional content gains and ideas about the nature of science in the inquiry group over the students who were included in this study. Additionally, students at a community college or online learners might have different experiences with an inquiry-based approach than the students in this study.

Finally, a longitudinal study working with the same class for a semester would be valuable future work. In this case, the students would still randomly be placed into two groups to test the approaches, but the inquiry group would be provided with more scaffolding, working up to a full inquiry approach over time to assess the impact of an increased comfort level with student-centered learning.

Chapter 6: Summary, Conclusions and Future work

6.1 Summary

Remote sensing observations of tropical cyclone rainbands are used to describe the vertical structure and temporal variability of stratiform rainbands. The rainbands presented in the this work were observed in August and September 2008 from Tropical Storm Fay, Hurricane Gustav, and Hurricane Ike in South Florida. This study represents one of the first times that such a wide variety of instrumentation was able to collect data from multiple landfalling systems since capturing data from landfalling tropical systems is challenging due to safety concerns, instrument limitations, and logistical difficulties. The availability of multi-wavelength radar observations allowed for the characterization of the detailed vertical structure of these rainbands and capture of the sub-kilometer-scale variability to create a high-resolution representation of rainbands over land. This includes a focus on the vertical structure of the wind components including locations of wind maxima and inflection points, conditions in the surface layer, and changes during rainband passage, as well as the small-scale (< 1 km) variability seen during these rainbands. This work will improve the understanding of the conditions that occur in an urban coastal environment with rainband passage, especially in the surface layer where winds can have a large impact on structures.

Fourteen cases from stratiform periods in outer rainbands of three tropical systems in August and September 2008 in South Florida are analyzed to study rainband wind structure. These cases are chosen due to their constant reflectivity profile with time, presence of a bright band located around 4.5 km, and light to moderate rainfall rate. With this data set, the vertical structure of wind profiles from rainbands of storms of different intensities and distances are able to be compared.

6.1.1 Vertical Structure of the Rainband

Results of wind speed profiles show that the maximum horizontal wind speed in the rainbands is typically between 1000-1500 meters in height, and remains nearly constant up to 3000 meters, then decreases between 3000 and 4000 meters AGL. This low-level wind maximum is called the inflection point of the log-wind layer, or Vh IP, Top of Log-wind Layer, and is located at the top of the HBL. Several rainband cases show evidence of a secondary horizontal wind maximum around 3500-5000 meters AGL. This secondary wind maximum is found to be stronger than the low level wind maximum in the four cases of stronger storms observed at further distances from storm center. In terms of wind direction, the profiles show a general veering with height of 20^{o}-30^{o} over the lowest 1000-1500 meters AGL, or up to the height of the wind maximum.

All rainbands show a logarithmic wind speed decrease below 500 meters, though it often changes slope in the lowest part of the surface layer (lowest 200 meters AGL). The depth of this lowest logarithmic profile is called the inflection point of the surface layer, or Vh IP, Top of Surface Layer. Mean horizontal wind between 65-120 meters AGL are used to solve for the various components of a log-wind equation. The goodness of fit to the linear plot is very high, and the calculated friction velocity is reasonable based on the rainband conditions. While the aerodynamic roughness length is found to be much more variable than previous observations, using the calculated components allows for the estimation of winds from 65-500 meters above ground level with decent accuracy. However, a constant value for extrapolating wind speeds near the surface in future storms appears unrealistic based on this data set. Using a mean z_0 value with individual u_* values by rainband calculates winds that are within 6 ms^{-1} of the actual wind speed at 90

meters AGL. There is not a consistent trend in whether the calculated wind speed over- or under-estimates the actual wind speed, but in terms of building codes, using a mean z_0 is an acceptable option for estimating wind speeds near the tops of tall buildings (200-400 feet) if wind speed values in that range are used for the z_0 calculation. However, using a mean z_0 value from 200-400 feet to assess wind speeds at 18 meters underestimates the winds by 2-5 ms^{-1}, even for weak (< 10 ms^{-1}) wind speeds. This suggests that using a mean z_0 is not an effective way to calculate near-surface wind speeds from winds aloft (and vice versa). Since this underestimation occurs with observed wind speeds that are less than 10 ms^{-1}, it will likely be more extreme under higher wind speeds, so based on this data set a mean z_0 does not seem to be valuable for determining building wind codes during rainband conditions.

Radial and tangential wind components are calculated and show a mean transition from radial inflow at low levels to radial outflow around 2500-3000 meters AGL. The radial inflow maximum is around a height of 500 meters, while maximum outflow is much more variable in height. The height of the maximum radial inflow is called the inflection point of the radial wind, or Vr IP.

Tangential wind profiles are all positive, with a peak between 1000-3000 meters AGL, where values are close to constant with height. Although most tangential profiles decrease in speed with height above 3000 meters, a few of the cases do show evidence of a small tangential wind maximum around 3000-4000 meters AGL, especially during the stronger storms Gustav and Ike. Tangential wind profiles by rainband closely match the mean horizontal wind in strength and structure, as they make up the largest component of total horizontal winds, although changes in wind directions appear to be associated with

changes in the radial wind. These findings on radial and tangential wind profiles are in agreement with those found during previous studies, both over water and over land.

A comparison of surface winds to HBL winds shows a mean ratio of 0.36 between 18 meter mean wind speeds and the mean wind speed at the top of the BL. This ratio is lower than even the lowest bound of 0.55 found by Powell and Black (1990) between ocean buoys and flight-level winds, and much lower than the 0.67 ratio found by Blackwell (2000) over land to flight-level winds. These much lower ratios could partially be due to the friction effects of being over land, the fact that these observations are located far from the storm center, and the fact that the mean HBL wind speeds are lower than those measured by previous studies

Temporal variability within Band 21 is examined with half hour averaged profiles during Band 21a and Band 21b to illustrate changes over a four hour period. Two striking features seen during this analysis are an ascending and strengthening low-level wind maximum during Band 21a that is gone an hour later by Band 21b, and a decrease in the low-level radial inflow over time. The differences in wind structure between the 30 minute averages during Band 21a and 21b further helps to illustrate that while both scenarios are stratiform rainbands, the location of the rainband sampled can cause the observed conditions to vary widely.

Data sets from various instruments were combined to compare non-precipitating periods before and after rainband passage with stratiform periods within the rainbands. In the case study presented, an increase in V_t is apparent over time that is related to the storm center moving towards the site. A consistent low-level wind maximum is present around 1000 meters AGL, and it appears to rise in height and broaden with rainband

passage. The depth of the radial inflow layer is shown to deepen during the rainband case study, and then return to a more shallow level after rainband passage.

Rainband characteristics can change drastically depending on storm intensity, storm-relative location, and rainband stage, so it is important to remember that even with several case profiles, these observations are still only point profiles in a much larger tropical system. While many of the observed wind structure components shown in this work agree with previous observations, the high resolution of this data set and wider variability in observing instruments allowed for the study of the variability in structure in greater depth. Although not all of these observations agree with previously published work, having several cases for analysis helps to solidify the belief that the differences seen could be partially due to the location over land, which makes this data set valuable for comparison with observations over the ocean.

6.1.2 Small-scale Vertical Motions

Four case studies are presented to showcase the mesoscale (< 5 km) and small-scale (< 1 km) variability within stratiform rainbands. Even with a constant melting level height, similar rain rates, and seemingly benign conditions, vertical fluctuations are present in the majority of the cases. The vertical velocity perturbations (w') are found to be on the order of 4 ms^{-1}, and are due to a combination of updraft and downdraft features and drop size variability. Attempts to deconvolve these two influences do not indicate that one is more dominant than the other consistently.

Eddy fluxes are shown for the four cases to represent vertical variability. Three of these cases (Bands 4a, 9a, and 21a) show vertical features extending from about 1000

meters up to the melting level that are on wavelengths of 3.5-5.3 km and are spaced about 15 minutes apart (10-15 km depending on rainband motion). The wavelengths of these features are shorter than those seen in finescale bands but longer and deeper than those seen in HBL rolls. It is hypothesized that the rolls are being triggered at low levels (<500 meters), and the instability in the atmosphere is carrying the features associated with them up to the melting level. On the other hand, the vertical features could be forced thermodynamically from the melting level. Three of the case studies suggest that a combination of forcing mechanisms are at work, with some of the filaments being generated above the melting level, and some just existing in the rain. It is likely that a combination of surface forcings and melting level/evaporation forcings are acting on these three cases, which can explain why the resulting length scales do not solely fit into the theory of any forcing mechanism. A blend of two or more mechanisms acting in conjunction could superimpose a new wavelength on the signal, making it impossible to determine which mechanism is more dominant.

The case study of Band 21b provides an interesting perspective of the differences between environmental conditions in the HBL and in stratiform rainbands. The fact that large vertical variability and the turbulent features are seen in Bands 4a, 9a, and 21a suggest that these are features related to band-specific dynamics. The fact that Band 21b does not show these vertical features and also is completely melting layer forced suggests that the other three cases that do have vertical features are most likely influenced by a combination of HBL rolls and melting level features, and that the HBL rolls may play a larger role in the vertical transport.

Unfortunately, vertical profiles of TKE with height do not support the previous conclusions, as they suggest that Bands 4a and 9a are gaining the most energy from turbulence above the HBL and near the melting layer, while both cases from Band 21 have the highest TKE near the surface, making them more likely to contain HBL rolls. This apparent disconnect between potential forcing mechanisms makes it difficult to determine the exact cause of the vertical features seen in the four cases.

6.1.3 Using Field Data in the Classroom

Finally, a study, based on these research results, for testing the most effective use of field data in an upper level meteorology classroom is described. This work involved designing a weeklong study conducted with senior meteorology majors at the University of Oklahoma to test whether a traditional laboratory approach or an inquiry laboratory approach changed attitudes about science and content knowledge growth and retention. Three stratiform rainband cases were used to encourage content growth regarding vertical structure and variability of wind and moisture components. The results suggest that both lab approaches were effective at improving content knowledge, with only minor significant differences in content growth or retention by group. Neither lab approach had an influence on changing the undergraduate senior meteorology students' attitudes toward science labs, either by enhancing preference toward inquiry-based labs or by enhancing preference toward traditional-style labs. Only one content area had a significant difference in knowledge growth and retention between the approaches, and that was radial wind, which could be explained by technological challenges encountered by both groups.

The two lab approaches used in this study were on the extreme ends of two lab styles, with the traditional lab being very rigid in instructions and individual work and the inquiry lab being very open-ended in instructions and conducted as a large group investigation. As both labs consisted of the extremes of their approaches, both labs had challenges. Some of the largest issues with the inquiry lab involved technology and adjustment to the inquiry process. As the majority of the inquiry students were unfamiliar with this approach, there was class-wide hesitation about where to start. The issues with Excel caused some students to focus so much on plotting that they could not devote their time to learning. While Excel was also a challenge for the TG, it wasn't so much of a stress because the students could work on the lab at their own pace and figure out how to plot on their own schedule. The main challenges with the traditional approach were the lack of interaction and the repetitiveness.

Overall, a blend of the two approaches is probably more effective than the extreme of either approach. The inquiry lab would work better if the students worked in smaller groups where they felt more welcome to speak up and explore their own ideas. Also, previous practice with Excel would have been helpful, as it was a major cause of issues in both groups. Based on this study, it appears that both inquiry and traditional approaches are effective for student learning, though students do get a better understanding of how science is done with the guided inquiry approach. While the inquiry approach does require a learning curve of deciding how to utilize the data which can cause frustration among the students, the students most comfortable with the technology seemed to get the most out of the inquiry experience.

6.2 Outlook and Future Work

The results presented in this work help to fill an important gap in hurricane rainband observations over land. Previous observations of rainbands over land are limited due to safety and logistical reasons, and direct comparisons of rainbands over water and over land are still challenging, especially at low levels where the amount of land influence on the rainband conditions is relatively unknown. This dissertation shows observations of many rainbands over land observed from a variety of instruments. While the data set does include a wide range of storm conditions, it is still too small to draw definite conclusions from. The main features described in Sections 6.1.1 and 6.1.2 can be connected with previous observations and scientific theory, but the variations between rainbands present many features that are difficult to explain with a limited data set.

Nevertheless, having 14 stratiform periods in 24 rainbands allowed for a high-resolution (~7 meters vertically) analysis of the conditions in the HBL and free atmosphere and provide a very valuable addition to previous research done on mean and small-scale conditions in hurricane rainbands. As technology continues to improve, remote sensing and in-situ hurricane observations can continue to examine the small-scale variability that exists in these storms. Capturing landfalling systems to compare with the results shown here will continue to be a challenge, but with the wide coverage of WSR-88D radars around the country, future VAD studies could be done. With an increased knowledge of landfalling hurricane rainband conditions, simulations and forecasts of hurricane impacts could be improved before a storm comes close enough to impact land.

Another area of potential future work would be to compare the results shown here to regular (non-cyclonic) tropical squall lines. There were a few stratiform anvils observed during the field campaign that could be used to compare drop size properties and vertical air motions. Additionally, convective periods could be used to calculate the log-wind profile near the surface and see if the values of wind stress (u_*) and surface roughness (z_0) change, even when occurring at the same location.

It is important to study and understand the layer of the atmosphere closest to the surface in order to better be able to predict storm conditions and their impact on life and property. This study has provided further evidence about the conditions that exist in tropical cyclone rainbands over land. Even in conditions that are thought of as stratiform, wind speed maxima and vertical motions are evident and understanding where they are located and how they change is important current and ongoing work.

Appendix A: Previously Published Figures in the Literature

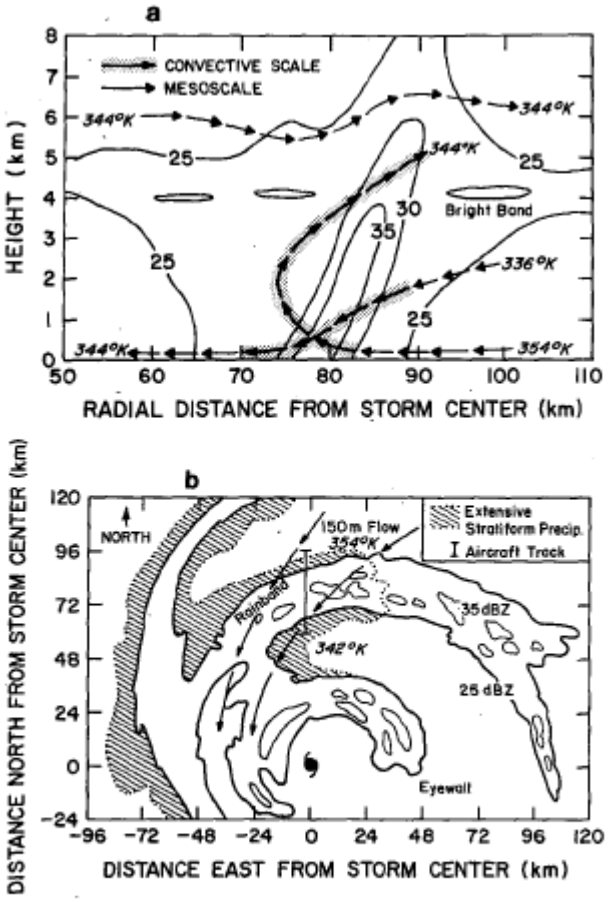

FIG. 18. (a) A schematic of the rainband in r, z coordinates. Reflectivity θ_e, mesoscale (arrows) and convective scale motions are shown. (b) Rainband in x, y coordinates. Aircraft track reflectivities, cells, stratiform precipitation and 150 m flow and θ_e values are shown.

Figure A1: Rainband schematics. From Barnes et al. 1983.

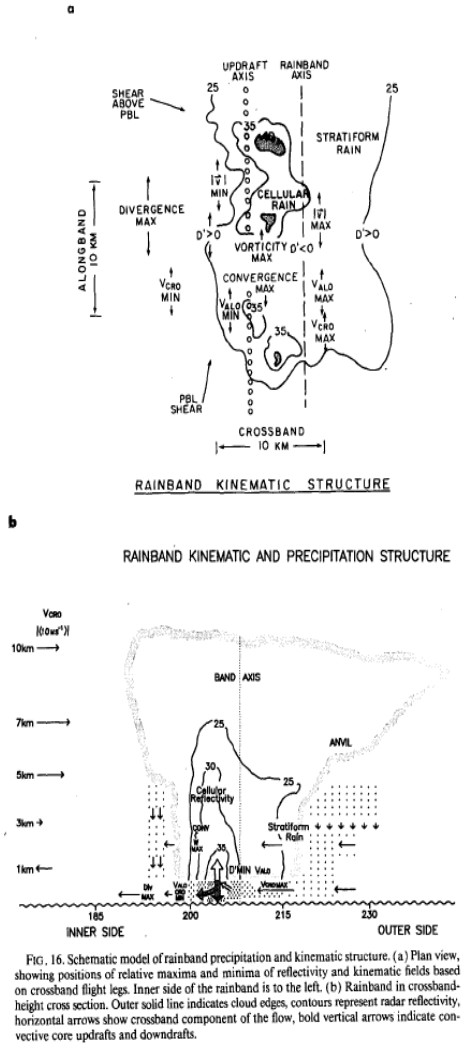

FIG. 16. Schematic model of rainband precipitation and kinematic structure. (a) Plan view, showing positions of relative maxima and minima of reflectivity and kinematic fields based on crossband flight legs. Inner side of the rainband is to the left. (b) Rainband in crossband-height cross section. Outer solid line indicates cloud edges, contours represent radar reflectivity, horizontal arrows show crossband component of the flow, bold vertical arrows indicate convective core updrafts and downdrafts.

Figure A2: Rainband schematics. From Powell 1990a.

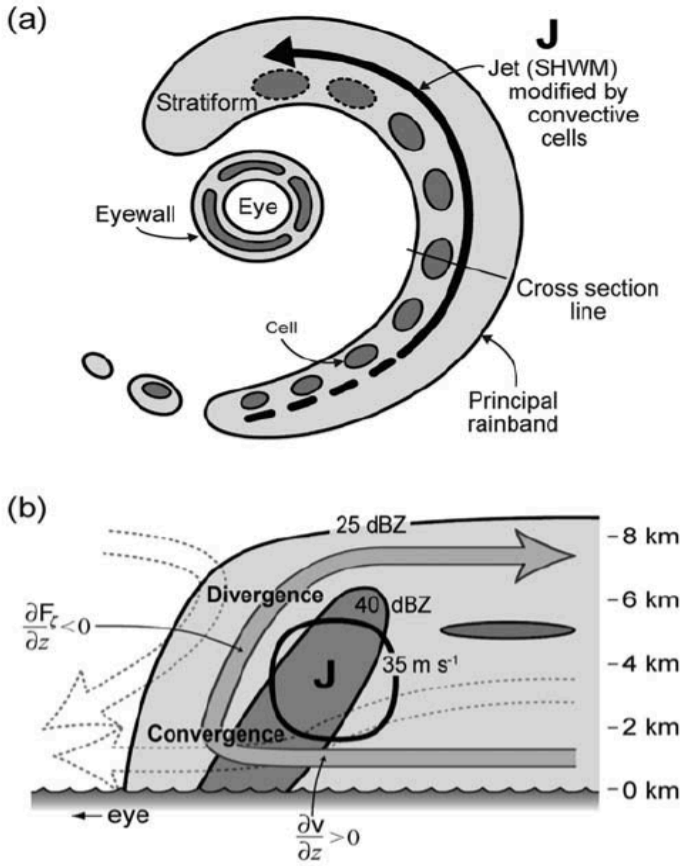

Figure 13. (a) Plan view schematic of the principal band within a mature, single-eyewall hurricane, with the SHWM (labeled as "jet") illustrated in relation to the convective elements within the rainband. The 25 dBZ region is indicated by light shading, and 40 dBZ region is indicated by darker shading. The cross section conceptualized in (b) is indicated by a line through the middle portion of the rainband. The size of the convective cells indicates the level of maturity, with the dashed border indicating collapsing cells. (b) Schematic of the vertical convective motions within rainband along the cross section indicated in Figure 13a. The reflectivity contours are consistent with Figure 13a. The clear arrow indicates the in, up, and out convective circulation conceptualized by BZJM, passing through a low-level convergence, vertical convergence of vorticity flux, and midlevel divergence regions indicated. The circled region labeled "J" indicates the same rainband tangential wind jet, with the associated low-level shear. Dashed arrows in the background indicate the low-level downdraft conceptualized by BZJM and the upper-level downdraft as a part of the three-dimensional flow.

Figure A3: Rainband schematics. From Hence and Houze 2008.

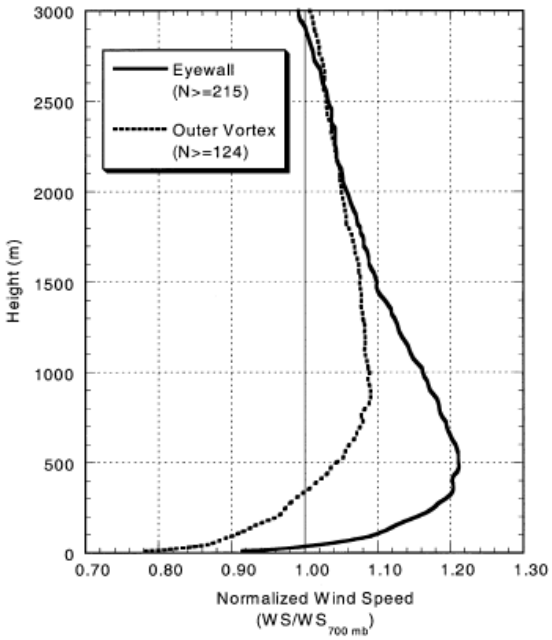

FIG. 8. Mean hurricane wind speed profiles for the eyewall and outer-vortex regions. Wind speeds are averaged and expressed as a fraction of the profile wind speed at 700 hPa. The minimum number of profiles used to construct the averages is also indicated.

Figure A4: Mean hurricane wind speed profiles for the eyewall (solid) and outer-vortex regions (dashed line). From Franklin et al. 2003.

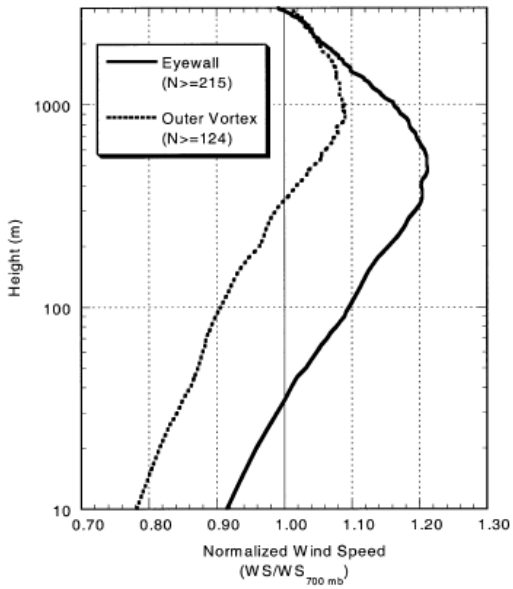

FIG. 9. As in Fig. 8 except that the height axis is plotted on a logarithmic scale.

Figure A5: As in Figure A4, but with y-axis plotted on a logarithmic scale. From Franklin et al. 2003.

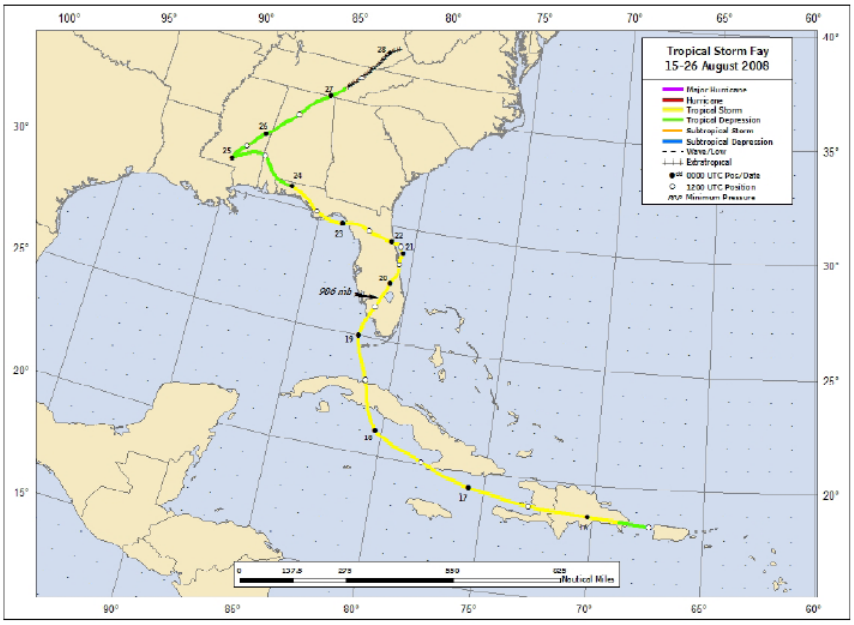

Figure A6: Best Track positions for Tropical Storm Fay, August 15th-26th, 2008. From the National Hurricane Center.

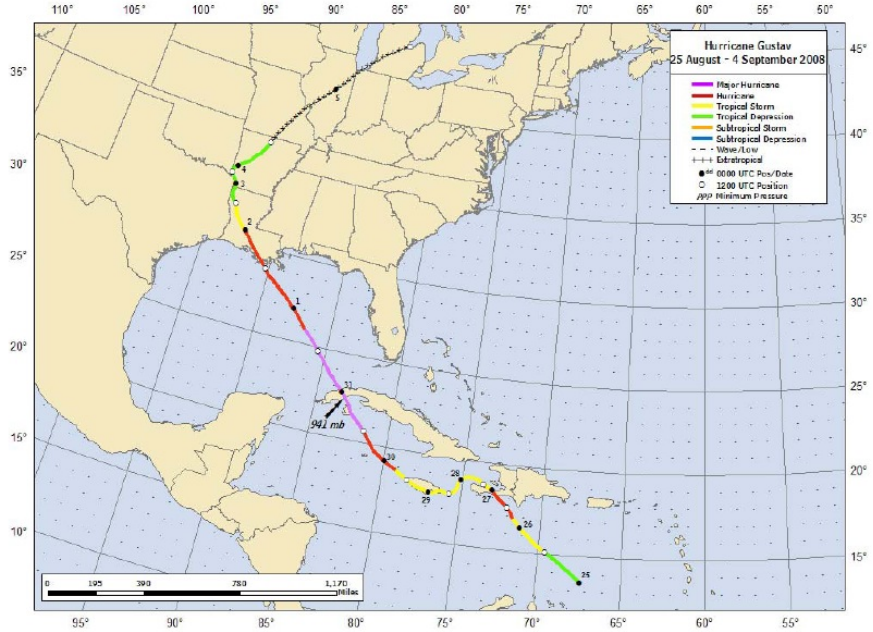

Figure A7: Best track positions for Hurricane Gustav, August 25th - September 4th,2008. From the National Hurricane Center.

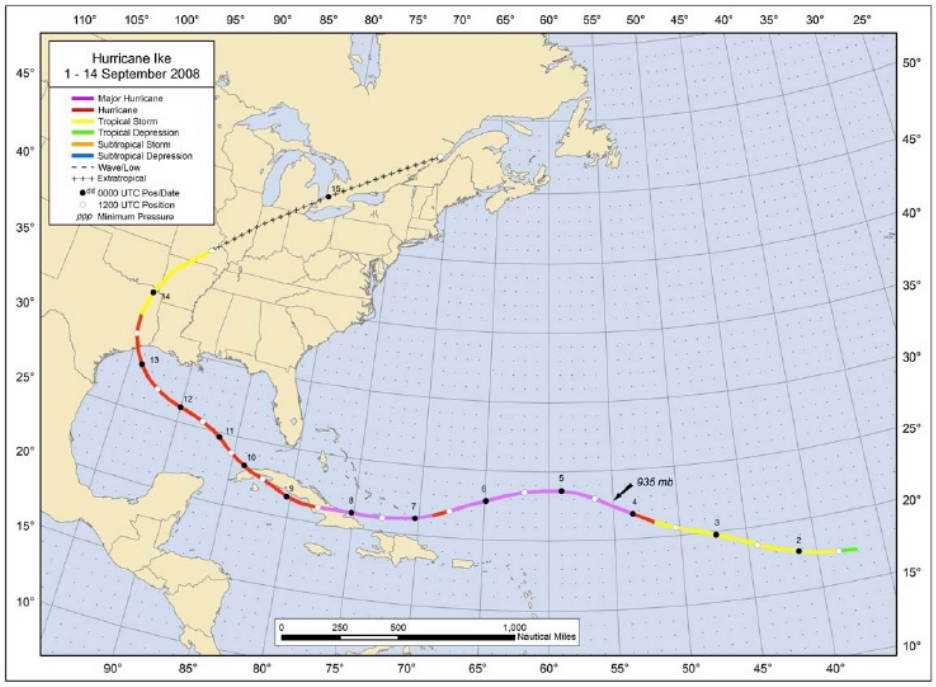

Figure A8: Best track positions for Hurricane Ike, 1-14 September 1st-14th, 2008. From the National Hurricane Center.

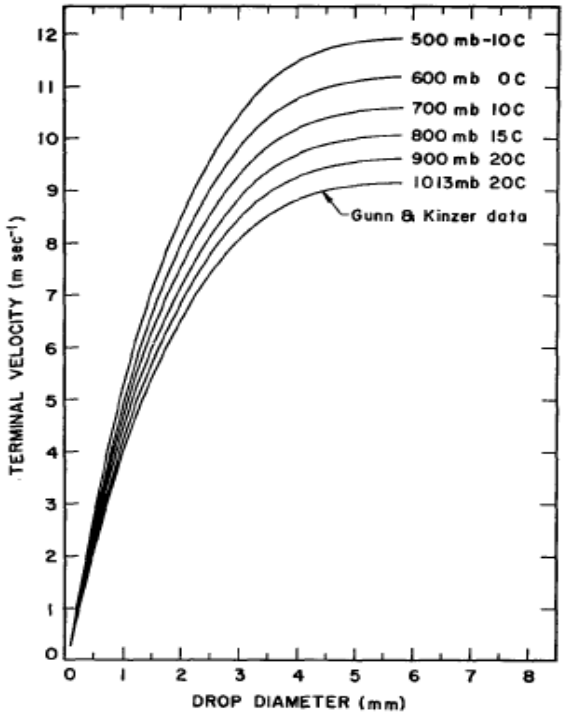

Figure A9: Terminal fall velocity of raindrops as a function of drop diameter. From Foote and duToit 1969.

Appendix B: Surveys, Instructions, and Sample Responses to Rainband Lab

B1: Pretest

Pre-test for Rainband Lab

ID Number: _____

Part 1: Science Labs

Think about your experience with science labs in general. Circle a number corresponding to how much you disagree or agree with each statement.

		Strongly Disagree	*Disagree*	*Neutral*	*Agree*	*Strongly Agree*
1. I enjoy learning how scientists work with data sets		*1*	*2*	*3*	*4*	*5*
2. I like working on my own during labs		*1*	*2*	*3*	*4*	*5*
3. I enjoy being able to use creativity during labs		*1*	*2*	*3*	*4*	*5*
4. I prefer to follow lab instructions in a step-by-step approach		*1*	*2*	*3*	*4*	*5*
5. It is important for me to be able to formulate and defend a scientific argument during labs		*1*	*2*	*3*	*4*	*5*
6. Labs allow me take control of my own learning		*1*	*2*	*3*	*4*	*5*
7. Technology allows me to do more interesting and imaginative work during science labs		*1*	*2*	*3*	*4*	*5*
8. Being able to design and conduct a scientific investigation improves my understanding of the material		*1*	*2*	*3*	*4*	*5*

Part 2: Rainband Profiles

These questions refer to profiles (variable vs. height) of wind and moisture in tropical cyclone rainbands. Answer them to the best of your ability. For questions 9 and 10 circle a number corresponding to how much you disagree or agree with each statement.

		Strongly Disagree	*Disagree*	*Neutral*	*Agree*	*Strongly Agree*

9. I feel that I know a lot about how wind speeds vary with height in rainbands		*1*	*2*	*3*	*4*	*5*
10. I feel that I know a lot about how moisture varies with height in rainbands		*1*	*2*	*3*	*4*	*5*

11. Describe what stratiform conditions are in a tropical cyclone (TC) rainband
12. Describe what a mean (horizontal) wind profile looks like in a TC rainband
13. Do you think all rainbands have the same mean horizontal wind profile? Why or why not?
14. Explain what radial and tangential winds are relative to a TC
15. Describe what a radial wind profile looks like in a TC rainband
16. Describe what a tangential wind profile looks like in a TC rainband
17. Would radial or tangential winds play a larger role in the mean horizontal wind? Why?
18. Describe what a moisture profile looks like in a TC rainband
19. Describe what might change in the wind and moisture profiles from before a rainband passage, to during the passage, to after the band has passed
20. If you were given observed profiles of the winds or moisture, how many rainbands would you need profiles from to feel confident that they describe the typical structure?

Question 21 refers to figures A-D:

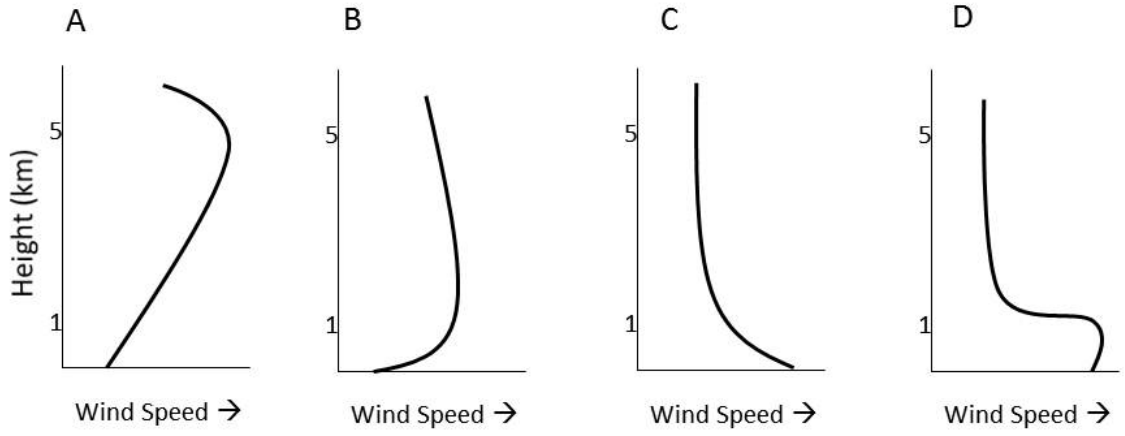

21. Which of the above profiles is most likely to be a mean wind profile in a tropical cyclone rainband? Explain your reasoning.

B2: Inquiry Lab Instructions

Wind Structure in Stratiform Rainbands Lab

Tuesday, November 8, 2011

ID Number: _____

You are given the following Excel files:

a) Mean Horizontal, Radial, and Tangential VAD Wind Speeds with height for three cases , each occurring during a stratiform period in a tropical cyclone rainband

b) 3 Soundings, occurring
   a. before Case 1 @ 1400 UTC
   b. before Case 3 @ 1500 UTC
   c. after Case 3 @ 2000 UTC

And the following supplemental files:

-WSR-88D still images and loops for the 3 cases

-Details about the storms and timing of the three cases

*Includes surface mean horizontal winds from tower at 14.5 meters and 18 meters

* Includes map of storm tracks

Scenario: Investigating Rainbands

Your research lab collects the above observations during Tropical Storm Fay and Hurricane Ike. Your job as a scientist is to determine what features are observed in the wind and moisture profiles during the stratiform rainbands. You should determine if these features are real and robust, if they can be tied to scientific explanations, and whether you can make any broad statements about stratiform rainbands based on your data set.

Your boss reminds you to study all three wind components, and also to look at how wind speed and moisture profiles change with band passage.

B3: Traditional Lab Instructions

Wind Structure in Stratiform Rainbands Lab

Wednesday, November 9, 2011

ID Number: _____

You are given the following Excel files:

c) Mean Horizontal, Radial, and Tangential VAD Wind Speeds with height for three cases , each occurring during a stratiform period in a tropical cyclone rainband
d) 3 Soundings, occurring
    a. before Case 1 @ 1400 UTC
    b. before Case 3 @ 1500 UTC
    c. after Case 3 @ 2000 UTC

And the following supplemental files:

-WSR-88D still images and loops for the 3 cases

-Details about the storms and timing of the three cases

*Includes surface mean horizontal winds from tower at 14.5 meters and 18 meters

* Includes map of storm tracks

Part 1. VAD mean horizontal wind profiles

1. Plot the VAD mean horizontal wind vs. height for each case.

    1a. Where is the wind maximum located in each case?

    1b. Describe the overall structure for each case.

2. Plot just the lowest 1 km for each case.

    2a. What does the wind speed do in the lowest 1 km in each case?

    2b. What do you hypothesize might be happening in the lowest levels to cause the wind speeds to have this profile?

3. Include the 2 surface tower data points on each plot. Does their location help to support your answer to Question #2b? Why or why not?

4. Average together the wind speeds and tower speeds from the three mean horizontal wind cases and plot them vs. height.

4a. Which of the features you noted in Question # 1b still appear in the main profile?

4b. Using the other supplemental storm information, what could explain the differences seen in the mean wind horizontal profiles?

4c. Do you feel confident based on the three cases of mean wind speed that the mean profile adequately describes the features observed during all tropical rainbands? Why or why not?

Part 2. VAD radial and tangential wind profiles

5. Plot the VAD mean radial wind with height for each of the three cases.

5a. Where does the maximum radial inflow occur in each case?

5b. At what height does the radial inflow transition to outflow?

5c. Compare the strength of maximum inflow and maximum outflow. Which one is stronger in each case?

5d. What happens above 3 km? Is this the same for all 3 cases?

6. Plot the VAD mean tangential wind with height for each of the three cases.

6a. What are the main features that you see?

7. Compare your radial, tangential and mean wind plots for each case.

7a.Which wind component plays the largest role in the mean winds?

7b. Is this what you expected to find? Why or why not?

Part 3. Rawindsondes

8. Plot both wind speed vs. height and temperature and dew point vs. height for all three soundings.

8a. What features do you see in the sounding wind speeds? Do they match or contrast with the features you noted in question #1?

8b. What features do you see in the moisture profiles?

Part 4. Changes during band passage

9. Using the soundings before and after Case 3, plot and compare the changes in wind speed and moisture profiles.

9a. What changes in wind speed do you see with band passage?

9b. What changes in moisture do you see with band passage?

B4: Supplemental Rainband Information

Rainband Case Information

*refers to overall storm conditions at the time of band observation over field site. The rest of the conditions are observed at the field site.

	Case 1	Case 2	Case 3
Date	8/18/2008	8/19/2008	9/9/2008
Time Period	16:40-17:40 UTC	3:53-4:11 UTC	17:27-17:38 UTC
Storm	Fay	Fay	Ike
Storm Winds*	50 kts	50 kts	70 kts
Storm Pressure*	1002 mb	995 mb	965 mb
Distance to storm center*	190.6	156.1	427.4
Direction of band approach	S/SSE	S/SW	E/SE
Band Observation Type	Cross-band	Cross-band	Along-band
Average Rainfall Rate	6.71 $mmhr^{-1}$	3.18 $mmhr^{-1}$	1.62 $mmhr^{-1}$
18 meter surface wind	4.50	8.38	6.38
14.5 m surface wind	2.64	6.29	4.38

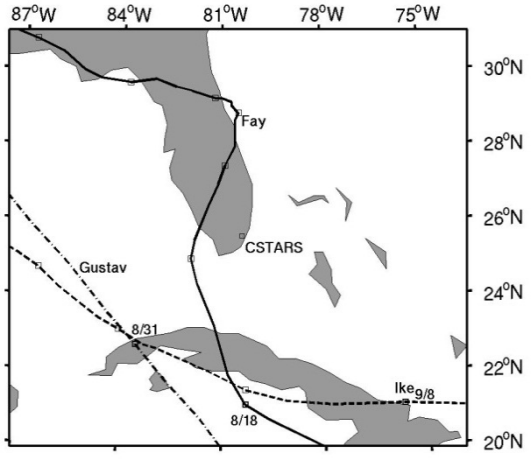

Map of Florida and Cuba. The marker represents the location of vertically pointing instruments from the CPS experiment at the University of Miami South Campus (CSTARS). The tracks of the three storms with rainbands sampled at CSTARS are also shown. Each position marker represents 00 UTC. Storm tracks are center positions from HURDAT.

B5: Posttest

Post-test for Rainband Lab

ID Number: _____

Part 1: Science Labs

Think about your experience with the rainband lab specifically. Circle a number corresponding to how much you disagree or agree with each statement.

		Strongly Disagree	*Disagree*	*Neutral*	*Agree*	*Strongly Agree*
1. I enjoy learning how scientists work with data sets		*1*	*2*	*3*	*4*	*5*
2. I like working on my own during labs		*1*	*2*	*3*	*4*	*5*
3. I enjoy being able to use creativity during labs		*1*	*2*	*3*	*4*	*5*
4. I prefer to follow lab instructions in a step-by-step approach		*1*	*2*	*3*	*4*	*5*
5. It is important for me to be able to formulate and defend a scientific argument during labs		*1*	*2*	*3*	*4*	*5*
6. Labs allow me take control of my own learning		*1*	*2*	*3*	*4*	*5*
7. Technology allows me to do more interesting and imaginative work during science labs		*1*	*2*	*3*	*4*	*5*
8. Being able to design and conduct a scientific investigation improves my understanding of the material		*1*	*2*	*3*	*4*	*5*

Part 2: Rainband Profiles

These questions refer to profiles (variable vs. height) of wind and moisture in tropical cyclone rainbands. Answer them to the best of your ability. For questions 9 and 10 circle a number corresponding to how much you disagree or agree with each statement.

		Strongly Disagree	*Disagree*	*Neutral*	*Agree*	*Strongly Agree*
9. I feel that I know a lot about how wind speeds vary with height in rainbands		*1*	*2*	*3*	*4*	*5*
10. I feel that I know a lot about how moisture varies with height in rainbands		*1*	*2*	*3*	*4*	*5*

11. Describe what stratiform conditions are in a tropical cyclone (TC) rainband
12. Describe what a mean (horizontal) wind profile looks like in a TC rainband
13. Do you think all rainbands have the same mean horizontal wind profile? Why or why not?
14. Explain what radial and tangential winds are relative to a TC
15. Describe what a radial wind profile looks like in a TC rainband
16. Describe what a tangential wind profile looks like in a TC rainband
17. Would radial or tangential winds play a larger role in the mean horizontal wind? Why?
18. Describe what a moisture profile looks like in a TC rainband
19. Describe what might change in the wind and moisture profiles from before a rainband passage, to during the passage, to after the band has passed
20. If you were given observed profiles of the winds or moisture, how many rainbands would you need profiles from to feel confident that they describe the typical structure?

Question 21 refers to figures A-D:

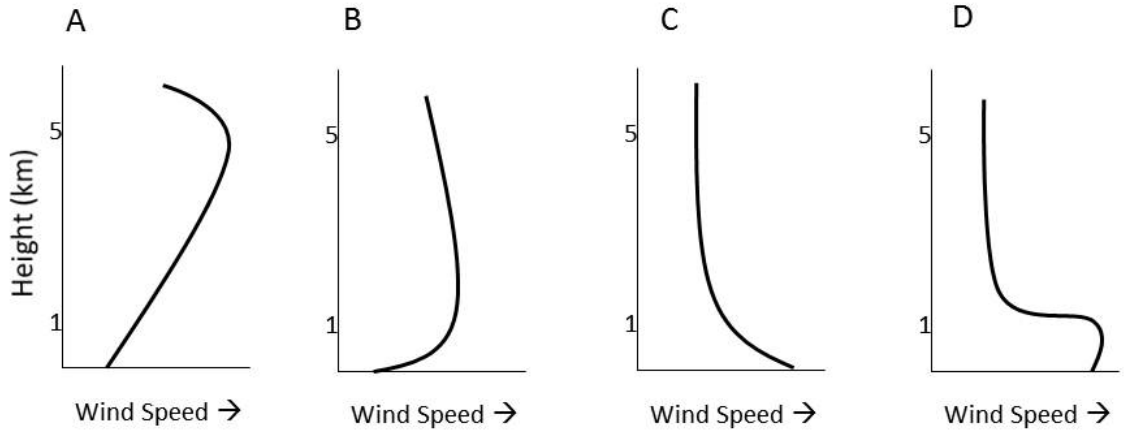

21. Which of the above profiles is most likely to be a mean wind profile in a tropical cyclone rainband? Explain your reasoning.

B6: Retention Test

Post-test for Rainband Lab

ID Number: _____

These questions refer to profiles (variable vs. height) of wind and moisture in tropical cyclone rainbands. Answer them to the best of your ability.

1. Describe what stratiform conditions are in a tropical cyclone (TC) rainband
2. Explain what radial and tangential winds are relative to a TC
3. Would radial or tangential winds play a larger role in the mean horizontal wind? Why?
4. Describe what might change in the wind and moisture profiles from before a rainband passage, to during the passage, to after the band has passed

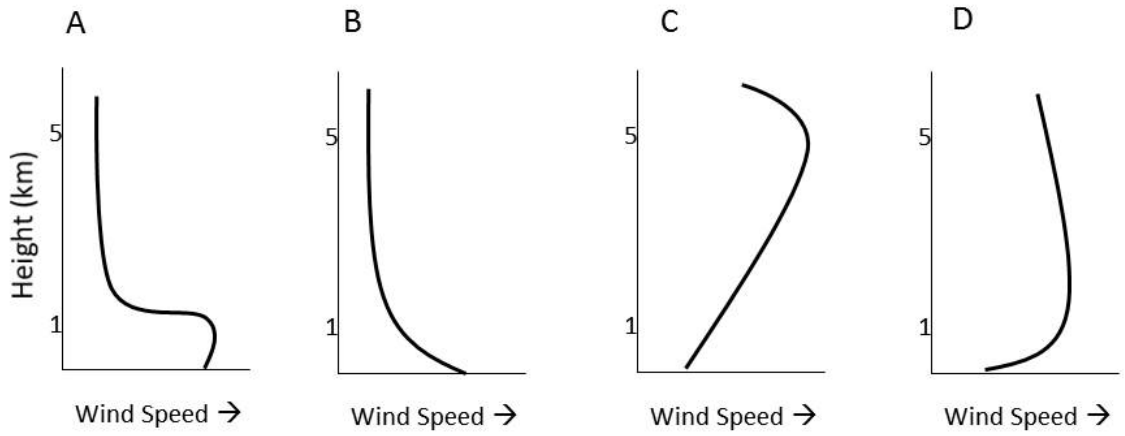

5. Which of the above profiles is most likely to be a mean (horizontal) wind profile in a tropical cyclone rainband? Explain your reasoning.

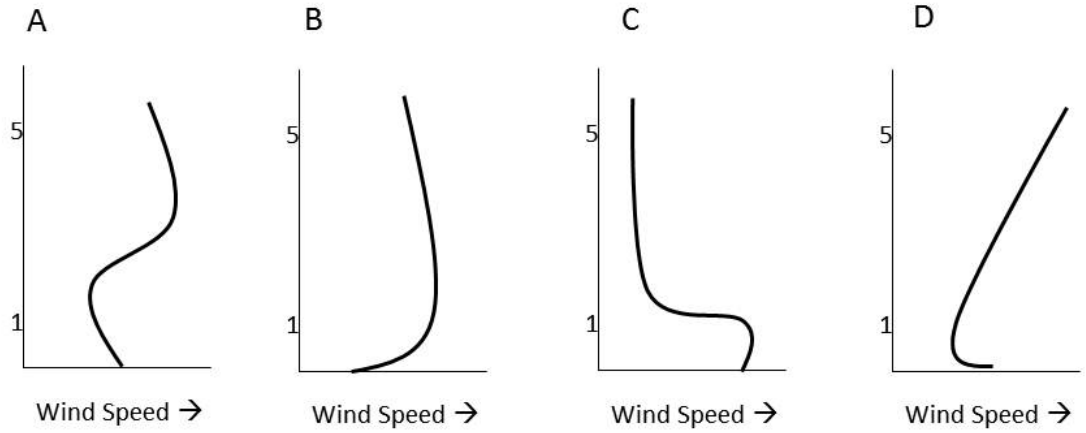

6. Which of the above profiles is most likely to be a tangential wind profile in a tropical cyclone rainband? Explain your reasoning.

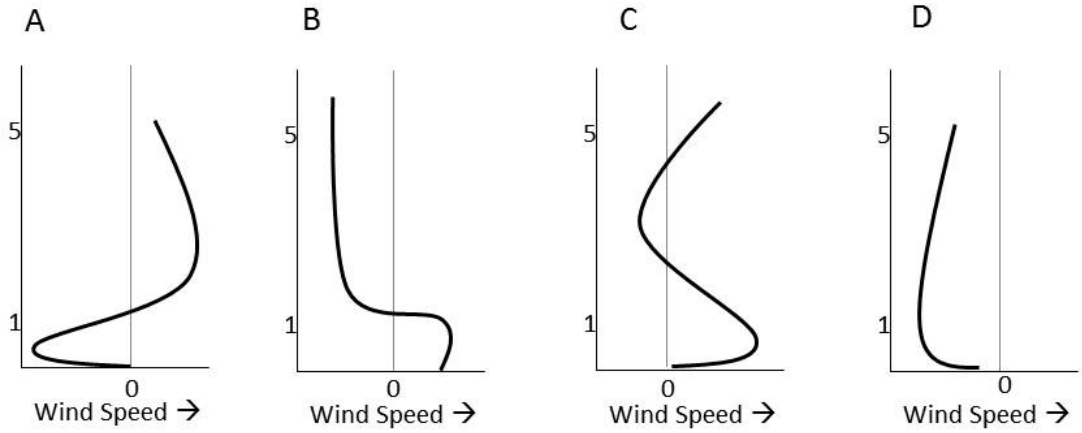

7. Which of the above profiles is most likely to be a radial wind profile in a tropical cyclone rainband? Explain your reasoning.

8. What do the mean horizontal wind speeds do near the surface?

9. What force causes this (#8) to occur?

B7: Sample Short Answers Responses with Rubric Scores

Rubric scores range from Level 0 (no credit) to Level 3 (full understanding). Student ID number is shown after each sample response.

Question	Sample Pretest Responses	Sample Posttest Responses
11. Describe what stratiform conditions are in a tropical cyclone (TC) rainband	Level 1: "Stratiform conditions refer to layers within the TC. Basically you have rising motion (updrafts) inside rainband then sinking motion (downdrafts) on both sides of the rain band.-42 Level 3: "Stratiform conditions are when the rainband is weaker and lighter precipitation because the clouds are stratus.-38	Level 3: "There is generally little vertical motion, high moisture content throughout the vertical, and winds that rapidly increase with height to a level just above the surface then slowly weaken.-61
12. Describe what a mean (horizontal) wind profile looks like in a TC rainband	Level 2: "The mean horizontal wind profile increases with height to about 700mb and then decreases above that point." -15 Level 3: "Strongest above the boundary layer then weakening."-27	Level 3: "Winds increase dramatically from the surface up to between 1 and 2 km where maximum wind speeds usually exist. The wind max could be at a higher altitude for strong TC. From 2-3 km up, winds tend to decrease slowly.-23
13. Do you think all rainbands have the same mean horizontal wind profile? Why or why not?	Level 1. "Yes, because the bands are all moving cyclonically."- 21 Level 3: "no. depends on cyclone strength, structure, size, and portion of a particular rainband within a cyclone"- 34 Level 3: "No, different forcing mechanisms combining in various ways are responsible for driving precip process. The different interactions will change how the horizontal profile looks"-26 Level 3: "I would think they would all be very similar as TC's are (mostly) uniform phenomena." -17	Level 2: "Roughly; some factors make certain profiles more variable and erratic than others." -40 Level 3: "No, some are associated with stronger or weaker TCs, maxima may occur in certain rainbands." -64 Level 3:" no, it depends on cross-band/along-band; strength of the storm, size of the storm, etc. but rainbands are likely to be similar in most cases."-34 Level 3: "No. because different environmental conditions contribute to how the profile evolves with heights. In case 1, there was a "nose" feature of max speeds, but in cases 2 and 3, speeds were instead constant with height in the same location."- 26 Level 3: "For the most part yes. Friction causes them to slow at the surface, then increase, then slowly decrease."- 17 Level 3: "No, based on analysis of different bands, they have general

		features, but height of maximum speeds can differ and rate of decay can differ." -15 Level 3: "Yes, based on the idea that all bands face friction (the cause of the curve at the surface." -13 Level 3 "To some degree. I believe all rainbands have the relatively same profile shape but eh magnitude of the values will differ depending on the cyclone strength the rain bands are a part of." -5
14. Explain what radial and tangential winds are relative to a TC	Level 1: "I think radial winds would be curved, circular like winds around a TC and tangential would always point straight out from curved flow (plus incorrect picture)"-35 Pre. Level 1: "Radial winds are in the same direction as the TC circulation. Tangential winds are tangent to the TC circulation. "-8 Level 2: "Tangential winds are winds blowing parallel to the rainband. Radial winds are winds blowing outward from the rainband."-20 Level 3: "Radial would be outward/inward winds while tangential would be flow along movement of TC"- 22	Level 2: "Tangential winds are the winds blowing tangent to tropical cyclone rotation. Radial winds are winds that blow toward center if a tropical cyclone."-15 Level 3: "Radial→ toward (-) or away from (+ center of TC. Tangential→ perpendicular to TC (cyclonic=+)." -40
15. Describe what a radial wind profile looks like in a TC rainband	Level 2: "A radial wind profile in a TC rainband would decrease with height, be stronger towards the surface."- 10	Level 3: "There is inflow near the surface up to about 3 km and then outflow above 3 km."-14
16. Describe what a tangential wind profile looks like in a TC rainband	Level 2: "Less varied than a radial wind profile." -6	Level 3: "Same answer as 12, but ~5% less magnitude."- 50
17. Would radial or tangential winds play a larger role in the mean horizontal wind? Why?	Level 3: "Tangential. If winds are mostly radial the low pressure will fill."-62 Level 3: "Tangential. They are the direct byproduct of cyclostrophic balance, whereas radial winds are a byproduct of the secondary flow."-46	Level 3: "Tangential, because the winds are in flow with TC circulation, which is dominating wind force due to primary PGF."-50 Level 3: "Tangential. The radial winds play key roles in upper/lower convergence, but a TC is essentially a strong

		cyclostrophic/gradient wind system, with the winds tending to be rotational around the center."-46
18. Describe what a moisture profile looks like in a TC rainband	Level 1. "Similar to the wind, I would expect moisture to increase moving in toward the center of the rainband."-61 Level 1: " More moist in the center of the rainband"-10 Level 2: "Saturated to the tropopause"-46 Level 3: "Column is mostly saturated in a TC rainband"-44	Level 2: "Moisture decreases, almost linearly, with height."-14 Level 3: "In a TC rainband, the moisture profile is saturated from lower level to upper levels with a few *slightly* drier pockets where the atmosphere is not as saturated (the dwpt is not exactly overlaid onto the temp)."-26 Level 3: "After a non-saturated layer close to the surface, there is a saturated layer between about 1 and 4 km. From there up the layer again is not saturated but very moist profile exists." -23
19. Describe what might change in the wind <u>and</u> moisture profiles from before a rainband passage, to during the passage, to after the band has passed	Level 2: "before: dry and wind blowing toward rainband. During: moist and strong winds. After: moist with winds blowing opposite as before" -22 Level 2: "Winds would go from calm to strong. Moisture profile would show an increase of moisture during the passage compared to before and after"-25 Level 3: "Before→ Drier, moderate winds. During→ moist, high winds. After→ moderate moisture, moderate wind (with more gusts than before)"-50 Level 3: "Winds will increase before passage as will moisture due to the approach of convergence zone. Winds will peak in band, as will moisture. Then lessen as divergence zone due to local subsidence approaches." -12	Level 3: "There is very little change before and after, and during would be windier and more moist." -39 Level 3: "Winds would increase during passage then decrease again. Moisture would vary very little before and after passage since the atmosphere is very near saturation throughout a TC."-28

20. If you were given observed profiles of the winds or moisture, how many rainbands would you need profiles from to feel confident that they describe the typical structure?	Unscored: "The more the better, but I would say about 10 in order to get a general idea." -12 Unscored: "I'm not really sure, maybe 5-10." -8	Unscored: "I still don't really know the answer to this question. Maybe 3 or 4 because that's how many we were given."- 8
21. Which of the above profiles is most likely to be a mean wind profile in a tropical cyclone rainband? Explain your reasoning.	Level 2: "B. Calmest in the eye, then strongest in the eyewall, then decreasing outward.-8	Level 3: "B. Winds are greatest at the surface theoretically [are strongest] but friction slows the wind down. The wind speed is maximized where surface friction no longer affects the winds."-21

References

Aberson, S. D., 2008: Large Forecast Degradations due to Synoptic Surveillance during the 2004 and 2005 Hurricane Seasons. *Mon. Wea. Rev.,* **136**, 3138-3150.

Agne, R. M., and D. J. Blick, 1972: A Comparison of Earth Science Classes Taught by using Original Data in a Research-approach Technique versus Classes Taught by Conventional Approaches not using Such Data. *Journal of Research in Science Teaching,* **9**, 83-89.

Anderson, R. D., 2002: Reforming Science Teaching: What Research says about Inquiry. *Journal of Science Teacher Education*, ***13*(1)**, 1-12.

Apedoe, X. S., 2008: Engaging Students in Inquiry: Tales from an Undergraduate Geology Laboratory-based Course. *Science Education,* **92**, 631-663.

Atlas, D., K. R. Hardy, R. Wexler, and R. J. Boucher, 1963: On the Origin of Hurricane Spiral Bands. *Geofis. Int.,* **3**, 123-132.

Baker, A. K., M. D. Parker, and M. D. Eastin, 2009: Environmental Ingredients for Supercells and Tornadoes within Hurricane Ivan. *Wea. Forecasting,* **24**, 223-244.

Barnes, G. M., J. F. Gamache, M. A. LeMone, and G. J. Stossmeister, 1991: A Convective Cell in a Hurricane Rainband. *Mon. Wea. Rev.,* **119**, 776-794.

Barnes, G. M., and G. J. Stossmeister, 1986: The Structure and Decay of a Rainband in Hurricane Irene (1981). *Mon. Wea. Rev.,* **114**, 2590-2601.

Barnes, G. M., E. J. Zipser, D. Jorgensen, and F. Marks, 1983: Mesoscale and Convective Structure of a Hurricane Rainband. *J. Atmos. Sci.,* **40**, 2125-2137.

Barrett, B. S., J. E. Woods, 2012: Using the Amazing Atmosphere to Foster Student Learning and Interest in Meteorology. *Bull. Amer. Meteor. Soc.,* **93**, 315-323.

Berg, R. (2009-01-23). "Tropical Cyclone Report Hurricane Ike." National Hurricane Center. http://www.nhc.noaa.gov/pdf/TCR-AL092008_Ike_3May10.pdf. Retrieved 2011-08-02.

Beven, J.L., and T B. Kimberlain, (2009-01-22) "Tropical Cyclone Report: Hurricane Gustav". National Hurricane Center. http://www.nhc.noaa.gov/pdf/TCR-AL072008_Gustav.pdf. Retrieved 2011-08-02.

Black, M. L., R. W. Burpee, and F. D. Marks, 1996: Vertical Motion Characteristics of Tropical Cyclones Determined with Airborne Doppler Radial Velocities. *J. Atmos. Sci.,* **53**, 1887-1909.

Blackwell, K. G., 2000: The Evolution of Hurricane Danny (1997) at Landfall: Doppler-Observed Eyewall Replacement, Vortex Contraction/Intensification, and Low-Level Wind Maxima. *Mon. Wea. Rev.,* **128**, 4002-4016.

Browning, K. A., and R. Wexler, 1968: The Determination of Kinematic Properties of a Wind Field Using Doppler Radar. *J. Appl. Meteor.,* **7**, 105-113.

Chang, C., and Y. Chang, 2010: College Science Students' Perception Gaps in Preferred-actual Learning Environment in a Reformed Introductory Earth Science Course in Taiwan. *Journal of Geography in Higher Education,* **34**, 187-203.

Chang, C., C. Hsiao, and J. P. Barufaldi, 2006: Preferred-actual Learning Environment "Spaces" and Earth Science Outcomes in Taiwan. *Science Education,* **90**, 420-433.

Chang, C., S. Mao, 1999: The Effects on Students' Cognitive Achievement when using the Cooperative Learning Method in Earth Science Classrooms. *School Science and Mathematics,* **99**, 374-379.

Chen, Y., and M. K. Yau, 2001: Spiral Bands in a Simulated Hurricane. Part I: Vortex Rossby Wave Verification. *J. Atmos. Sci.,* **58**, 2128-2145.

Chiappetta, E. L., 2008: Historical Development of Teaching Science as Inquiry. In J. Luft, Bell, R. L., Gess-Newsome (Eds.), *Science as Inquiry for Secondary Setting*. Washington, DC: National Science Teachers Association.

Clayton, D. S., and C. Gautier, 2006: Scientific Argumentation in Earth System Science Education. *Journal of Geoscience Education,* **54(3)**, 374-382.

Cohn, S.A., W.O.J. Brown, C.L. Martin, M.E. Susedik, G. Maclean, and D.B. Parsons, 2001: Clear Air Boundary Layer Spaced Antenna Wind Measurement with the Multiple Antenna Profiler (MAPR). *Annales Geophysicae*, **19(8),** 845 - 854.

D.B. Parsons, 2001: Clear Air Boundary Layer Spaced Antenna Wind Measurement with the Multiple Antenna Profiler (MAPR*). Annales Geophysicae*, 19(8), 845 – 854.

Cohn, S. A., J. Hallett, and J. M. Lewis, 2006: Teaching Graduate Atmospheric Measurement. *Bull. Amer. Meteor. Soc.,* **87**, 1673-1678.

Colin, J. and R. Faivre, 2010: Aerodynamic Roughness Length Estimation from very High-resolution Imaging LIDAR Observations over the Heihe Basin in China. *Hydrol. Earth Syst. Sci.*, **14(12)**, 2661-2669.

Committee on the Development of an Addendum to the National Science Education Standards on Scientific Inquiry, National Research Council, 2000: *Inquiry and the National Science Education Standards: A Guide for Teaching and Learning.* The National Academies Press.

Cutrim, E. M., D. Rudge, K. Kits, J. Mitchell, and R. Nogueira, 2006: Changing Teaching Techniques and Adapting New Technologies to Improve Student Learning in an Introductory Meteorology and Climate Course. *Adv. Geosci.,* **8**, 11-18.

Dunion, J. P., C. W. Landsea, S. H. Houston, and M. D. Powell, 2003: A Reanalysis of the Surface Winds for Hurricane Donna of 1960. *Mon. Wea. Rev.,* **131**, 1992-2011.

Eastin, M. D., and M. C. Link, 2009: Miniature Supercells in an Offshore Outer Rainband of Hurricane Ivan (2004). *Mon. Wea. Rev.,* **137**, 2081-2104.

Foote, G. B., and P. S. Du Toit, 1969: Terminal Velocity of Raindrops Aloft. *J. Appl. Meteor.,* **8**, 249-253.

Foster, R. C., 2005: Why Rolls are Prevalent in the Hurricane Boundary Layer. *J. Atmos. Sci.,* **62**, 2647-2661.

Franklin, C. N., G. J. Holland, and P. T. May, 2005: Sensitivity of Tropical Cyclone Rainbands to Ice-Phase Microphysics. *Mon.Wea.Rev.,* **133**, 2473-2493.

Franklin, J. L., M. L. Black, and K. Valde, 2003: GPS Dropwindsonde Wind Profiles in Hurricanes and Their Operational Implications. *Wea. Forecasting,* **18**, 32-44.

Gall, R., J. Tuttle, and P. Hildebrand, 1998: Small-scale Spiral Bands Observed in Hurricanes Andrew, Hugo, and Erin. *Mon. Wea. Rev.,* **126**, 1749-1766.

Gamache, J. F., and R. A. Houze, 1982: Mesoscale Air Motions Associated with a Tropical Squall Line. *Mon. Wea. Rev.*, **110**, 118–135.

Gardner, C. M., P. E. Simmons, and R. D. Simpson, 1992: The Effects of CAI and Hands-On Activities on Elementary Students' Attitudes and Weather Knowledge. *School Science and Mathematics,* **92**, 334-336.

Gautier, C., 2006: A Personal Experience of Designing Earth System Science Instruction Based on Learner-centered Environment Paradigm. *Journal of Geoscience Education,* **54(3),** 208-209.

Gautier,C., and R. Solomon, 2005: A Preliminary Study of Students Asking Quantitative Scientific Question for Inquiry-based Climate Model Experiments. *Journal of Geoscience Education,* **53(4)**, 432-443.

Gentry, R. C., 1983: Genesis of Tornadoes Associated with Hurricanes. *Mon. Wea. Rev.,* **111**, 1793-1805.

Grundstein, A., J. Durkee, J. Frye, T. Andersen, and J. Lieberman, 2011: A Severe Weather Laboratory Exercise for an Introductory Weather and Climate Class Using Active Learning Techniques. *Journal of Geoscience Education,* **59**, 22-30.

Hence, D. A., and R. A. Houze Jr., 2008: Kinematic Structure of Convective-scale Elements in the Rainbands of Hurricanes Katrina and Rita (2005). *J. Geophys. Res.,* **113**. D15108, doi:10.1029/2007JD009429.

Howard, D. R., and J.A. Miskowski, 2005: Using a Module-based Laboratory to Incorporate Inquiry into a Large Cell Biology Course. *Cell. Biol. Educ*., **4**, 249-260.

Illari, L., J. Marshall, P. Bannon, S. Lee, R. Najjar, J. Botella, R. Clark, A. Kumar, T. Sikora, T. Haine, K. J. Mackin, G. A. McKinley, M. Morgan, and A. Tandon, 2009: "Weather in a Tank" Exploiting Laboratory Experiments in the Teaching of Meteorology, Oceanography, and Climate. *Bull. Amer. Meteor. Soc.,* **90**, 1619-1632.

Ishihara, M., Z. Yanagisawa, H. Sakakibara, K. Matsuura, and J. Aoyagi, 1986: Structure of a Typhoon Rainband Observed by Two Doppler Radar. *Journal of the Meteorological Society of Japan*, **64** (6), 923-939.

Jones, R. W., 1986: Mature Structure and Motion of a Model Tropical Cyclone with Latent Heating by the Resolvable Scales. *Mon. Wea. Rev.,* **114**, 973-990.

Jorgensen, D. P., 1984: Mesoscale and Convective-Scale Characteristics of Mature Hurricanes. Part II. Inner Core Structure of Hurricane Allen (1980). *J. Atmos. Sci.,* **41**, 1287-1311.

Jorgensen, D. P., and P. T. Willis, 1982: A Z-R Relationship for Hurricanes. *J. Appl. Meteor.,* **21**, 356-366.

Kepert, J., 2001: The Dynamics of Boundary Layer Jets within the Tropical Cyclone Core. Part 1: Linear Theory. *J. Atmos. Sci.,* **58**, 2469-2484.

Khain, A., B. Lynn, and J. Dudhia, 2010: Aerosol Effects on Intensity of Landfalling Hurricanes as Seen from Simulations with the WRF Model with Spectral Bin Microphysics. *J. Atmos. Sci*., **67**, 365-384.

Kim, D., K. R. Knupp, and C. R. Williams, 2009: Airflow and Precipitation Properties within the Stratiform Region of Tropical Storm Gabrielle during Landfall. *Mon. Wea. Rev.,* **137**, 1954-1971.

Knupp, K. R., J. Walters, and M. Biggerstaff, 2006: Doppler Profiler and Radar Observations of Boundary Layer Variability during the Landfall of Tropical Storm Gabrielle. *J. Atmos. Sci.,* **63**, 234-251.

Knupp, K. R., J. Walters, and E. W. McCaul Jr., 2000: Doppler Profiler Observations of Hurricane Georges at Landfall. *Geophys.Res.Lett.,* **27**, 3361-3364.

Krockover, G. H., D. P. Shepardson, P. E. Adams, D. Eichinger, and M. Nakhleh, 2002: Reforming and Assessing Undergraduate Science Instruction Using Collaborative Action-Based Research Teams. *School Science and Mathematics,* **102**, 266-284.

Lorsolo, S., J. L. Schroeder, P. Dodge, and F. Marks, 2008: An Observational Study of Hurricane Boundary Layer Small-scale Coherent Structures. *Mon. Wea. Rev.,* **136**, 2871-2893.

Lorsolo, S., J. A. Zhang, F. Marks, and J. Gamache, 2010: Estimationand Mapping of Hurricane Turbulent Energy Using Airborne Doppler Measurements. *Mon. Wea. Rev.*, **138**, 3656-3670.

Mao, S., and C. Chang, 1998: Impacts of an Inquiry Teaching Method on Earth Science Student's Learning Outcomes and Attitudes at the Secondary School Level. *Proceedings of the National Science Council, Republic of China,* **8(3)** 93-101.

Marks, F. D., 1985: Evolution of the Structure of Precipitation in Hurricane Allen (1980). *Mon. Weather Rev.,* **113**, 909-930.

Marks, F. D., 2003: State of the Science: Radar View of Tropical Cyclones. *Meteorological Monographs,* **30**, 33-33.

Marks, F. D., and R. A. Houze, 1984: Airborne Doppler Radar Observations in Hurricane Debby. *Bull. Amer. Meteor. Soc.,* **65**, 569-582.

Marks, F. D., and R. A. Houze, 1987: Inner Core Structure of Hurricane Alicia from Airborne Doppler Radar Observations. *J. Atmos. Sci.,* **44**, 1296-1317.

Marks, F. D., P. Dodge, and C. Sandin, 1999: WSR-88D Observations of Hurricane Atmospheric Boundary Layer Structure at Landfall. Preprints, 23rd Conf. on Hurricanes and Tropical Meteorology, Dallas, TX, Amer. Meteor. Soc., 1051-1054.

Masters, F. J., H. W. Tieleman, and J. A. Balderrama, 2010: Surface Wind Measurements in Three Gulf Coast Hurricanes of 2005. *J. Wind Eng. Ind. Aerodyn.,* **98**, 533-547.

May, P. T., 1996: The Organization of Convection in the Rainbands of Tropical Cyclone Laurence. *Mon. Wea. Rev.,* **124**, 807-815.

May, P. T., G. J. Holland, and W. L. Ecklund, 1994: Wind Profiler Observations of Tropical Storm Flo at Saipan. *Wea. Forecasting,* **9**, 410-426.

Moon, Y., and D. S. Nolan, 2010: The Dynamic Response of the Hurricane Wind Field to Spiral Rainband Heating. *J. Atmos. Sci.,* **67**, 1779-1805.

Morrison, I., S. Businger, F. Marks, P. Dodge, and J. A. Businger, 2005: An Observational Case for the Prevalence of Roll Vortices in the Hurricane Boundary Layer. *J. Atmos. Sci.,* **62**, 2662-2673.

National Committee on Science Education Standards and Assessment, National Research Council, 1996: *National Science Education Standards.* The National Academies Press.

Nolan, D. S., 2005: Instabilities in Hurricane-like Boundary Layers. *Dyn. Atmos. Oceans,* **40**, 209-236.

Novlan, D. J., and W. M. Gray, 1974: Hurricane-spawned Tornadoes. *Mon. Wea. Rev.,* **102**, 476-488.

Oh, P. S., 2011: Characteristics of Abductive Inquiry in Earth Science: An Undergraduate Case Study. *Science Education,* **95**, 409-430.

Park Rogers, M. A., and S. K. Abell, 2008: The Design, Enactment, and Experience of Inquiry-based Instruction in Undergraduate Science Education: A Case Study. *Science Education,* **92**, 591-607.

Parker, L. C., G. H. Krockover, D. C. Eichinger, and S. Lasher-Trapp, 2008: Ideas about the Nature of Science Held by Undergraduate Atmospheric Science Students. *Bull. Amer. Meteor. Soc.,* **89**, 1681-1688.

Powell, M. D., 1987: Changes in the Low-level Kinematic and Thermodynamic Structure of Hurricane Alicia (1983) at Landfall. *Mon .Wea. Rev.,* **115**, 75-99.

Powell, M. D., 1990a: Boundary Layer Structure and Dynamics in Outer Hurricane Rainbands. Part I: Mesoscale Rainfall and Kinematic Structure. *Mon. Wea. Rev.,* **118**, 891-917.

Powell, M. D., 1990b: Boundary Layer Structure and Dynamics in Outer Hurricane Rainbands. Part II: Downdraft Modification and Mixed Layer Recovery. *Mon. Wea. Rev.,* **118**, 918-938.

Powell, M. D., and P. G. Black, 1990: The Relationship of Hurricane Reconnaissance Flight-level Wind Measurements to Winds Measured by NOAA's Oceanic Platforms. *J. Wind Eng. Ind. Aerodyn.,* **36,** 381-392.

Powell, M. D., P. P. Dodge, and M. L. Black, 1991: The Landfall of Hurricane Hugo in the Carolinas: Surface Wind Distribution. *Wea. Forecasting,* **6**, 379-399.

Powell, M. D., E. W. Uhlhorn, and J. D. Kepert, 2009: Estimating Maximum Surface Winds from Hurricane Reconnaissance Measurements. *Wea. Forecasting,* **24**, 868-883.

Powell, M. D., P. J. Vickery, and T. A. Reinhold, 2003: Reduced Drag Coefficient for High Wind Speeds in Tropical Cyclones. *Nature,* **422**, 279-283.

Qingchao, K., M. Xiufang, and H. Guangyan, 2008: Design and Effectiveness of Scientific Inquiry Learning Based on Campus Weather Station. *2008 International Conference on Proc. Computer Science and Software Engineering*, **5**, 602-607.

Romine, G. S., and R. B. Wilhelmson, 2006: Finescale Spiral Band Features within a Numerical Simulation of Hurricane Opal (1995). *Mon. Wea. Rev.,* **134**, 1121-1139.

Sato, K., 1993: Small-Scale Wind Disturbances Observed by the MU Radar during the Passage of Typhoon Kelly. *J. Atmos. Sci.,* **50**, 518-537.

Schwendike, J., and J. D. Kepert, 2008: The Boundary Layer Winds in Hurricanes Danielle (1998) and Isabel (2003). *Mon. Wea. Rev.,* **136**, 3168-3192.

Simmons, M., X. Wu, S. Knight, and R. Lopez, 2008: Assessing the Influence of Field- and GIS-based Inquiry on Student Attitude and Conceptual Knowledge in an Undergraduate Ecology Lab. *CBE Life Sci . Educ.,* **7**, 338-345.

Skwira, G. D., J. L. Schroeder, and R. E. Peterson, 2005: Surface Observations of Landfalling Hurricane Rainbands. *Mon. Wea. Rev.,* **133**, 454-465.

Spratt, S. M., D. W. Sharp, P. Welsh, A. Sandrik, F. Alsheimer, and C. Paxton, 1997: A WSR-88D Assessment of Tropical Cyclone Outer Rainband Tornadoes. *Wea. Forecasting,* **12**, 479-501.

Smith, R. K., and M. T. Montgomery, 2012: Hurricane Boundary-layer Theory. *Q. J. R. Meteorol. Soc*., **136**, 1-6.

Spronken-Smith, R., J. O. Bullard, W. Ray, C. Roberts, and A. Keiffer, 2008: Where Might Sand Dunes be on Mars? Engaging Students through Inquiry-based Learning in Geography. *Journal of Geography in Higher Education,* **32**, 71-86.

Spronken-Smith, R., and S. Kingham, 2009: Strengthening Teaching and Research Links: The Case of a Pollution Exposure Inquiry Project. *Journal of Geography in Higher Education,* **33**, 241-253.

Stewart, S. R., and S. W. Lyons, 1996: A WSR-88D Radar View of Tropical Cyclone Ed. *Wea. Forecasting,* **11**, 115-135.

Stewart, S.R., and J.L. Beven, J.L., (2009-02-08) "Tropical Cyclone Report: Hurricane Fay". National Hurricane Center. http://www.nhc.noaa.gov/pdf/TCR-AL062008_Fay.pdf. Retrieved 2011-08-02.

Stull, R.B., 1988: *An Introduction to Boundary Layer Meteorology*. Kluwer Academic Publishers, 666 pp.

Vickery, P. J., D. Wadhera, M. D. Powell, and Y. Chen, 2009: A Hurricane Boundary Layer and Wind Field Model for Use in Engineering Applications. *J. Appl. Meteor. Climatol.,* **48**, 381-405.

Weckworth, T. M., J. W. Wilson, R. M. Wakimoto, and N. A. Crook, 1997: Horizontal Convective Rolls: Determining the Environmental Conditions Supporting their Existence and Characteristics. *Mon. Wea. Rev*., **125**, 505-526.

Weckworth, T. M., T. W. Horst, and J. W. Wilson, 1999: An Observational Study of the Evolution of Horizontal Convective Rolls. *Mon. Wea. Rev*., **127**, 2160-2179.

Willoughby, H. E., F. D. Marks, and R. J. Feinberg, 1984: Stationary and Moving Convective Bands in Hurricanes. *J. Atmos. Sci.,* **41**, 3189-3211.

Wurman, J., and J. Winslow, 1998: Intense Sub-kilometer-scale Boundary Layer Rolls Observed in Hurricane Fran. *Science,* **280**, 555-557.

Yarger, D. N., W. A. Gallus, M. Taber, J. P. Boysen, and P. Castleberry, 2000: A Forecasting Activity for a Large Introductory Meteorology Course. *Bull. Amer. Meteor. Soc.,* 81, 31-39.

Yuter, S. E., D. Kingsmill, L. B. Nance, and M. Löffler-Mang, 2006: Observations of Precipitation Size and Fall Speed Characteristics within Coexisting Rain and Wet Snow. *J. Appl. Meteor. Climo.*, **45**, 1450-1464.

Zhang, J. A., R. F. Rogers, D. S. Nolan, and F. D. Marks, 2011: On the Characteristic Height Scales of the Hurricane Boundary Layer. *Mon. Wea. Rev.,* **139**, 2523-2535.